

Phase I Inspection of the Stay Cable System on the US 231 William H. Natcher Bridge over the Ohio River

Kentucky Transportation Center Research Report — KTC16-01/KHIT77-1F

DOI: <http://dx.doi.org/10.13023/KTC.RR.2016.01>

KTC's Mission

We provide services to the transportation community through research, technology transfer, and education. We create and participate in partnerships to promote safe and effective transportation systems.

© 2016 University of Kentucky, Kentucky Transportation Center

Information may not be used, reproduced, or republished without KTC's written consent.

Kentucky Transportation Center
176 Oliver H. Raymond Building
Lexington, KY 40506-0281
(859) 257-4513

www.ktc.uky.edu

Research Report
KTC-16-01/KHIT77-1F

**Phase I Inspection of the Stay Cable System on the US 231 William H. Natcher Bridge over
the Ohio River**

By
Theodore Hopwood II, P.E.
Program Manager

Sudhir Palle, P.E.
Associate Engineer III Research

Danny Wells
Researcher

Bobby W. Meade
Researcher

Jared Fairchild
Transportation Technician II

Christopher Goff
Transportation Technician II

Kentucky Transportation Center
College of Engineering
University of Kentucky
Lexington, Kentucky

In cooperation with
Kentucky Transportation Cabinet
Commonwealth of Kentucky

The contents of this report reflect the views of the authors, who are responsible for the facts and accuracy of the data presented herein. The contents do not necessarily reflect the official views or policies of the University of Kentucky, the Kentucky Transportation Center, the Kentucky Transportation Cabinet, the United States Department of Transportation, or the Federal Highway Administration. This report does not constitute a standard, specification, or regulation. The inclusion of manufacturer names or trade names is for identification purposes and should not be considered an endorsement.

January 2016

1. Report No. KTC-16-01/KHIT77-1F	2. Government Accession No.	3. Recipient's Catalog No.	
4. Title and Subtitle Phase I Inspection of the Stay Cable System on the US 231 William H. Natcher Bridge over the Ohio River		5. Report Date January 2016	
		6. Performing Organization Code	
7. Authors, Theodore Hopwood II, Sudhir Palle, Danny Wells, Bobby W. Meade, Jared Fairchild, and Christopher Goff		8. Performing Organization Report No KTC-16-01/KHIT77-1F	
9. Performing Organization Name and Address Kentucky Transportation Center College of Engineering University of Kentucky Lexington, KY 40506-0043		10. Work Unit No. (TRAIS)	
		11. Contractor Grant No. KHIT 77	
12. Sponsoring Agency Name and Address Kentucky Transportation Cabinet State Office Building Frankfort, KY 40622		13. Type of Report and Period Covered Final	
		14. Sponsoring Agency Code	
15. Supplementary Notes Prepared in cooperation with the Kentucky Transportation Cabinet, Federal Highway Administration, and U.S. Department of Transportation. Study Title: Natcher Bridge Cable Inspection			
16. Abstract <p>The US 231 Natcher Bridge was opened in 2002. By 2006 cracking was observed in the plastic piping that protected the stay cable strands from the environment at both the deck and tower anchorages. Over time the extent of cracking increased and an investigation was initiated to assess the types of deterioration impacting the cables, their causes and their impacts on the integrity of the stay cables.</p> <p>From 2012-2015, a series of in-depth field inspections were performed using visual and nondestructive testing. Most of this work focused on the piping at the deck anchorages. The inspections disclosed voids in cable grouting, bad welds in the plastic piping and deterioration of the co-extruded outer layer of the piping. Water was detected during inspections of the cable ends at the anchor heads along with minimal corrosion of the strands and anchorages. The water and samples of the plastic piping were evaluated and found to be problematic.</p> <p>No direct indications of cable corrosion damage were observed, but ultrasonic testing of the strand wires at the deck anchorages revealed possible signs of corrosion. Thermography of the tower anchorages provided extensive grout void indications. Recommendations are provided to address remaining concerns related to the condition of the strands at the towers and to evaluation of strands of selected stay cables at the deck anchorages.</p>			
17. Key Words Cable Stayed Bridges, Cables, Corrosion, Cracking, Nondestructive Evaluation, Plastic Piping, Plastic Sheathing, UV damage, Welding		18. Distribution Statement Unlimited with the approval of the Kentucky Transportation Cabinet	
19. Security Classification (this report) Unclassified	20. Security Classification (this page) Unclassified	21. No. of Pages 182	22. Price

Table of Contents

TABLE OF CONTENTS.....	I
TABLE OF FIGURES	III
EXECUTIVE SUMMARY	VII
1. INTRODUCTION	1
Relevant Bridge Features.....	1
Background on Stay Cable Problems	2
KTC Initial Work on the Stay Cables.....	3
2012 Phase I Work.....	4
2. 2013 KTC PHASE I WORK.....	6
GPR and IRT Detection of Grout Voids.....	6
Inspection of HDPE Piping Problems	8
Evaluation of Grout Voids and the Presence of Water.....	9
Crack Inspections/Evaluations	10
Evaluating the Condition of Other Piping Elements	11
Evaluating Map Cracking on the White HDPE Piping.....	12
Various Attendant Tasks and Analyses	14
3. SUMMARY AND CONCLUSIONS.....	16
KPFF and SCS Investigations.....	17
Grout Voids	17
Water in the Stay Cables.....	19
Cracking of the HDPE Piping	19
Micro-Cracking of the White HDPE.....	22
Results of Various KTC Tasks.....	25
Stay Cable Problem Issues and Priorities for Follow-on Work	26
4. RECOMMENDATIONS	28
5. REFERENCES.....	28
6. TABLES	31
7. FIGURES	40
8. APPENDIX 1 Description of HDPE Piping Condition States.....	98
9. APPENDIX 2 Applied Technical Services Review of HDPE Piping Fractures at the Deck	

Anchorage 104

10. APPENDIX 3 Microbac Report on Analysis of HDPE Piping Specimens from the Natcher Bridge..... 146

Table of Figures

Figure 1. US 231 William H. Natcher Bridge over the Ohio River near Owensboro, KY and Rockport, IN.	40
Figure 2. Cable configuration for the Natcher Bridge (Symmetrical for Upstream and Downstream).	41
Figure 3. Cross-section of Natcher Bridge Deck on Main and Side Suspended Spans.	41
Figure 4. Deck Anchorages.	42
Figure 5. Tower Anchorage.	42
Figure 6. Tower Anchorage and HDPE Piping Terminology.	43
Figure 7. Deck Anchorage Sectional View Showing Key Components (VSL).	43
Figure 8. Tower Anchorage Sectional View Showing Key Components (VSL).	44
Figure 9. Protective Cap on Deck Anchorage during Removal.	44
Figure 10. Deck Anchorage Showing Heavy Grease Coating on Strands/Wedges/Anchor Head. Note Water inside Anchorage Piping being Collected.	45
Figure 11. Helically Wound Ribbing on Stay Pipes.	45
Figure 12. Crack in Connection Sleeve Coupler at Cable B22D. Note Inked Cutting Outline.	46
Figure 13. Connection Sleeve and Coupler after Coupon Extraction. Note Grout (Red Arrow) and the Transition Pipe (Blue Arrow).	46
Figure 14. Extracted Coupon (Inner View). Note Fracture Face (Red Arrow) and Lack of Fusion Area in Electrofusion Weld (Blue Arrow).	47
Figure 15. Fatigue Fracture Surfaces. Note Concentric Beach Marks in Top View.	47
Figure 16. Locating Voids in Deck Anchorage Piping Using Sounding (October 2010).	48
Figure 17. Locating Voids in Deck Anchorage Piping Using the Time-of-Flight Method (October 2010).	48
Figure 18. UK IR4TD Personnel Taking IR Pictures of the Deck Anchorage Piping (October 2010).	49
Figure 19. KTC Personnel Using GPR to Locate Voids in Deck Anchorage Piping (October 2010).	49
Figure 20. Grout Void Indication on GPR Monitor Screen.	50
Figure 21. Deck Anchorage Sectional View Showing Strand Wedge Anchor.	50
Figure 22. Detecting Grout Voids in Connection Sleeves by GPR using a GSSI Palm Antenna.	51
Figure 23. Sectional View of Grout Void Disposition in Deck Anchorage Connection Sleeves.	51
Figure 24. Measuring Grout Voids Based upon GPR and Sounding Tests.	52
Figure 25. Use of a Man Lift to Take Thermal Images of the Stay Cable Piping at Various Heights above Deck Level.	52
Figure 26. Camera Operator Taking Thermal Images of the Stay Cables from a Man Lift.	53
Figure 27. Camera Operator Taking Thermal Images of Anchorages at the Tower Decks.	53
Figure 28. Images of Deck Anchorage Connection Sleeve of Cable B5U Infrared (Thermal) Image (a) Showing Void under Connection Sleeve Piping Compared to (b) GPR Detected Defect Shown in Visual Image.	54
Figure 29. Example of Defect Analysis for the Deck Anchorage Connection Sleeve of Cable B1D. Image Taken a Deck Level Position 0.	54
Figure 30. Infrared Images of Deck Anchorage at C6U.	55
Figure 31. Infrared Image of the Tower Anchorage Connection Sleeve Pipe Section for Cable B3D and Thermal Profile for the Dashed Line Shown in the Infrared Image.	56

Figure 32. Thermal Image Taken at Tower B of Cables B20D-B22D Showing the Effect of Solar Reflectance in Inhibiting Detection of Grout Voids	57
Figure 33. Thermal Image of Stay Pipe at Cable B12U Showing Possible Void	57
Figure 34. View from Hole Cut in Connection Sleeve Pipe. Grout Void Area Showing Stay Pipe End Fitting Embedded in Top of Grout.	58
Figure 35. KTC Technician Operating the Articulating Camera of Videoscope inside a Grout Void in a Connection Sleeve.....	58
Figure 36. Grout Interface between the Inner Wall of the Connection Sleeve Pipe and the Stay Pipe.....	59
Figure 37. Picture Taken by Videoscope inside a Grout Void Looking Upward Where the Stay Pipe Passes Through the Reducer.	59
Figure 38. Picture Taken by Videoscope Showing a Reducer Crack inside a Grout Void.	60
Figure 39. Picture of a Grout Void Taken Upward with Daylight Visible Through a Crack in the Reducer. Note the Tide Mark Rings on the Inner Wall of the Connection Sleeve Indicating Past Presence of Water in the Cable.	60
Figure 40. Picture inside a Grout Void Showing the Presence of Water in a Grout Void.	61
Figure 41. Water Leaking from a Grout Void in the Connection Sleeve Pipe at Stay Cable B12D.....	61
Figure 42. Circumferential Crack in Reducer above Grout Void in Stay Cable B12D.....	62
Figure 43. Water Gushing from Void in Cable B2U after Tape Covering Hole was Removed.	62
Figure 44. Arm’s Length Crack Inspection of the HDPE Piping at the Deck Anchorages.	63
Figure 45. Crack Growth from Coupler Butt Weld into Connection Sleeve Pipe Section (Looking Downward).	63
Figure 46. Complex Condition State 6 Cracking – A Single Crack at the Top of the Pipe Which Grew Radially in both the Clockwise and Counter-clockwise Direction to the Bottom of a Coupler (Looking Upward).	64
Figure 47. Simple Condition State 3 Cracking Perpendicular to Axis of Piping.....	64
Figure 48. Bottom Side of HDPE Reducer Where Cracks Growing Clockwise and Counter-Clockwise from the Top Side Merge.....	65
Figure 49. Bottom Side of HDPE Reducer Where Cracks Growing Clockwise and Counter-Clockwise from the Top Side Terminate.....	65
Figure 50. (a) Measuring Large Crack Opening with a Vernier Caliper; (b) Measuring Small Crack Opening with a Comparator Gage.....	66
Figure 51. Sawtooth Edge of Fatigue Crack with Arrow Pointing in the Direction of Propagation.....	66
Figure 52. Fracture Surface Marks (Steps) Indicating Clockwise (Right- to- Left) Crack Growth Typical of Low-Cycle Fatigue Crack Propagation at Reducer-to-Connection Sleeve Pipe Butt Weld.	67
Figure 53. Individual Crack Sites That Merge to Create Stepped Crack Faces.....	67
Figure 54. Large Crack Opening without Signs of Significant HDPE Deformation.	68
Figure 55. Crack Growth in Reducer Indicated by Marks.	68
Figure 56. Crack Growth in Connection Sleeve Pipe Indicated by Marks	69
Figure 57. Coupler Crack at Tower Anchorage on Cable B1U.....	69
Figure 58. Cables B4D and B5D at Tower Anchorage Showing Gaps Created by Butt Weld Fracture between Reducers and Pipe Sections of Connection Sleeves.	70
Figure 59. Slippage of Coupler off Transition Pipe at Tower Anchorage B4D due to Shear Failure of Electrofusion Welds.	70
Figure 60. Longitudinal Cracking of Reducer at Lag Bolt Retrofit Added During Construction.	71

Figure 61. Typical 40 ft. Stay Pipe Segment with Helical Ribbing Intact.....	72
Figure 62. Severe Disbonding of Ribbing from Stay Pipe Segment (2009).	73
Figure 63. Cracking of Ribbing Still Bonded to Stay Pipe (2013).....	74
Figure 64. Ribbing Detaching from Stay Pipe near Deck Anchorage	74
Figure 65. Ribbing Detaching from Stay Pipe near Tower Anchorage (2013).	75
Figure 66. Grout Plug with Minor Cracking.....	75
Figure 67. Grout Plug in Transition Pipe Having Extensive Cracking.	76
Figure 68. Missing Grout Plug.	76
Figure 69. Neoprene Boot at Deck Anchorage with Superficial Damage.	77
Figure 70. Neoprene Boots at the Upstream Side (Span 9) of Tower B Showing Missing Boot Retaining Bands.....	77
Figure 71. Detached Neoprene Boot at Tower Anchorage of Stay Cable B13U.	78
Figure 72. Barges Off-Loading Coal at the Neighboring Rockport Power Station in Indiana.	78
Figure 73. Contrasting Appearance of the Stay Cable HDPE Piping between 2009 and 2013.	79
Figure 74. Penetrant Test Showing Indelible Ink Bleeding into Micro-cracks at the Topmost Portion of a Stay Pipe.....	79
Figure 75. Ink Marks around the Periphery of Stay Pipe B2U Pipe Showing Ink Bleeding into Micro-cracks at the Mid Portion of the Pipe (Upper Arrow) and No Bleeding Is Present on the Lower Portions (Lower Arrow).	80
Figure 76. Close up Picture of Ink Marks on the Bottom Side of the Connection Sleeve at B20U Showing Signs of Minor Micro-cracking (Ink Bleeding).	80
Figure 77. Ink Mark on Coupler Showing the Absence of In Bleeding/Micro-cracking.	81
Figure 78. Differences in Micro-cracking in a Stay Pipe Adjacent to the Ribbing.....	81
Figure 79. “Candy-Stripe” Appearance of Stay Pipes Due to Micro-cracking Variations at the Helically Wound Ribbing.	82
Figure 80. KTC Researcher Using a Digital Microscope Camera to Take Close-up Pictures of Micro-cracking on the Surface of the Coextruded HDPE Pipe of a Connection Sleeve.....	83
Figure 81. Magnified Image of the Surface of a Coextruded HDPE Pipe Showing Micro-cracking. Note Coat Fines/Soils Embedded in the Micro-cracks.....	83
Figure 82. KTC Technician Using Hand Plane to Take Scrape Samples from the Surface of the White HDPE.	84
Figure 83. Surface of Coextruded HDPE Piping after Taking a Surface Scrape Sample.	84
Figure 84. Magnified Picture of the Surface of a Coextruded HDPE Pipe Adjacent to A Scrape Showing the Interwoven Pattern of the Micro-cracking with Depth into Surface down to Sound HDPE.....	85
Figure 85. Scrape Location on Transition Pipe Showing Micro-cracking Penetration of White Coextruded HDPE Down to the Black Base Material.	85
Figure 86. Spalling of Coextruded HDPE on Surface of a Connection Sleeve.	86
Figure 87. FTIR Scan from Scrape Sample of White Coextruded HDPE from Connection Sleeve Pipe Exhibiting Micro-Cracking.	86
Figure 88. FTIR Scan from Scrape Sample of White HDPE from Coupler with No Signs of Micro-Cracking.	87
Figure 89. A Porous Grout Sample Extracted from A Void in Connection Sleeve C19D.	87
Figure 90. Crack Width Gage Installed at Butt-Weld Crack at a Reducer.	88
Figure 91. Drill with Rasp Bit Being Used to Create Bevel in a Butt-Weld Crack Prior to Plastic Welding. 88	

Figure 92. Weld Repair of Crack in Reducer at Stay Cable B23D. 89

Figure 93. Completed Weld Repair in a Previously Cracked Reducer. 89

Figure 94. Failed Repair Weld (Ref. Figure 89) Discovered Several Months after Completion of Repair. . 90

Figure 95. Applying Stopaq® Paste to a Seal Crack in a Reducer..... 90

Figure 96. Covering the Stopaq® Paste Seal with Tedlar Tape. 91

Figure 97. Failure of Stopaq® Paste Seal Found Several Months after the Repair..... 91

Figure 98. Tedlar Tape Applied over Crack in a Reducer and Reducer-Stay Pipe Gap. 92

Figure 99. The Application of STOPAQ® Tape to Seal the Reducer-Stay Pipe Gap and Prevent Water
Intrusion into the Grout Void..... 92

Figure 100. Measuring Resistance of an Electrofusion Weld at the Weld Nipples on a Coupler..... 93

Figure 101. Broken Heating Wire of Electrofusion Weld and Missing Weld Nipples of Cracked Reducer. 93

Figure 102. Re-welding HDPE Plug Cut from a Connection Sleeve at a Void Access Hole..... 94

Figure 103. Water Leaking from Neoprene Boot at Tower Anchorage of Cable C7D (Ref. 11)..... 94

Figure 104. Finite Element Analysis of Effect of a Grout Void to the Reducer-Stay Pipe Area under
Loading (Ref. 17). 95

Figure 105. Commercial Cable Wrap Used as a Spot Repair on Stay Cable B22D (Arrow)..... 95

Figure 106. Zipper Sleeve on the US 17 Talmadge Memorial Bridge at Savannah, GA. 96

EXECUTIVE SUMMARY

The US 231 William H. Natcher Bridge, spanning the Ohio River near Rockport, IN and Owensboro, KY was opened on October 21, 2002. The first recorded observations of high density polyethylene (HDPE) cracking were noted in an annual consultant inspection report dated July 2006. Most of these problems related to several cables at the tower anchorages that experienced weld cracking of connection sleeve end fittings, which are termed couplers and reducers in this report.

KTC researchers first observed the cable cracking in May of 2009. By then, extensive cracking was apparent in the HDPE piping at the deck anchorages. At that time, water found inside the cables was sampled along with grease and an unknown material, which was later identified as a cementitious grout. In September 2009, KTC assembled a team of experts that visited the bridge and performed a preliminary evaluation of the stay cables and conducted initial tests of several nondestructive evaluation methods. During that work, a cracked weld at a coupler was sectioned, and several pieces of pipe were removed for laboratory inspection. The laboratory evaluation revealed that the cracking was due to fatigue from a defective weld (lack of fusion). A sample of black powder removed from the top of the stay cable piping was identified as coal dust probably from a nearby power plant. A portion of the HDPE piping made of a thin coextruded white outer layer and a thicker black base layer showed micro-cracking of the white surface with dark deposits in the cracks (probably coal dust fines).

In 2010, KTC researchers performed follow-on evaluations to detect grout voids inside the HDPE cables. They used sounding to detect 40 large voids in the upstream cables at the deck anchorages. Three other nondestructive evaluation methods were successfully demonstrated on the voids including two hands-on methods, ground penetrating radar (GPR) and time-of-flight ultrasound and one remote method, infrared thermography (IRT).

In 2011 follow-on work was halted due to construction on a nearby bridge. A five-phase plan was developed to investigate the cable problem with active work on Phase I of the plan scheduled to begin in 2012. The first part of the Phase I work began that year. Two consultants, Siva Corrosion Services (SCS) and KPFF Consulting Engineers (KPFF) were employed to inspect the lower deck anchorage (SCS) and perform ultrasonic testing on the strand ends.

KPFF performed ultrasonic testing (UT) on each wire in each strand at the deck anchorages seeking reflections indicative of cracked strands. Most of the strands (86 percent) gave no UT indications. The remainder, some 429 strands provided "atypical" returns which could be attributable to corrosion damage (but not cracking). KPFF recommended periodic re-testing of the strands to detect future degradation". They identified cables B10D, B15D and C8U as being problematic due to the large number atypical ultrasonic indications on them.

SCS testing of the protective grease in the anchorage found it to be in poor condition. It was replaced. SCS also observed a significant amount of water draining from the anchor head areas on 90 of the 96 stay cables after several days of rain. SCS examined and photographed the anchorages and performed several tests to assess the wedging of the strands in the anchor heads. SCS also took samples of the original grease, grout, rainwater and water that drained from the anchor heads and performed laboratory tests to analyze their impacts on potential corrosion of the strands. The rainwater was the most problematic issue. SCS recommended Borescoping the voids, evaluating the quality of the grout,

inspecting the tower anchorages, inspecting strands and repairing the piping to prevent further water infiltration.

In 2013 KTC conducted the second part of the Phase I work. The first portion of that work was grout void detection and sizing using GPR testing by KTC, which was supplemented by IRT performed by the UK Mechanical Engineering Department Institute of Research for Technical Development (IR4TD). GPR was used to examine the connection sleeves at the reducer ends on the deck anchorages. Once testing was completed, the grout void sizes were measured by their maximum length along the connection sleeves. IRT was used to remotely scan the stay cables (from a man-lift) and the tower anchorages (from the tower work platform). The GPR and IRT results indicated grout voids at all of the deck anchorages in upper portion of the connect sleeves. The GPR void indications ranged from several to more than 50 inches. GPR and IRT results for the deck anchorages were generally in good agreement. IRT testing of the tower anchorages indicated grout voids in all of the connection sleeves that were successfully scanned (65 of 96 cables). Most of those void indications were large.

After that work KTC inspected the deck anchorage piping of all 96 cables. That work included:

- performing arm's length (and closer) inspections of the HDPE piping of the deck anchorages,
- accessing the interior of grout voids to assess the internal conditions and determine whether water was entering the voids,
- examining for cracks in the HDPE piping to determine root causes and growth mechanisms,
- taking digital pictures of the anchorage assemblies including the connection sleeve assemblies, exposed portions of the transition pipes and the adjacent portions of the stay pipes,
- taking digital pictures of cracking the anchorage piping, measuring crack openings and classifying the piping issues (i.e., condition states),
- taking digital pictures of the tower anchorage HDPE piping using a high resolution camera and telephoto lens from deck level and the tower platforms,
- taking digital pictures of stay pipe ribbing, grout plugs and neoprene boots showing signs of distress,
- evaluating map cracking on the exterior (white) surface of the HDPE piping including conducting ink penetrant tests around the periphery of the pipes/sleeves, taking digital pictures of the map cracking and extracting samples of HDPE for laboratory analyses,
- performing ultrasonic testing of electrofusion and butt welds,
- assessing the chloride content in grout samples extracted from the cables,
- placing crack gages on HDPE piping to evaluate potential long-term crack activity, and
- repairing or sealing cracks in HDPE piping and replacing HDPE plugs cut out of the connection sleeves to evaluate the voids.

KTC researchers cut holes near the base of most grout voids and inspected the void interiors using a videoscope. Inspections revealed that the stay pipes had extended through the voids and terminated in grout just below the base of the voids. This finding indicated that none of the strands were directly exposed to the rainwater collecting in the voids. KTC researchers observed water ponding in 20 of the voids. At several larger voids, the KTC inspection found them completely full of water shortly after rainfalls. The videoscope revealed signs of water having been present in most of the dry voids. The presence of water in the voids was typically related to cracks in the HDPE.

Consultant biennial inspections conducted in 2013 and 2015 found water in some neoprene boots at the tower anchorages. The number of boots that contained water increased over that period.

Most of the cracking at the deck anchorages occurred in the couplers and reducers located at the ends of the connection sleeves. KTC researchers found only four stay cables at the deck anchorages with no cracks. The number of cracks detected by KTC at the deck anchorages increased significantly between 2009 and 2013.

A crack growth pattern assessment by Applied Technical Services (based upon pictures taken by KTC researchers) indicated that most of the cracks originated at the top of the HDPE piping transverse to the longitudinal axis. The cracks radiated circumferentially in both directions until they arrested at the bottom of the piping. The cables appeared to experience unidirectional bending in the vertical plane. Cracks in the reducers appeared primarily related to the underlying grout voids and welds issues. The coupler cracks were primarily related to welds. KTC created a model of the HDPE piping's condition states to permit classification of presence/types of cracking into 9 categories. KTC used that to determine the prevalent types of cracking of the HDPE piping. Ratchet marks on the surfaces of the cracks indicated that they were probably experiencing low-cycle fatigue.

KTC researchers took high-resolution pictures of the tower anchorages. Those pictures were used to inspect the HDPE piping at the tower anchorages for cracks. On five stay cables at the tower anchorages no cracking was observed. At the tower anchorages some cracks possessed wider openings/gaps than observed at similar cracks at the deck anchorages. Also, several of the tower anchorages exhibited shear failures in the coupler electrofusion welds and significant slippage between the connection sleeve couplers and the transition pipes. Summaries of KTC's inspection work and other consultants' findings are provided in Tables 5-8.

KTC researchers documented the disbonding of helically wound ribbing/strakes on the stay pipes. KTC researchers first observed the ribbing disbonding in 2009. The extent of that damage is difficult to assess. The ribbing is intended to prevent rain/wind vibrations in the stay cables so its loss can be problematic.

To detect micro-cracking in the HDPE piping KTC researchers wiped indelible ink marking pens at 90° quadrants around the piping. When multiple ink marks were made on the piping, ink flowed into the micro-cracks. This produced visible indications of the cracking. In most cases, the micro-cracking was present with the most severe amount on the upper portion of the HDPE cable components with less – or no – micro-cracking on the lower surfaces due to higher UV exposure. In some cases, the micro-cracking appeared to be consistent around the periphery of the HDPE components. KTC researchers found that all 96 stay cables have surface micro-cracking (map cracking) on at least some of the HDPE components.

Coal fines from a nearby power plant, as well as soils were lodged in the numerous fine cracks, giving the previously white cables a dingy gray appearance. Some of the HDPE piping, notably the all-white couplers and reducers did not exhibit this deterioration to the same extent as the coextruded

white HDPE on the outer surfaces of the stay pipes, connection sleeve pipe segments and the transition pipes. Since 2009 the stay cables' change in appearance of the stay cables has become more pronounced due to the micro-cracking worsening and the uptake of more debris in the cracks. KTC researchers found the map-cracking extended into the white HDPE. This resulted in the embrittled material spalling off piping surfaces. KTC researchers provide a test laboratory, Microbac, with samples of both poor and good performing HDPE from the bridge for evaluation. The laboratory reported poor oxidation resistance, which indicated that the material was susceptible to UV degradation and not suitably stabilized for use in exterior exposure. The base black HDPE which comprises most of the piping thickness had adequate oxidation resistance.

KTC researchers and SCS performed limited maintenance at the deck anchorages. SCS replaced deteriorated grease on the anchor head and added new gaskets for reinstalling the protective caps. KTC researchers used several different repairs to seal cracks in the HDPE piping. This included the use of plastic welding and different sealing materials. The bulk of the cracks were sealed with a UV-resisting tape. Researchers also placed crack gages at 8 locations where the existing cracks were sealed.

KTC researchers also tested grout samples taken from connection sleeves for chlorides and determined the chloride-contents were below those specified for post-tensioned grouted strands. Therefore, chlorides in grout were not considered problematic.

Based upon the Phase I test results, KTC has not identified any concerns that would justify re-cabling the bridge. KTC originally proposed a five-phase plan to investigate and repair the cables. The remaining phases need to be carried out to resolve the on-going stay cable problems. The Phase II work will entail evaluating strands in the piping at or near the deck and tower anchorages for signs of wire corrosion. The tower anchorages require arm's length inspections including assessment of connection sleeves for grout voids and investigating inside those voids. The protective caps at the towers need to be removed and the anchor heads, wedges and strand tails inspected for corrosion. The Phase II work should be considered safety inspections. Additionally, UT should be performed on the strands to look for cracking. The Phase II testing will identify the current conditions of the strands. In Phase III, a consultant experienced with cable-stayed bridges will perform design and construction reviews, analyze existing reports on the bridge, perform structural monitoring and other work deemed necessary to identify the root cause(s) of the stay cable problems. The consultant will also prepare and evaluate options for cable rehabilitation and replacement. In Phase IV, the consultant will prepare plans for repairing or replacing the stay cables at the direction of KYTC. Phase V will encompass the rehabilitation project's construction.

1. INTRODUCTION

The US 231 William H. Natcher Bridge, spanning the Ohio River near Rockport, IN and Owensboro, KY was opened on October 21, 2002 (Figure 1). At that time, it was the longest inland cable-stayed bridge in the U.S. Currently is the sixth longest bridge of that type. Since the completion of the four-lane section of US 231 from I-64 in Indiana, the traffic volume over the bridge has gradually increased. Work is underway to connect the bridge with the William H. Natcher Parkway to I 65. That will create an almost nonstop route that links I-64 and I-65 allowing traffic using those routes to by-pass Louisville.

Relevant Bridge Features

The main structure of the Natcher Bridge has a conventional two-tower layout employing diamond shaped pylons that are each 374 feet tall. Its main span is 1,200 feet long with two side spans that each measure 500 feet (Figure 2). The deck is 67 feet wide (Figure 3). The bridge has 96 stay cables that terminate at deck and tower anchorages. The stay cables are arranged in harp configurations with 48 cables connecting the deck with each of the pylons/towers on both the upstream and downstream sides of the bridge. To identify stay cables in this report, the following numbering scheme will be used. First, the tower or pylon is designated (e.g., Tower B or C). This is followed by the cable number (1-24) and finally the upstream or downstream side of the bridge (e.g., U or D). For example C11D denotes 11th cable on Span 10 (the Indiana side span) on the downstream side adjacent to the southbound lanes (Reference Figure 2).

The stay cables range in length from 170.17 feet to 606.87 feet. The cable diameters range from 5.51 to 8.58 inches. The cables contained between 18 to 61 steel strands (0.6-inch diameter) each of which contains seven 0.2-inch diameter wires. The strands were fabricated by greasing the wires and encasing them in polyethylene sheaths. High density polyethylene (HDPE) pipe/sheathing contains the strands to form the stay cables. Once the cables had been placed, the strands pre-tensioned, and HDPE piping assembled by welding, the interior of the HDPE piping was filled with a cementitious grout. According to the designer the HDPE pipes serve several functions:

- Provides additional layer of protection.
- Prevents water from entering the cables.
- Blocks UV light that can damage the strands sheath.
- Provides a smooth aerodynamic shape to the cable.
- Acts as a form for grouting (1).

The bridge has similar cable anchorage designs at both deck level and at the towers (Figures 4 and 5). In this system, the stay cable pipe is inserted into one end of a connection sleeve, with a transition pipe inserted into the other end (Figure 6). At the stay cable end of the connection sleeve, there is a reduced diameter fitting to accept the stay pipe. The report refers to that fitting as the “reducer”. A constant diameter fitting is attached to the other end of the connection sleeve to accept the transition pipe. That fitting is termed the “coupler”. Both of these fittings are butt-welded to the connection sleeve. Both fittings contain exposed helical wire wrappings on the inside faces that are connected at each end to external weld nipples. The stay cable pipe and transition pipe are thermally welded to the connection sleeve couplers and reducers (respectively) in slip fittings using a process termed

electrofusion welding. In that process, an impressed current is run through the wires from an external power source attached to the weld nipples. The wires heat the HDPE plastic of the couplers and reducers causing them to melt locally and subsequently to fuse with the stay pipes and transition pipes, respectively on cooling. The heating wires are wound along the inner faces of the reducers (in the small diameter portions) and the couplers so as to create two separate welds running circumferentially and mate the slip-fitted pieces together. This provides some redundancy if one of the welds fails.

A stay pipe is inserted into the small diameter portion of the reducer (Figure 7). At the end of the stay pipe there is an end fitting that narrows the diameter of the stay pipe and contains a steel band that acts as a reinforcement. Inside the connection sleeve, the strands emerge from the stay pipe, splay slightly and run down the length of the connection sleeve embedded in grout. Near the end of the connection sleeve, the sheaths are removed from the strands and the bare strands are inserted into tubes (separation sheaths) inside the transition pipe that run down to the anchor head. These tubes are wedged in countersunk holes in the anchor heads. The tubes are filled with grease prior to insertion of the strands to provide corrosion protection. The bare strands are run through the holes in the anchor head. On the exterior side of the anchor head, those holes are beveled. The strand tails are secured in tension by wedges inserted into beveled holes in the exterior face of the anchor head. According to the manufacturer, the anchorage assemblies were supplied with the tube portion pre-grouted to hold the tubes in place (2). At the anchorages, the strands are continually encased in HDPE starting with the stay cable, then the connection sleeve and finally the transition pipe (which fits in a notch in the anchor head). The tower anchorages are a similar to the deck anchorages with shorter connections sleeves and the guide pipes embedded in the tower concrete (Figure 8). The anchor head is enclosed in a steel “protection cap” to prevent the strand ends/wedges/and back face of the anchor head from direct exposure to the atmosphere (Figure 9). Those items are coated with a grease intended to provide corrosion protection (Figure 10).

The constant section piping, including the stay cables, connection sleeves and transition pipes are coextruded with a thin outer white layer of HDPE and an inner layer pigmented with carbon black. The stay piping has helically wound HDPE ribbing attached to the white coextruded HDPE which is intended to promote the piping shedding water to preclude wind-rain vibration problems (Figure 11). The couplers and reducers butt welded to the connection sleeve pipes are made from solid white HDPE pipe and are probably made by injection molding. The transition pipe is made from three pieces: an extruded pipe of solid carbon black pigmented HDPE, a molded transition piece and a coextruded pipe similar to the pipe segments of the connection sleeves. The pieces are assembled by butt welding. The only part of the transition pipe exposed to the atmosphere is a short segment of the coextruded pipe.

Background on Stay Cable Problems

Problems were encountered with stay cables during/shortly after the bridge was constructed. In 2002, during construction, four strands were found to have experienced wedge slippage involving two cables (3). A follow-on investigation was performed. This found that most strand ends at the deck anchorages extended beyond the specified 2-inch length from the anchor plates. The investigators concluded that three of the strand slippages were probably due to uneven wedge seating. No cause could be ascribed to the slippage of a fourth strand. The strands were resealed and re-tensioned at the tower anchorages.

The first recorded observations of HDPE cracking that the KTC investigators obtained were documented in an annual consultant inspection report performed in July 2006 (4). Most of those

problems related to several cables at the tower anchorages that experienced weld cracking of connection sleeve couplers and reducers.

KTC Initial Work on the Stay Cables

KTC investigators were apprised of the situation in late 2007 and made their first onsite inspection of the bridge in May 2009 with KYTC officials from the Central Office and District 2. At that time, KTC investigators working at the deck level observed numerous cracks in HDPE piping. They took pictures of all the HDPE deck anchorage piping including magnified images of visible cracks. While at the jobsite, they worked with KYTC personnel to remove several protective caps and found small amounts of water in the caps and water leaking from holes in the anchor heads. KTC personnel collected samples of the water, protective grease and irregularly shaped solid debris found in a protective cap. They also met with the bridge designer from Parsons Brinkerhoff and showed him the HDPE cracking at the deck anchorages. He was unable to determine the cause of those cracks.

KTC investigators subsequently took the samples to IMR of Louisville for analyses. The water was analyzed using energy dispersive spectroscopy. It contained slight amounts of organic acids, chlorides and nitrates along with a significant amount of sulfates that were later ascribed to calcium sulfonate in the protective grease. They also reviewed the HDPE piping cracks and categorized the pipes into nine condition states by the type of piping element affected, the presence of cracking and crack locations.

In September 2009, KTC assembled a team of UK and outside experts in corrosion, polymers, plastic welding, modal analysis, failure analysis, ground penetrating radar (GPR) and infrared thermography (IRT). The group visited the bridge to: familiarize itself with the cracking problems; conduct some preliminary testing using modal analysis, IRT (with external heating) and GPR; and take an HDPE fracture sample for follow-on evaluation. At several anchorage locations the reducers had completely detached from the connection sleeves due to fractures in the butt welds. At those locations the connection sleeves had deflected transversely relative to the strands which could only be the result of large voids in the grout. One of the attendees was able to insert a stiff wire into the connection sleeve at an opening created by the weld fracture and the transverse displacement. The wire was run down the pipe section about 4 feet. Upon withdrawal, it was found to be wet along most of its length. Both the GPR and IRT using external heating were unable to detect this large void.

The upper portion of a cracked connection sleeve coupler at cable anchorage B22D containing the electrofusion weld and a transverse crack was cut for removal (Figures 12, 13). The piece was easily extracted, which indicated poor electrofusion weld bonding to the transition pipe. Laboratory inspection of the weld revealed that only a small portion of the heated HDPE had melted resulting in incomplete fusion (Figure 14). Also, the fracture was due a penny-shaped fatigue crack that grew out of a groove for the heating wire. It propagated outward until it became a through-thickness crack. The crack became unstable and ran completely around the coupler's circumference (Figure 15). The fatigue initiation point was on top of the coupler indicating cable deflection in the vertical plane. Those findings suggested that some of the electrofusion welds were of questionable quality and could be responsible for some of the (fatigue) cracking observed.

The results of the KTC 2009 work were presented to KYTC officials and a series of laboratory tests were performed by KTC using GPR with a higher frequency (2.6 GHz) probe than used in the

previous field tests. Also, IRT was used with ambient thermal response rather than impressed heating. Both of those tests proved successful and plans moved ahead to employ those in field trials on deck anchorage piping that were conducted in October 2010. KTC contracted with a nondestructive test firm, Radarview, to demonstrate the time-of-flight ultrasonic test method that was being used on other bridges to inspect external prestressing ducts for grout voids. The initial tests centered on several connection sleeves that had fractured at the reducer butt weld and deflected transversely. As a comparison, KTC researchers used a 3-pound hammer to strike the outer surface of the HDPE piping and listened to the resulting sound (Figure 16). The grouted portion of the HDPE piping gave a noticeably different ring from the void locations where the grout was absent. By rapping the piping at various location along and around the piping, the boundaries of the voids were detected and marked with indelible ink pens. The validity of the sounding method was confirmed using the time-of-flight tests (Figure 17).

As part of the 2010 test, KTC investigators used sounding to examine 40 other connection sleeves that had cracks in their reducers, but were otherwise intact. Those tests indicated that many of the connection sleeves had grout voids running from the reducers at various distances into the pipe sections of the connection sleeves. The presence of those voids and their sizes were verified using both thermography with pictures taken from deck level using a telephoto lens (Figure 18) and GPR (Figures 19, 20) by running the probe along the connection sleeve (5). It appeared that many of the piping cracks were associated with the voids under the reducers.

These findings were presented to KYTC officials along with a plan to perform an in-depth evaluation of the cable piping to assess the damage and defects (grout voids and bad welds) in the stay piping, along with assessment of the HDPE material/welds to determine if they were satisfactory or defective (6). Due to construction closure of the KY 161 Bridge at Owensboro, the in-depth work did not occur in 2011, though KTC researchers visited the bridge to determine traffic needs for that work and, while there, observed what they believed to be increased cracking on the stay piping at the deck anchorages. They also developed a five-phase work plan to address the stay cable piping issues and effect a resolution to them.

2012 Phase I Work

Once the preliminary KTC work was completed and successful void detection methods developed, work began on Phase I of the five-phase KTC project. Due to funding limitations, the Phase I work was divided into two parts to be performed in consecutive years. From June to August 2012, KPFF Consulting Engineers and Siva Corrosion Services (SCS) conducted investigations at the deck/lower anchorages of the bridge for KTC (Figure 21).

KPFF performed ultrasonic testing (UT) of the strand ends at the anchor heads to inspect as far up the strands as possible to detect wire fractures (7). KPFF engineers worked at the Dywidag Systems International laboratory in Bolingbrook, IL to provide a proof of concept for the UT method that was able to detect half-depth notches in wires in strands at a distance of 9 feet under all loading conditions. Due to near-field ultrasonic noise, UT could not detect flaws 2 1/2" from the strand end. Concurrent with that work, SCS removed the protective caps at the deck anchorages and visually inspected the interior faces of the protective caps, anchor plates, wedges and strand tails for corrosion and strand tails and wedges for evidence of possible loss of tensioning.

SCS collected water present at each cable, measured the volume and analyzed it to determine whether it could contribute to corrosion. SCS also collected rainwater during its time on the bridge. Additionally, SCS evaluated the anticorrosive grease applied on the anchor plates, strands and wedges to determine its ability to protect those pieces from corrosion.

The KPFF field work took place during three weeks in July 2012. After removing the protective caps and anti-corrosive grease, KPFF personnel ground the strand ends flat to provide suitable contact surfaces for the ultrasonic transducers. During that period KPFF personnel conducted UT tests on all 96 cables – 3053 strands (21371 wires).

KPFF personnel found no flaw indications on 2624 strands (86 percent of the strands). However, on 429 strands, KPFF personnel detected atypical A-scan returns from one or more wires that might be typical of corrosion damage (loss of wire section) or some other issue. KPFF found no UT indications typical for fractured wires. KPFF also noted the “significant” amount of water leaking from the anchorages after the caps were removed and expressed concerns about corrosion and its possible impact on the fatigue strength of the strands/wires.

The KPFF recommendations included:

- Monitoring the stay cables “frequently and closely for degradation.”
- Performing further laboratory tests to classify wire damage due to general corrosion (e.g., loss of section) or small cracks.
- Considering the UT data in conjunction with the work done by SCS to evaluate the potential for corrosion damage (for each cable) for overall analyses of the strands.
- Performing in-depth evaluation and future inspections of cables B15D, B10D, C08U and due to the high number of atypical UT returns encountered from those cables.

SCS performed a detailed visual inspection of all 96 lower cable anchorages and collected and tested water, grout and grease samples from those anchorages (8). SCS personnel photographed the sites with the caps in place and removed. They observed the thick deposits of protective grease that were slathered over the anchorage components and found that the grease was discolored and in need of replacement. The grease was removed to permit visual inspection of the anchorages. The exposed steel anchorage components were inspected and photographed. Only light surface rust was observed on the strands tails, anchor heads and wedges. Conductivity tests were performed between strand tails to determine if there was excessive corrosion build up between the strands, wedges and bevels in the anchor heads. The lengths of the strand tails were measured and some variance in the length was observed. However, that issue was also noted during construction (9). The ends of the strand tails were sounded with hammer strikes to identify any anomalous responses indicative of loss of pretension.

Water draining from the opened anchorage was collected for future volume measurement and laboratory analyses. When available, samples of rainwater were collected for laboratory analyses. Grout found inside the protection caps was taken for laboratory analyses. SCS personnel tried to examine the backsides of the anchor heads with a borescope inserted through unused holes in the anchor heads. Those attempts were thwarted by a heavy build-up of the grease on the backsides of the anchor heads. New grease was obtained and applied to the anchorage components. Also, KTC obtained new flange gaskets used by SCS to replace the original ones when reinstalling the protective caps.

Samples were taken to the SCS laboratory for analyses. The laboratory tests of grease samples indicated that they had mixed with water to form emulsions. SCS noted that the emulsions would not provide the same corrosion protection as the original grease. The rainwater collected was slightly acidic. Corrosion rate tests using the rainwater showed that exposed steel wires would corrode rapidly leading to failure of the strands. SCS noted that on other projects, water infiltrating greased and sheathed strands (like those used in the Natcher Bridge) had caused strand failure within seven years.

SCS found water in 90 of the 96 deck anchorages. The pH values of the entrained water were basic due to interaction with the alkaline grout in the cables. In a contact with steel wires the pH values dropped over time and the cable water samples promoted corrosion similar to that of the rainwater samples.

SCS recommended:

- Performing bore scoping at exposed voids to document the corrosion condition of strands.
- Attempting to insert borescope into the top of grease-filled anchorage sections (may not be completely filled with grease).
- Performing intrusive cable inspection at select locations to test grout quality.
- Opening/inspecting all upper anchorages.
- Opening/inspecting 10 lower anchorages in 2013 to document the condition of strands. Opening/inspecting these locations again in four years to document the progression of corrosion and section loss.
- Repairing the stay cable pipes to prevent additional water infiltration into the cables.

2. 2013 KTC PHASE I WORK

From June-October 2013, KTC investigators and researchers from the UK Mechanical Engineering Department Institute of Research for Technical Development (IR4TD) conducted follow-on inspections of stay piping on the Natcher Bridge. The KTC work included:

- Detecting and sizing grout voids at the deck anchorages,
- Detecting and sizing potential grout voids at the tower anchorages,
- Detecting water intrusion/collection in grout voids,
- Documenting cracking/flaws in the HDPE piping at the deck and tower anchorages,
- Assessing the deterioration on the outer (white) layer of the coextruded and white HDPE piping at the deck anchorages and lower portions of stay piping,
- Assessing electrofusion/butt welds in lower anchorage piping, and
- Performing miscellaneous tasks.

GPR and IRT Detection of Grout Voids

Field work began on June 3, 2013. The GPR testing was performed by the KTC Pavements, Materials and Geotechnical Section and the IRT testing was conducted by the IR4TD team with oversight of the work managed by the KTC Bridge Preservation Section.

The GPR testing was performed during June 3 – 7 and 17 – 24, 2013. The testing employed a Geophysical Survey Systems (GSSI) SIR 3000 data collector and a 2 GHz Palm antenna (Figure 22). The antenna was moved down the pipe sections of the connection sleeves using the reducer-to-pipe butt welds as a datum. A void would present from the datum down the pipe sections until it ended (at varying distances for each anchorage). The distance of the void varied from the top of the cable to the bottom as the connection sleeves were inclined.

When the fluid grout initially was pumped into the piping at the transition pipe below the connection sleeve, it did not completely fill the connection sleeves creating the voids. Typically, the surface of the fluid grout settled to form a horizontal surface and solidified leaving a void that was longer at the top of the pipe than it was at the bottom (Figure 23).

The pipe was divided into quadrants about its circumference and scans were performed along the length of the cable at the 3, 6, 9 and 12 o'clock positions. After a scan was completed at a given position and the end of the void determined the location was marked with an indelible pen and its length from the datum was measured (Figure 24). Once all the scans had been completed, the inspection personnel roughed out a border of the void on the outside of the pipe using an ink pen. They also conducted initial checks of the GPR void locations by sounding them with a hammer. The marked void boundaries were subsequently used by KTC Bridge Preservation Section personnel in opening the voids to allow internal inspection. GPR testing revealed grout voids in connection sleeve pipe sections at all deck anchorages. The GPR void measurements for each cable are provided in Appendix 1 to assist with future re-grouting operations intended to eliminate the voids.

The IR4TD team performed infrared thermography (IRT) inspections on the cables June 17 – 21, 2013, on the downstream cables and in the towers September 23 – 27, 2013, for the upstream cables (10). The intent was to perform thermal imaging along the entire length of the HDPE encased cables from the deck- to the tower anchorages. The team used a portable Long Wave Infrared (LWIR) camera (FLIR Thermo Vision Model SC660) with a special lens to take the infrared images. The camera had 640 × 480 pixel resolution and operated in the long-wave infrared region (7.5–13 μm) with a temperature resolution of 0.1°C. The camera was factory calibrated to measure temperatures between -10°C – 90°C (14°F to 194°F). To ensure successful inspection, the team took IRT images at deck level and at 10, 20 and approximately 50 feet above the deck using a man lift (Figures 25 and 26). IRT images were also taken from the tower platforms shooting downward at the tower anchorages (Figure 27). The images were post processed using special software programs to identify defects and construct thermal images that encompassed the cable's full length. GPR and sounding location marks for the cable voids were used as references to compare with the IRT results for the defects (Figure 28).

At the deck anchorages, the thermal imaging detected void indications in all of the connection sleeves. They were present in the upper portion of the connection sleeves running from the reducer into the pipe section of the sleeves. IR4TD investigators measured the void sizes non-dimensionally as percentages of the lengths of the connection sleeve pipe. In the pipe section of the connection sleeve, defect (i.e. grout void) is identified as an increase in the temperature profile from the surrounding area of the cable. The defect length is identified as L_D in pixels, while the connect sleeve pipe length is identified as L in pixels (Figures 29 and 30). The defect size (%D) was referred to as dimensionless percentage and calculated as follows:

$$\%D = \frac{L_D}{L}$$

Thermal images taken of the connection sleeve pipe sections at the tower anchorages were taken on June 20 and 21, 2013 at about 10:00 am CDT. They produced similar results, detecting grout voids in numerous cables (Figure 31). Researchers encountered problems in imaging all of the anchorages due to poor visual access to some cables hampering thermal imaging from the tower platforms. Another problem related to solar reflections which obscured the thermal images from some cables (Figure 32).

Results of the grout void thermal imaging of the deck anchorage connection sleeve pipe sections are presented in Tables 1 and 2. The results of the grout void thermal imaging of the tower anchorage connection sleeve pipe sections are presented in Tables 3 and 4.

Both thermal imaging and GPR testing detected grout voids in the deck anchorage connection sleeve pipe sections of all of the cables except for B13U which was only detected by GPR. Thermal imaging provided larger void indications than GPR testing though most of the two tests provided indications within 10 percent of each other. Thermal imaging indicated grout voids in the tower anchorage connection sleeve pipe sections on all of the cables that were successfully scanned (65 out of 96). Due to lack of physical access to the tower anchorage piping, those indications could not be confirmed by another test method.

The IR4TD investigators recommended performing additional thermal imaging tests at the towers to obtain more complete grout void data. The improvements would be realized by using different lenses and conducting the tests at different times.

Thermal images of the stay pipes only revealed one small void in stay cable B12U (Figure 33). Thermal imaging did not provide any evidence of voids at the connection sleeve couplers.

Inspection of HDPE Piping Problems

From June 11 to October 14, 2013 KTC Bridge Preservation Section personnel inspected the deck anchorage HDPE piping of all 96 cables. The work included:

- performing arm's length (and closer) inspections of the HDPE piping of the deck anchorages,
- accessing the interior of grout voids to assess internal conditions and determine whether water was entering the voids,
- examining for cracks in the HDPE piping and assessing them to determine root causes and growth mechanisms,
- taking digital pictures of the anchorage assemblies including the connection sleeve assemblies, exposed portions of the transition pipes and the adjacent portions of the stay pipes,
- taking digital pictures of cracking the anchorage piping, measuring crack openings and classifying the piping issues (i.e., condition states),
- taking digital pictures of the tower anchorage HDPE piping using a high-resolution camera and telephoto lens from deck level and from the tower platforms,
- taking digital pictures of stay pipe ribbing, grout plugs and neoprene boots showing signs of distress,

- evaluating map cracking on the exterior (white) surface of the HDPE piping including conducting ink penetrant tests around the periphery of the pipes/sleeves, taking digital pictures of the map cracking and extracting samples of HDPE for laboratory analyses,
- attempting ultrasonic testing of electrofusion and butt welds,
- assessing the chloride content in grout samples extracted from the cables,
- placing crack gages on HDPE piping to evaluate potential long-term crack activity, and
- repairing or sealing cracks in HDPE piping and replacing HDPE plugs cut out of the connection sleeves to evaluate the voids.

In part, pictures were taken to establish a visual record of the deck anchorage piping condition in mid-2013 for comparison with previous pictures taken in 2009 and 2010 and for follow-on comparisons of piping condition in future years.

Evaluation of Grout Voids and the Presence of Water

A major concern of this project was the presence of grout voids in stay cables primarily at the reducer end of the connection sleeves. Those voids were associated with cracking in the reducers. Another concern was the presence of standing water in the voids and the possibility of this water coming into direct contact with exposed strands in the void areas.

Access holes were cut in connection sleeve pipes at the lowest point in the void at each cable as indicated by the GPR testing. This usually resulted in the access hole being cut at the interface between the grout and the void. To evaluate the interior of the voids thoroughly, KTC employed an articulating videoscope inspection camera with sufficient reach (9 feet) to access the interiors of the deck anchorage grout voids. At every location examined, the stay pipes had penetrated into the connection sleeve pipes and were visible typically including a portion of the black stay pipe end fittings which were either partially or completely embedded in the grout (Figure 34). Access holes were not used in a few locations where GPR and FTIR tests indicated small grout voids (usually 2 to 8 inches long) as most of space inside the connection sleeves were filled with grout.

The videoscope cable with the camera on its tip was inserted into the access hole and an operator manipulated the camera by moving the cable in and out and articulating it to view the voids and search for any signs of distress in the stay cables or the presence of water (Figure 35). Pictures showed that the set grout had typically formed a flat horizontal surface between the black inner wall of the connection sleeve pipe and the white exterior wall of the stay pipe (Figure 36). Inside the voids, the camera revealed void areas between the stay pipes and the inner face of the connection sleeve pipe which were available to collect and hold any water that could enter the void from cracks in the reducers or gaps in the reducer electrofusion welds (Figure 37). Pictures taken in the voids with the camera revealed daylight penetrating through open cracks in the reducers (Figures 38 and 39). In several cases, the video camera detected drops of water in voids that may be due to condensation (Figure 40). The videoscope was used on 46 of the downstream and 34 of the upstream stay cables. Of the cables inspected using the videoscope, about 70 percent showed potential signs of the current/past presence of water inside the voids (e.g., beach marks on the interior walls of the connection sleeve pipes shown in Figure 39).

In cutting the access holes for void inspections, KTC personnel encountered water in the voids on several occasions. A significant amount of water flowed from the 1-1/2 in. diameter access hole

when inspecting the void at cable B12D (Figure 41). That void had a length of about 26" measured from the connection sleeve reducer butt weld to the farthest point along the top of the connection sleeve pipe. KTC personnel videotaped most of this event and it appears that all or most of the void space was filled with water. At that location, the reducer had a relatively tight circumferential crack (Figure 42). KTC personnel questioned whether this crack opening was sufficient to allow water into the void and subsequently considered that the reducer electrofusion weld might have been incomplete letting moisture to enter the void in the gap between the reducer and the stay pipe. A similar event occurred when cutting an access hole in the connection sleeve at cable C13U. At cable B3U, KTC researchers inspected the cable in mid-June 2013. They repaired a relatively tight crack in the reducer using Tedlar tape. They also cut an access hole near the bottom of the grout void. Due to various operational issues, they were unable to re-plug that access hole after completing their work. They sealed the grout hole with Tedlar tape and did not return to permanently close the hole until late September. At that time, they observed the tape covering the hole bulging outward. When they removed the tape, a large amount of water gushed from the void (Figure 43). There was no crack-related opening above the void and the end of the stay pipe was encased in grout. It is likely that the water in the void entered from the gap between the end of the reducer and the stay pipe. That would indicate that the two electrofusion welds were not adequately sealing the slip joint between the reducer and stay pipe.

During inspections in the grout voids, KTC researchers encountered water in voids at 20 locations. That water was probably similar to the rain water that SCS found to be acidic and corrosive to exposed steel strands in laboratory tests.

Crack Inspections/Evaluations

The deck anchorage HDPE piping was visually inspected at arm's length for the presence of cracks (Figure 44). Each crack was photographed. Then, the maximum crack openings were measured, crack tips (where present) were marked and dated and the cracks were categorized by location on the piping termed "Pipe Condition States" developed after 2009 KTC inspection. Those nine condition states are described in Appendix 1. At the deck anchorages all of the cracks were located in the connection sleeves – primarily in couplers and reducers though some butt-weld cracking extended into the pipe section of connection sleeves (Figure 45).

In many cases the cracking was circumferential about the pipes and generally perpendicular to the axis of the piping. In some cases the cracking pattern was relatively complex (Figure 46). In others, the cracks were simple circumferential transverse cracks (Figure 47). Some cracks began at the top of the piping and grew around the pipe in both the clockwise and counter-clockwise directions. At some locations on the bottom side of the reducers or couplers, those cracks merged (Figure 48). In others, the cracks terminated without merging (Figure 49). At most crack locations, the crack had completely or almost completely parted the piping elements. Therefore, crack opening/gap measurements were taken as a measure of crack severity rather than crack length. Large crack openings were measured using a caliper while tighter cracks were measured using a small crack comparator (Figures 50a and 50b). Crack gaps were measured at the topmost portion of the piping (0°) and at quadrants numbered clockwise when looking at a cable from the topside.

At the outer surfaces of the pipes, sawtooth marks were observed on the edges of the cracks which are indicative of cyclic crack growth (Figure 51). At several locations where the reducer-to-connection sleeve pipe butt weld fractured, the connection sleeve pipe was displaced about 1 inch

transversely to the reducer end (Figure 52). The large size of crack ratchet marks on the fracture faces indicate low-cycle fatigue. At several locations, multiple adjacent cracks were evident, which will probably merge to form a coherent fracture (Figure 53). No fractures showed signs of significant localized elongation/necking although many had significant gaps between the mating crack faces (Figure 54). The cracking process was on-going during the course of the inspection work. Some crack tips marked by the consultant conducting a fracture-critical bridge inspection in May 2013 had extended by the time KTC researchers inspected them in July and October 2013 with some crack growth in excess of 1 inch (Figures 55 and 56). The deck anchorage HDPE pipe conditions are summarized in Tables 5-8.

Subsequent to the KTC field work, Applied Technical Services (ATS) Louisville was engaged to review the fracture pictures from the deck anchorages and interpret the crack growth patterns. The ATS report is provided in Appendix 2.

KTC did not have close access to the tower anchorage piping. However, high resolution digital pictures (4288 x 2848 pixels) were taken at the tower and the deck (3687 x 7311 pixels) of those locations. Crack information was obtained from viewing those pictures (primarily crack condition states). Most of the cracking observed at the tower anchorages was similar to that in the deck anchorages, with nearly all of the cracks in the connection sleeves – primarily in the couplers and reducers (Figure 57). At the tower anchorages some cracks possessed wider openings/gaps than observed at similar cracks at the deck anchorages (Figure 58). Also, several of the tower anchorages (B1D and C24D) exhibited shear failures in the coupler electrofusion welds and significant slippage between the couplers and transition pipes (Figure 59). That same type of failure had been observed with a lesser amount of slip at several of the deck anchorages B7U and B12U.

At several of the tower anchorages, lag bolts had been installed as field retrofits to secure couplers and reducers to transition pipes and stay pipes respectively (indicating that the electrofusion welds were not adequately joining the HDPE elements). In some cases, the bolts resulted in unusual crack patterns such as longitudinal cracks (Figure 60). In addition to the digital pictures, other tower anchorage information (especially related to cracks) was obtained from an annual consultant inspection report that involved rope descent and hands-on access which enabled direct measurements of crack openings (11). In some cases, KTC's review of the digitized pictures conflicted with the findings of that report. KTC researchers went over those instances closely to resolve the differences. The tower anchorage HDPE pipe conditions are also summarized in Tables 5-8.

Evaluating the Condition of Other Piping Elements

During the course of KTC's inspections, the condition of items related to the HDPE piping were photo-documented to determine their condition and assess whether they should be the subject of remedial actions. Those items included the ribbing/strakes that were attached to the stay pipes, the grout plugs that were inserted in the stay cables during grouting operations and the neoprene boots that sealed the opening between the steel guide pipes/girder connections and the transition pipes. No attempt was made to remove the boot bands and move any boots for internal inspections. That is generally performed to inspect the neoprene damper between the guide pipe and transition pipe to see if the dampers are deformed by excessive stay cable vibrations (12). That was not pursued as there had been no history of severe stay cable vibrations on the bridge and the wind-ties were intact without signs of major disturbances.

Short sections on the ends of the stay pipes do not have ribbing as they are slip-fit into the reducer ends of the connection sleeves and welded to them by the electrofusion welds in the neck of the reducers. The stay pipes were provided to the jobsite in 40 ft. lengths and butt-welded in the field to assemble the stay pipes (Figure 61). The sections could be observed as the butt-welding upset the coextruded stay pipe welds producing visible black bands from the black base HDPE at every weld location. The ribbing had been shop welded to the stay pipe sections. It was intended to prevent the formation of water rivulets which could be problematic under certain conditions (e.g., wind-rain vibrations).

Beginning with the 2009 KTC inspections, failures of ribbing were observed on the stay pipes (Figure 62). When KTC personnel returned for subsequent inspections, the tangles of loose, detached ribbing were not visible as they probably had been blown from the stay pipes by the wind. Close examination of the ribbing at various locations in 2013 indicated that it had been fracturing along its length and had become detached from the stay pipes (Figures 63-65). The disbonding of the ribbing appeared to occur randomly throughout the length of all of the stay cables. The extent of ribbing loss is difficult to determine due to the lengths of cable and the distance from which the ribbing must be observed either at deck level or from the towers. When the ribbing detaches, it leaves remnants of the weld with the stay pipe making inspection at distance other than arm's length impractical. To date, there have been no signs of wind-rain vibration on the bridge. The cross ties were observed to be intact. Therefore, the impact of lost ribbing is probably not a pressing concern.

The grout plugs appeared to be made from a different material than the HDPE, possibly nylon. Some of the plugs were generally intact although they showed signs of minor deterioration by cracking (Figure 66). In most cases the plug cracking is more pronounced (Figure 67). Several grout plugs showed signs of coming out of the piping and some were missing primarily from stay pipes (Figure 68).

The neoprene boots at the deck anchorages were typically in good condition. One boot showed signs of what appeared to be minor construction-related damage (Figure 69). All of the stainless steel retaining bands were in place on the deck anchorage boots. That was not the case at the tower anchorages where the retaining bands were missing on the tower anchorage boots for cables B13U – B17U (Figure 70). At that location, the neoprene boots for cables B13U and B17U had slid down the transition pipes leaving a large gap between the steel guide pipe and the transition pipe (Figure 71).

The consultant inspection noted bulging of some of the tower anchorage neoprene boots along with leakage of water and other indications of water collecting in the boots (13). Water inside the boots was noted at 14 anchorages.

Evaluating Map Cracking on the White HDPE Piping

During the 2009 inspections, KTC personnel noted a slight variance of color between some of the coextruded white HDPE piping (e.g., transition pipes, connection sleeves and stay piping). Most of that piping, along with the connection sleeve reducers and coupler that were cast from white HDPE had a bright white appearance. In late 2009, a sample of the white coextruded HDPE that had a darkened appearance was examined under a, optical microscope revealing that the surface had many fine interconnected micro-cracks (i.e. map-cracking). The cracks appeared filled with a dark material that was later found to be, in large part, coal dust fines. The Rockport Power Generating Station (Indiana Michigan Power Inc.) is a coal-fired power plant has large open piles of coal that come from barges and railcars (Figure 72). The plant is located in Indiana approximately one mile from the Natcher Bridge and

the coal piles are located in line of sight of the bridge between the power plant and the river. Wind carries the dust fines off of the open coal piles. A portion of the fines are deposited on the cables with some becoming lodged in the micro-cracks. That was determined by sampling surface deposits and SEM testing in 2010 (14). A white HDPE sample taken from a reducer did not exhibit signs of micro-cracking. However, by 2013 most of the coextruded piping (and a few of the couplers and reducers) had acquired a darker grayish appearance (Figure 73).

Prior to their field work, KTC researchers sought to determine why the white HDPE of the coextruded pipe exhibited micro-cracking while the all-white HDPE of the couplers and reducers were performing satisfactorily. The probable cause of the micro-cracking was believed to be related to UV degradation of the HDPE. KTC sought a method to analyze the surface white HDPE for the presence/absence of UV stabilizers. In 2011, KTC provided FTIR samples of the two types of materials taken from the bridge in 2009 to an FTIR equipment manufacturer for evaluation. Subsequently, the firm responded with test results that indicated the presence of “aromatic antioxidant or UV absorbers” and provided spectra from the two materials that clearly showed peak differences. Based upon that data, KTC acquired an FTIR unit and made plans to extract thin samples from the stay cables to evaluate them for the presence of light stabilizers (e.g., hindered amine light stabilizers or HALS).

During work on the bridge in 2010, KTC researchers noticed that darkening of the white HDPE was most prevalent on the upper portions of the piping. That would be most likely if the micro-cracking was due to UV exposure which would be greatest on the upper portions of the piping. KTC researchers wiped indelible ink marking pens at 45° points around the piping with the topmost point marked as 0° and the bottommost point as 180°. The pipe elements marked included the transition pipes, connections sleeves (which were categorized as couplers, pipe sections and reducers) and the stay pipes. When multiple ink marks were made on the piping, the ink flowed into the micro-cracks producing visible indications of the cracking (Figure 74). In most cases, the micro-cracking was present as expected with the most severe cases on the upper portion of the HDPE cable components. The lower surfaces exhibited less (or no) micro-cracking (Figures 75 and 76). In some cases, the micro-cracking appeared to be consistent around the periphery of the HDPE components. Typically, the all-white connection sleeve couplers and reducers exhibited little or no micro-cracking (Ref. Figure 77). Apparently, the process of bonding ribbing to the stay pipes impacted the micro-cracking patterns adjacent to the ribbing giving some stay pipes a “candy stripped” appearance (Figures 78 and 79). KTC researchers used a digital microscope/camera to take close-up pictures of the surface micro-cracking (Figure 80). A magnified image shows the complex interconnected nature of the cracking and the dark coal/soils lodged in the cracks (Figure 81).

In addition to the ink marking tests, KTC researchers took scrape samples of the HDPE piping from many stay cables and cable components – transition pipes, stay pipes and connection sleeve couplers, pipes and reducers (Figure 82). At some locations the white coextruded HDPE on the upper (0°) portion of the piping had become embrittled, having a powdery consistency. At those locations the powder had to be removed before the KTC researchers could get down to coherent material that could be scrape sampled. That underlying material would be extensively micro-cracked. A typical scrape swath in a micro-crack area usually removed some underlying HDPE that lacked the extensive map-cracking pattern (Figure 83). The scraping process revealed the interconnectivity of the micro-cracking with depth (Figure 84). In one case, the micro-cracking in the coextruded HDPE was observed to have

penetrated down to the black base HDPE (Figure 85). In several locations, the white coextruded HDPE exhibited spalling (Figure 86).

After completing the field testing and obtaining over 200 slice samples, KTC researchers used transmission FTIR to produce IR “fingerprints” to the samples (Figures 87 and 88). The red traces are FTIR scans of the actual test materials, while the blue scans are reference scans of similar materials in an FTIR scan library. Both sample traces correlate with ones for HDPE in the scan library. They sought to correlate the surface condition of the HDPE samples with the presence of UV light stabilizers (e.g., HALS). They were unable to reproduce the results similar to those provided by the equipment manufacturer in 2011 and sought assistance from that firm in interpreting the scans. After several discussions, with their technical experts, that effort was abandoned.

At the direction of KYTC officials, KTC contacted Microbac Laboratories, Inc. of Boulder, CO a test laboratory familiar with evaluating polymers to assist in evaluating the samples collected. At that time, KTC researchers had two questions: 1) why do some white HDPE piping components exhibit micro-cracking and some not?; and 2) does the micro-cracking pose any risk for fracture propagation into (and through) the black base HDPE? The latter question stemmed from the observation that some of the micro-cracking had penetrated completely through the white coextruded HDPE down to the black base material that constituted most of the piping’s wall thickness (Ref. Figure 85). To that end, in 2014, KTC initially provided the test laboratory with two “chunk” samples of coextruded HDPE with both the white outer layer and the black base material taken from a cracked coupler on cable B22D in 2011. The samples had micro-cracking that was less pronounced than that encountered on most coextruded piping in 2013. KTC also provided 30 slices of the white outer layer of the coextruded piping extracted during the 2013 field work. Those samples represented good and bad performing white HDPE from both solid piping (couplers and reducers) and coextruded material. Subsequently, the test laboratory requested additional “chunk” coextruded pieces from both the topmost and bottommost portions of the piping. Those were used to perform various laboratory analyses including stress crack testing. The laboratory test report is attached in Appendix 3.

Various Attendant Tasks and Analyses

In addition to the main tasks described above, KTC conducted several additional tasks as part of the 2013 (and 2014) field work. Those included: attempting ultrasonic testing of electrofusion and butt welds, assessing the chloride content in grout samples extracted from the cables, placing crack gages on HDPE piping to evaluate potential long-term crack activity, repairing or sealing cracks in HDPE piping, measuring resistance in electrofusion weld nipples and replacing HDPE plugs cut out of the connection sleeves to evaluate the voids.

KTC intended to conduct ultrasonic tests of the piping butt welds and electrofusion welds. The testing of the butt welds was intended to detect any subsurface cracking that might be forming. The HDPE piping was being subjected to variable stresses that caused fatigue cracking in the welds. In 2009, KTC extracted a fractured coupler segment that contained a fatigue crack that initiated at a heating wire within the electrofusion welds growing from the inside of the coupler to its outer surface before travelling in both directions around the coupler (Ref. Figure 15). The fracture mechanism of the butt welds, generally appeared to initiate at or near the top of the piping and grow in visible steps typical of low-cycle fatigue.

KTC researchers attempted to perform ultrasonic testing to evaluate the welds. They tried to acquire sample pieces of butt and electrofusion welds from the stay cable supplier and other sources but were unsuccessful. KTC researchers avoided removing exemplary welds from the bridge cables for laboratory ultrasonic tests and the one representative sample extracted in 2009 had been cut up for other tests. They attempted to perform several field trials using ultrasound but were unable to interpret the test results. Some straight beam tests of the electrofusion welds for lack of fusion appeared to be promising, but they could not be interpreted without cutting apart the welds. Lacking representative sample welds to perform laboratory evaluations (as done by KPFF in evaluating strand/wire cracking), ultrasonic testing was not going to provide usable results. Therefore, that task was abandoned.

After cutting the access holes in the connection sleeves at the base of the voids and inspecting the interior, KTC researchers extracted grout samples prior to plugging the holes. Typically, the grout at the base of the voids was in a plastic state when being pumped into the interior of the piping. The topmost portion of the solidified grout was typically covered with porous or flakey small pieces of grout (Figure 89). Grout specimens were taken from 96 stay cables. Chloride content tests were performed on 10 of those samples using the Germann Rapid Chloride Test that provides results consistent with the AASHTO T260 Standard Method of Test for Sampling and Testing for Chloride Ion in Concrete and Concrete Raw Materials. The chloride concentrations ranged from 0.005 to 0.04 percent by weight of grout. Those values are less than the allowable acid-soluble maximum of 0.08 percent (15).

As part of this work, KTC researchers installed crack width gages bridging cracks in the deck anchorage piping – the couplers and reducers. The intent was to perform subsequent long-term monitoring of changes in the gaps of cracks at various cables to determine if the crack widths were expanding. Previous visual inspections of anchorages by consultants and KTC (from the deck) seemed to indicate that some crack widths were increasing. The gages were affixed to the HDPE piping on either side of a crack by screws with the gages aligned along the length of the piping (Figure 90). Ten gages were installed on both the upstream and downstream stay cables – 5 gages per tower. At some installations, problems were encountered in attaching the flat-based gages to the round piping which caused the centering mark on the grids to displace when the tape holding the two gage pieces was cut. Close-up pictures were taken in those cases for future reference in reading the gages.

KTC researchers applied several types of repairs to the cracked HDPE elements at the deck anchorages. One type of repair used at three locations involved employing plastic welding to span the crack gaps. Typically, a drill with a rasp bit was used to cut a bevel along the length of the crack (Figure 91). Then a handheld plastic welder was used weld the cracked pieces together in one pass (Figure 92). The completed repairs were intended primarily for sealing these pieces and as only one pass was used with 5/32-inch diameter HDPE welding rods, the repair had low strength (Figure 93). Several months after one repair was completed, a follow-on inspection revealed that the crack gap had widened and the weld fractured (Figure 94). Weld repairs were performed at several other locations. After observing that failure, KTC researchers applied 3M™ Tedlar (polyvinyl fluoride) tape over the plastic welds including the failed one. A second type of repair used a putty/sealer, STOPAQ® PASTE CZH. The product is a viscous polymer molding paste with cold-flow and self-healing properties capable of being applied over polyethylene surfaces. The putty was applied over a crack and subsequently covered with Tedlar tape (Figures 95 and 96). Several months after the repair, KTC researchers unwrapped the tape to inspect the putty and found that the crack gap had widened and the putty had failed (Figure 97). The crack was then

covered with the Tedlar tape. All of the other cracks in the HDPE piping at the deck anchorages were sealed using the Tedlar tape. At stay cable B2U, the cracks in the reducer above the grout void had been sealed with tape. An access hole was cut in the connection sleeve at the base of the void (as indicated by previous GPR testing). Before the grout void could be inspected, KTC researchers had to leave the bridge. They taped the access hole closed and returned to site several weeks later. They discovered water a large amount of water the grout void. As the HDPE cracks remained sealed, KTC researchers believed the water probably entered in the gap between the stay pipe and the reducer (and poor electrofusion welds). Tape was applied over that gap to prevent water from entering the void (Figure 98). At cable B12D, where water was also present in the grout void, KTC researchers applied STOPAQ® wrapping tape around the reducer-stay pipe gap (Figure 99). This material remains soft and relatively pliable. After it was applied, it was overwrapped with Tedlar tape for UV protection. Most of the reducer-stay pipe gaps were sealed prior to KTC researchers completing their field work. The bulk of the crack and gap sealing performed on the anchorage HDPE piping consisted of wrappings with Tedlar tape.

Using a voltmeter, KTC researchers performed resistance measurements on the weld nipples of electrofusion welds on the deck anchorage couplers and reducers (Figure 100). The tests were used to determine if continuity still existed between the weld nipples. That would indicate the condition of the weld wiring and indicate if it was damaged. In some cases, broken weld wires were observed at gaps in cracks at the electrofusion welds – usually along with missing weld nipples (Figure 101). KTC researchers performed measurements with the potential for future repairs at the electrofusion welds by re-applying at current and re-melting the HDPE piping. This would be done to repair those welds showing lack of fusion (e.g., at the reducer-stay pipe gaps) and to re-weld connections showing signs of electrofusion weld shear failures and modest (< 1 inch) slippage (Ref. Appendix 2 Condition Category 8). The former task would require using straight-beam ultrasound to identify lack of fusion areas in the existing welds, which may be possible if KTC can obtain suitable exemplary welds for laboratory testing. Intact electrofusion welds had resistance reading on the order of a few ohms. Potentially failed electrofusion welds typically under tight cracks (Ref. Appendix 2 Condition Categories 3 & 6) had resistance readings in the hundreds to thousands of ohms. Completely failed electrofusion welds showed no continuity between the weld nipples.

All of the HDPE plugs generated by cutting access holes in the connection sleeves were re-attached by plastic welding (Figure 102). At several connection sleeve locations, KTC researchers had removed 1-inch x 3-inch pieces of HDPE in the coextruded pipe sections to provide samples for Microbac to analyze in late 2014. They had planned to insert HDPE filler pieces in the holes and close them by welding. The plastic welding unit malfunctioned during that work. As a stopgap, KTC researchers inserted the filler piece in the holes, sealed the gaps with caulk and covering the repair with Tedlar tape.

KTC researchers attempted to survey the deck profile but were unable to do so due to a constant low amplitude vibration in the suspended bridge deck.

3. SUMMARY AND CONCLUSIONS

The US 231 Natcher Bridge contains deficiencies in its stay cable system related to its construction and materials. It is unknown whether design issues have contributed to these deficiencies. What is significant is that every stay cable possessed some problem or group of problems that could negatively

impact – directly or indirectly – the cables’ anticipated service life. These problems could also detract from the aesthetics of the bridge. The maintenance manual for the bridge notes, “Stay cable corrosion protection should allow all stay cables to last more than 50 years” (16). The bridge/stay cables have been in service for 14 years and have experienced distress that may contribute to a reduction of that anticipated performance. The Phase I inspection results for each component/problem are addressed below along with their anticipated impacts on future stay cable performance. While these primarily relate to the stay cables at the deck anchorages, some remote evaluations were performed on the tower anchorages. This discussion addresses those findings as well. Additional information needs/actions are also discussed.

KPFF and SCS Investigations

Investigations by others have found that corrosion occurs at anchor heads to varying degrees (17). The KPFF and SCS investigations of strands and lower anchorages did not reveal any major problems related to the structural integrity of the cables (e.g., fractured strands). Those investigations provided several findings that are of major concern. One was the detection of water inside the stay cables. The SCS inspection discovered water seeping from the bottom anchorages of nearly all stay cables (in various quantities) after several rain episodes. At that time, the cracks in the HDPE deck anchorage piping had not been sealed. The protective grease covering the strand tails, wedges and anchor heads was discolored and found to be less protective than fresh grease. The rainwater samples collected were shown to cause rapid corrosion in steel wires. The KPFF inspection uncovered a second major concern – the finding of atypical ultrasonic indications from 14 percent of the strands with a high number of those from three stay cables – B10D, B15D, C8U and C11U. Based upon their work and experience on other investigations of cable-stay bridges, SCS and KPFF recommended:

- 1) Conducting a similar investigation at the tower anchorages including ultrasonic testing of the strands
- 2) Determining the condition of strands (and grout) at various locations at the deck and tower anchorages
- 3) Keeping water out of the lower anchorage hardware under the protective caps
- 4) Maintaining corrosion protection (i.e. the protective grease)
- 5) Performing periodic ultrasonic testing and visual inspections in the deck anchorages (of the strands and anchor heads/wedges). The need for periodic re-inspections is based upon the possibility that if wires in a strand have experienced corrosion damage (e.g., pitting) they may fracture over time due to the interaction of corrosion and fatigue.

Grout Voids

Stay cable shop drawings provided by the stay cable supplier for both the deck and tower anchorages show the stay pipes terminating in the narrow diameter portion of the reducers where the electrofusion welds were located. At the deck anchorages, internal inspections of the voids revealed that in most cases, the stay pipes had extended various distances past that into the connection sleeve pipe sections (in some cases more than 48 inches past the reducer-connection sleeve pipe butt weld). When access holes were cut into the base of the voids, the stay pipes ends were found to be embedded in the grout and in most cases, part of the tension rings at the ends of the stay pipes were partially visible.

In the stay cable grouting operations, filling plugs were cut in the HDPE transition pipes and grout was pumped inside travelling down the transition pipe to the anchor heads and upward into the connection sleeve pipe. KTC researchers believe that when the plastic grout hit the end of the stay pipe/tension ring, it basically sealed off the stay pipe hole (which was also filled with the greased and sheathed strands) and began pushing grout up the air pocket in the space between the inner wall of the connection sleeve pipe and the outer wall of the stay pipe. That created a situation in that space in which the trapped air was compressed by the plastic grout as it was moving upward filling the cavity in the compression sleeve. It is presumed that a pressure gage on the grout pump/line indicated a high pressure which stopped the grouting operation at the transition pipe, causing the grout to incompletely fill the connection sleeve. Thereafter, the grouting hole was plugged. Subsequently, another grouting hole was cut in the stay pipe above the reducer and the pumping operation continued with grout flowing up and down the stay pipe. As the lower end of the stay pipe had been plugged by the first grouting operation, the grout from the second pumping operation filled the short section of stay pipe below the pumping hole and routed the rest of the grout up the stay pipe. This operation continued until the pumping pressure became excessive and a new grouting hole was cut at or above the end point of the previous grouting operation. Typically, several grout plugs were observed on the bottom sides of the stay pipes along their length up to the tower anchorages. The FTIR pictures of the tower anchorages indicated that there were significant grout voids in this case above the reducers inside of the connection sleeve pipes and probably into the transition pipes. As KTC researchers did not have close access to the tower anchorages, those grout voids could not be investigated fully and their cause is not known.

Inspecting most of the grout voids was considered necessary because KTC researchers were concerned that strands might be in contact with standing rain water inside the voids. The SCS report noted that rain water samples taken in the area were slightly acidic and would cause corrosion in exposed wires. KTC's findings indicate that the location where the strands were splayed from the stay pipes was embedded in grout below the base of the voids. While exposed strands in that location might be exposed to wet grout, the SCS report noted that water in grout tended to be basic rather than acidic and would probably not pose a corrosion problem.

At the deck anchorages, grout voids of various sizes were detected in all of the stay cables at the reducer end of the connection sleeves (see Tables 5-8). Seventy-nine of those detected by GPR were over 12-inches long as measured from the reducer/connection sleeve pipe butt weld with 28 of those exceeding a length of 36-inches. Thermal imaging did not detect grout voids at the coupler ends of the connection sleeves. GPR was not used at those locations although sounding had been used in a limited number of tests by KTC in 2010, none of which indicated the presence of voids.

At the tower anchorages, thermal imaging void detection was hindered due to several technical issues. All 65 of the successful thermal images revealed grout voids in the connection sleeve pipes. Thirty-six of those were greater than 50 percent of the length of the connection sleeve pipes. It is likely that some of the tower transition pipes are not filled with grout.

The grout voids pose problems related to stay cable integrity. They can contribute indirectly to wire corrosion and make them more susceptible to cracking. They can also contribute to damage of the anchorage components (anchor heads and wedges). They directly are a cause of cracking problems in the stay cable HDPE piping. Any repair actions including those to prevent further cable cracking must include filling the grout voids at the deck and tower anchorages.

Water in the Stay Cables

Water inside the stay cables poses a major corrosion threat to the wires. As previously noted, the wires are inside greased and sheathed strands for most of their length inside the stay cables. Inside the connection sleeves, the strands splay out where they exit the stay pipes and travel down the connection sleeve pipes. Fortunately, the grout voids were above those locations and no uncovered strands were directly exposed to rainwater inside the grout voids.

KTC researchers found large amounts of standing water in voids at three stay cables and the presence of water in 20 of the voids that they inspected. Videoscope inspections revealed indications that water had been present inside dry voids of many of the stay cables. The indications typically were tide marks on the inner walls of the connection sleeve pipes. The absence of water in more voids during the inspections was probably due to a lack of rain prior to that work. SCS personnel collected water discharges from most of the anchor heads after the protective caps were removed for their inspections. In some cases, the collected large amounts of water after several days of rain. That water probably came from four potential locations: 1) down the stay pipes from cracks in the HDPE piping at the tower anchorages, 2) through the reducer-stay pipe gaps, 3) through cracks in the couplers and reducers, and 4) leakage at the neoprene boots. For cases 1-3, grout voids function as containers that collect the rain water before gradually releasing it downward through the transition pipe and through gaps and holes in the anchor heads. If the voids were not present, much less water could enter the piping.

For the water in the voids to reach the anchor heads, it had to penetrate through the about 10 feet of grout inside the connection sleeve and transition pipes. If the water penetrated at the neoprene boots, it would run down the steel guide pipes and enter the anchor head area through various joints in the HDPE anchorage piping or mating surfaces in the steel anchorage components. The former case poses questions about the continuity and permeability of the grout inside the deck anchorages. The latter case can be evaluated by removing a neoprene boot shortly after a rain event and checking for water inside the steel guide pipe.

The 2013 consultant inspection report noted the presence of water in the neoprene boots at the tower anchorages at 14 locations (Figure 103). A recent 2015 consultant inspection found that the number of boots with water had increased to 29 (18). SCS personnel have observed a similar problem on a cable-stayed bridge in another state (19). It is likely due to either leakage where the boot laps the guide pipe or to porosity in the boot material. The large gaps in some HDPE piping at the tower anchorages lead to water vapor entering the upper portions of anchorages inside the connection sleeves and condensing. The SCS report noted that some deck anchorage anchor heads had open holes that, according to the plans, should have been stopped by rubber plugs. They may also be missing from the tower anchor heads. Moisture from condensation could cause corrosion at the anchor heads.

Water in the cables is related to breaches in the HDPE piping at cracks and probably incomplete electrofusion welds in the reducers. It may also result from a lack of water-tightness in the neoprene boots. Any repairs to the stay cables must eliminate the presence of water inside the cables.

Cracking of the HDPE Piping

Cracking of the HDPE piping occurred almost entirely at the connection sleeve reducers and couplers. Over time, the number of those components with visible cracking has increased significantly and the crack openings have increased at some locations. In other cases, existing cracks have grown in length.

Consultant inspections performed in 2011 and 2013 showed new cracking or changes in cracks in 15 tower anchorages and 11 of the deck anchorages. KTC researchers performed deck-level inspections of the deck anchorages in 2009 and the arm's length inspections addressed in this report in 2013. In 2009, they observed 26 stay cables with no cracking. The 2013 inspection found that only four cables had not cracked. Most of the cracks found during the 2013 KTC inspection would be readily observable from deck level.

Based upon the ATS assessment of crack growth patterns, it appears that the cable movements were primarily unidirectional in the vertical plane (Appendix 2). There has been no evidence that the cables were subject to unusual or extreme motions (e.g., rain/wind induced vibrations). Cracks usually formed on the top side of the cables and propagated downward on either side. ATS noted that the butt-weld fractures originated in the heat affected zones of the welds. Some of the cracks appear to be related to fatigue in the electrofusion welds which may be due to lack of fusion between the slip-fit pieces. Those cracks would grow from the inner face of the piping through the thickness of the pipe component and then travel around the periphery from both edges of the through-thickness crack. At the bottom of the pipe, the clockwise and counter-clockwise moving cracks would usually intersect, move to the edges of a component (for the couplers) or overlap each other and stop growing. In some cases, the cracks had not yet quit growing and crack tip markers placed several months apart showed significant growth. Since most of the HDPE cracking was in the solid white couplers and reducers, ATS recommended extracting specimens from them and subjecting the specimens to tensile and impact tests to determine if their mechanical properties were satisfactory.

In the case of the deck anchorage reducers, grout voids appear to be a major factor. Tabatabai proposed that the solidification of the grout at an angle at the base of the voids created an uneven transfer of stresses from the strands to the reducers. That results in the connection sleeves bending in the vertical plane when the cables are stressed either by traffic or thermal loading (20). That would create a negative moment on the piping in the void area and promote cracking at the top of the pipes (Figure 104). Measurements of crack gaps on the tops and bottoms of the piping (the 0° and 180° positions respectively) showed no size tendency at either location on the cracked reducers. Several deck connection sleeves with long grout voids – C4U, C19D and C20D – developed complete fractures at the reducer – connection sleeve pipe butt-welds. The reducers remained attached to the stay pipes while the connection sleeve pipe was displaced transversely (cracking condition state 4). The voids may have been localized areas where the cables had greater flexibility due the lack of grout and acted as stress concentrators that also promoted cracking. As previously noted, the visible ratcheting marks on the cracks indicated that the growing cracks experienced low-cycle fatigue probably due to thermal stresses.

As previously discussed there were some shear failures of the electrofusion welds with significant displacements of the separated stay pipes and reducers at the tower anchorages. At the time of construction, slippage of electrofusion welds at those locations must have been a concern as lag bolts were installed adjacent to some of those welds to prevent further shear failures and joint slippages. Review of KTC's high-resolution tower pictures showed that some retrofit locations had cracking associated with the lag bolts and the continued integrity of those joints is in question.

Based on KTC arms-length inspections at the deck anchorages, the consultant biennial inspection report of 2013, and review of KTC's high resolution pictures of the tower anchorages the cracking conditions for the HDPE piping at the deck and tower anchorages were as follows:

- No stay cable HDPE piping is without cracks at both the deck and tower anchorages
- No cracking was observed in the HDPE stay pipes
- 5 stay cables have intact HDPE piping at the deck anchorages
- 3 stay cables have intact HDPE piping at the tower anchorages

At the deck anchorages, the most common crack condition states were:

- Type 1 (69)
- Type 2 (23)
- Type 3 (20)

At the tower anchorages, the most common crack condition states were:

- Type 2 (52)
- Type 3 (31)
- Type 6 (11)

As previously noted, KTC researchers used crack openings (gaps) as a measure of severity. For the deck anchorages the following crack opening data were collected (representing the maximum crack openings):

- < 0.125 inches (41)
- 0.125 inches – 0.500 inches (80)
- > 0.500 inches (0)

Using the consultant biennial inspection report and high resolution pictures, the crack openings at the tower the following crack opening data was collected:

- < 0.125 inches (27)
- 0.125 inches – 0.500 inches (65)
- 0.500 inches – 0.750 inches (7)
- > 0.750 inches (4)

The fact that the crack openings at the tower anchorages were greater than those at the deck anchorages may relate to gravity and downward slippage of the pipes. What is interesting is that some of the cracks at the deck anchorages had large gaps. That indicates the HDPE piping is in tension. Generally, the crack openings at the deck anchorages were greater at the reducers than at the couplers which might be explained by the presence of the grout voids, but some couplers had crack openings as wide as the ones in the reducers.

One interesting point to note is that KTC and others inspecting the Natcher Bridge stay cables did not find any signs of cracking in the stay pipes. The presence of tensile stresses and alternating stresses has not proven problematic in the longest portions of the cables. That indicates the cracking problems may mostly be related to grout voids and improper welds at the anchorages. The implication is that the cracking repairs will only need to be affected at the stay cable ends.

The recent 2015 consultant inspection report for the Natcher Bridge revealed continued HDPE piping crack activity in the form of new cracks emerging, growth of existing cracks around the piping and widening of crack openings. The report indicated that new crack activity was observed in over 30 locations in both tower and deck anchorages. The consultant's evaluations of crack activity at the deck anchorages were hampered by KTC researchers taping over cracks in 2013.

The cracks in the HDPE piping require repair, but before that is done, a better understanding of why the cracking occurs is necessary. The cracking is on-going and any repairs that are proposed must arrest or compensate for it. Key actions to address the cracking problem include assessing cyclic cable stresses due to loading and thermal stresses, reviewing construction practices for the installation of cables/piping, and reviewing the structural design. It should be noted that the cable supplier had minimal involvement with cable installation on this bridge (21).

Micro-Cracking of the White HDPE

All 96 stay cables have micro-cracking on at least some their HDPE components. The HDPE specimens provided to Microbac for laboratory testing were subjected to constituent analysis (Thermal Desorption Gas Chromatography/Mass Spectrometry or TD GC/MS), (High Performance Liquid Chromatography or HPLC), UV performance (Oxidative Induction Time or OIT testing) and mechanical testing (the Pennsylvania Edge Notch Test or PENT).

The TD GC/MS testing was performed by several methods to seek the common UV stabilizer additives used in polymers – hindered amine light stabilizers or HALS). Thermal Desorption Gas Chromatography is a process whereby a polymer sample is heated producing volatiles or semivolatiles that are transferred into a GC column in a carrier gas stream. The volatiles are separated as compounds in the GC column and each volatile is subjected to analysis as to the amount and type of chemicals present in the sample. That test was used to evaluate white HDPE from both solid and coextruded samples at various depths.

The HPLC testing is similar to TD/GC MS. The testing was used to determine the antioxidant (AO) concentration of the white coextruded layer of the chunk HDPE samples from connection sleeves removed in 2014. The AO concentration is a measure of UV resistance of the white HDPE.

OIT testing measures the level of thermal stabilization of the material tested. The test uses an instrument having a chamber in which a polymer is melted in an inert gas atmosphere. The liquid polymer is then exposed to an oxygen atmosphere. When the liquid polymer begins to oxidize, it gives off heat. The instrument detects the temperature increase. The interval between the exposure of oxygen to the liquid polymer and the onset of the exothermic reaction is termed the Oxidative Induction Time (in minutes). The test is a measure of the polymer's resistance to oxidation with better UV resistance resulting in longer OITs. That test was used to evaluate white HDPE from both solid and coextruded samples at various depths.

The PENT test was used to test the stress crack resistance/slow crack growth resistance. In that test, the chunk specimens extracted from connection sleeves (top and bottom) in 2014. Those were given a single edge notch and placed in a chamber filled with heated air. The specimen was placed in a constant load fixture with a timer that recorder when the pre-notched specimens broke into two pieces (in hours). The longer time to failure was indicative of better crack resistance.

The Microbac report findings are summarized as follows:

“Based on the cumulative body of test results reported herein, one can conclude the following:

1. The white coextruded material (and/or white base material for those samples not manufactured via coextrusion) displays evidence of UV exposure-induced degradation (via outdoor weathering) as evidenced by Map Cracking, which has occurred within approximately ten years of service.
2. The white coextruded material (and/or white base material for those samples not manufactured via coextrusion) displays very poor oxidation resistance as evidenced by very low OIT test results, although some few examples of higher OIT performance are in evidence.
3. The white coextruded material appears to NOT contain any HALS, which would be the typical additive used to stabilize white (non-black) PE materials used in outdoor service applications.
4. The white coextruded material contains varying levels of antioxidants (AO), from poorly-stabilized to well-stabilized.
5. The black pipe sheathing base material displays adequate to good oxidation resistance as evidenced by OIT test results from 19 to 56 minutes.
6. The black pipe sheathing base material displays varying levels of stress crack resistance (SCR) performance, from less well-performing (22-39 hours) to well-performing (>1000 hours).

The cumulative high-level takeaways from this testing program would be:

7. In general the white coextruded (or otherwise manufactured) material is NOT suitably stabilized for use within an outdoor service environment.
8. It is surmised that multiple different white materials were used in the manufacture of the products used within the stay cable protection system.
9. It is surmised that multiple different black materials were used in the manufacture of the products used within the stay cable protection system.
10. Through wall fractures initiating in the compromised white coextruded layer may arrest in the black material, with higher probability of this occurring for those black base materials with well-performing SCR (i.e. >1000 hours).
11. It should be noted that some system components, specifically the molded couplers and reducers, display acceptable field performance (i.e. they do NOT show map cracking and related weathering), although the materials test data contained herein would indicate the presence of oxidative degradation. No explanation is offered to explain this inconsistency.”

The report indicates that the white HDPE material is generally susceptible to oxidation (UV damage). The 2013 KTC inspection revealed that some pairs of connection sleeves (e.g., B3D and B3U) had little or no signs of micro-cracking while most of the others did. The white co-extruded HDPE of the stay pipes, transition pipes and connection sleeve pipes seems more prone to micro-cracking than the all-white HDPE couplers and reducers. The reason for that difference could not be deduced from the Microbac test results. Based upon the Microbac findings, it is likely that even the HDPE components that KTC researchers considered as performing well in 2013 will eventually exhibit micro-cracking.

Insight into the performance of the white co-extruded HDPE material can be gained in reviewing a certificate of performance from the material supplier (22). The supplier subjected samples of the co-extruded piping to an accelerated weathering test (Xenotest 1200) for 10,000 hours. The supplier noted that this was equivalent to 10 years of service. That testing produced “micro-fissures” (e.g., micro-cracks) that were at a maximum of 10 percent of the co-extruded material thickness (2 mm). As of 2013, the Natcher Bridge had been in service for 12 years. The micro-cracks in the co-extruded material exceeded the amount predicted by the supplier. At one scrape test location KTC researchers observed that the micro-cracking had penetrated down to the black base material of a transition pipe (Ref. Figure 84).

KTC researchers did not perform measurements on how deeply of the micro-cracks penetrated into the white co-extruded layers of the piping. The white co-extruded HDPE has become embrittled and is beginning to spall from the surface of some of the piping. The rate of that deterioration has not been determined. In 2013 this was not widespread. Eventually, it is anticipated that the white co-extruded HDPE will dissipate leaving the black base HDPE exposed to UV attack. The Microbac report stated that the percentage of carbon black in the base HDPE was sufficient to give it long term UV resistance. Another concern of KTC researchers is the possibility that the micro-cracking might reflect into the black base material, especially since the HDPE was subject to live stresses and some of the micro-cracks appeared aligned perpendicularly to those stresses. The Microbac report concluded that the black base material taken from the connection sleeves had a range of stress crack performance. That may require investigation in the future. The difference between the supplier’s test results and the HDPE performance at the bridge is that the supplier’s test likely did not reflect all of the environmental factors present in the field (e.g., freezing and thawing). In 2014 the Post-Tensioning Institute considered rigorous UV exposure testing for HDPE pipes than used to qualify the Natcher Bridge material (and the US 62/68 Harsha Bridge at Maysville).

Recognition of the Natcher Bridge micro-cracking relates to the darkening of the stay cables due to coal dust and soil build-up in the micro-cracks. If that had not occurred, the micro-cracks probably would have not been detected for several more years until spalling became more pervasive. For several years, KTC researchers questioned why the US 62/68 Harsha Bridge that was constructed a year before the Natcher Bridge did not show similar stay cable discoloration (noting the KTC had not performed close inspections of the Harsha Bridge stay cables). In 2014, the white HDPE cables on the Harsha Bridge began showing signs of darkening. It is likely that the Harsha Bridge had the same rate of micro-cracking as the Natcher Bridge, but lacked a nearby major source of airborne fines to become trapped and discolor the stay cables.

Eventually, KYTC may consider applying a wrap over the co-extruded cable to prevent further UV damage and accommodate any potential stay pipe cracking that might occur after the on-going cracking problem has been addressed. Prior to the development of the coextrusion process, Tedlar tape was commonly used for wrapping black-pigmented HDPE stay cable piping. That material may be considered for use in wrapping the cables. In 2009, a proprietary cable wrap was applied as a spot repair to a connection sleeve where a piping sample was extracted (B22D). When that repair was inspected in 2013, it was performing well (Figure 105). Another firm markets a similar wrap that acts as ribbing in

breaking up water rivulets to prevent rain/wind vibration. Those materials may be considered if the Cabinet eventually decides to wrap the stay cables.

Results of Various KTC Tasks

KTC employed/attempted miscellaneous tasks as part of the 2012/2013 Phase I field work. Some of those tasks should be expanded either on the deck or tower anchorages or both. SCS and KTC performed remedial work on the stay cables at the deck anchorages during the course of the Phase I work. SCS replaced water-contaminated grease on the anchor heads, strand tails and wedges and replaced damaged gaskets on the protective caps. KTC sealed all of the cracks on the deck anchorage HDPE piping and also sealed the reducer-stay pipe gaps to eliminate the most likely sources of water from entering the voids. KTC also provided several types of repairs including plastic welding of cracks. Follow-on inspections of those repairs can provide insight into future repair options. The bridge maintenance manual prescribed the use of welding to repair damaged HDPE (23). KTC employed single-pass welds in an effort to seal the cracks. A crack repair using welding and another using a putty sealer both failed in a few months. Future repairs using plastic welding would need to be multiple-pass welds after beveling the HDPE cracks. The root cause of the cracking must be identified and addressed before welding can be relied upon to re-join the broken pieces. However, it is the opinion of KTC researchers that plastic weld repairs are not likely to remain intact under the current conditions impacting the bridge cables.

KTC did not repair cracks/breaches in the HDPE piping at the tower anchorages. A temporary repair of those locations should be performed in the near future after the condition of exposed strands at has been determined.

The crack gages KTC installed provide some insight about continuing crack growth in the stay cable piping. The gages can be applied over cracks sealed by taping enabling inspectors to identify subsequent changes in crack openings while preventing water from entering the pipe openings.

KTC researchers sought to identify the condition of the electrofusion welds by performing resistance readings at the weld nipples and attempting to evaluate the welds internally using ultrasonic testing. The resistance readings were performed successfully. KTC has retained those readings and they can be provided in the event that future weld repairs can be affected by re-melting the existing welds. The latter action was hampered by lack of exemplary samples for laboratory calibration of an acceptable ultrasonic test procedure. As past efforts to obtain those samples proved unsuccessful, it is unlikely that the nondestructive testing can be used. Repair of the electrofusion welds may be of limited benefit as many of those are cracked, the heating wires are broken in some instances and show high resistance in others.

The Natcher Bridge grout samples taken by KTC researchers were sufficient to measure the chloride contents, but not thoroughly characterize the material. Grout properties can affect corrosion susceptibility even with low chloride contents (24). If the greased and sheathed strands are intact, the grout properties will probably not impact strand corrosion susceptibility. Grout condition probably is a factor of concern at the anchorages where damaged or otherwise pervious grout may allow moisture in the cables to cause corrosion problems in the anchor head area.

Stay Cable Problem Issues and Priorities for Follow-on Work

The KTC Phase I work has not identified any concerns that would justify re-cabling the bridge. A series of actions focusing on specific concerns and actions to assess their severity or remediate them are presented. Most of this work can be completed over the next few years. The original KTC plan envisioned a five-phase project of which the Phase I work is complete. KTC researchers believe that plan is still viable though the timeframe has expanded due to various factors. Phase II includes evaluation of the tower anchorages and the strands. Phase III entails an in-depth consultant review of the construction work/sequence impacting the cables, a design review of the bridge, reviews of relevant reports and documents, possible instrumentation of the bridge and data analysis, review of the current condition of the stay cables and development of a report that identifies the root causes of stay cable problems, proposing a repair procedure and evaluating options for repair or replacement of the cables. Phase IV would involve a consultant preparing plans to either repair or replace the stay cables at the direction of KYTC. Phase V is the construction phase of the rehabilitation project.

The highest priority task is the assessment of the strands' condition. KTC/KPFF/SCS findings warrant additional work to evaluate the condition of the strands at various locations in the stay cables/anchorages. If the strand sheaths show no signs of distress (e.g., cracking, rust staining, bulging) the strands can be considered intact. Evaluation of strand condition is a safety issue. If corrosion has damaged the wires inside strands, they can fail eventually due to fatigue even if the corrosion process is arrested.

For assessing strand integrity at the deck level anchorages, KTC has identified 11 cables that are candidates for assessing strands inside the HPDE piping. The selection criteria were:

- KTC and SCS detection of water inside the piping/anchorages,
- Cracking condition states 4, 7 and 8,
- Cracks in reducers and couplers with openings > 0.25 inches, and
- The number of anomalous UT returns (KPFF) > 15 percent.

KPFF requested in-depth inspections of stay cables B10D, B15D, C8U, and C11U due to a high number of anomalous UT returns and those were included in the final list of stay cables for strand inspections. Two other stay cables B2U and B12D were included due to the large quantities of water encountered in their grout voids. The 11 stay cables selected for strand inspection at the deck anchorages are: B10D, B12D, B15D, C10D, C20D, B2U, B19U, C8U, C11U, C18U and C23U.

Additionally, the integrity of the strands at each of the tower anchorages needs to be determined after "hands-on" inspections of the anchorage piping. This would include visual inspections of strands exposed by pipe cracking. Inspection of strands enclosed inside the tower HDPE piping will be performed after determining the presence or absence of grout (e.g., grout voids), the presence or absence of water inside those voids determined, and video scoping of the interiors of any grout voids. Also, the strand ends at the towers need to be tested using ultrasound to detect potential distress (i.e. cracks or anomalous/atypical UT returns). Thereafter, strands inside the tower piping can be accessed and evaluated.

The work at the towers and the strand assessments must be completed before performing any remedial tasks on the bridge. The only additional task would be to temporarily repair cracks and gaps in the deck and tower anchorage piping to prevent the entry of water inside the stay cables to provide short-term protection while KYTC is considering/implementing more permanent actions.

An in-depth study is needed to determine the root cause(s) of the on-going HDPE pipe cracking. That study should also provide a detailed plan to halt the HDPE piping cracking, execute repairs to the fractured HDPE pipe components along with any other necessary revisions to the bridge, and provide an inspection procedure to address future concerns about stay cable strand integrity. The latter task would address current performance of Natcher Bridge stay cables not anticipated in previous guidance documents (25, 26). All HDPE piping cracks at the deck and tower anchorages need to be temporarily sealed until they are permanently repaired.

The micro-cracking and subsequent spalling of the white coextruded HDPE piping requires investigation the rate of deterioration. Beyond aesthetics, the micro-cracking may reflect into the black HDPE base material at some locations and cause the pipe to crack away from welds. That possibility requires attention at some point. The ribbing/strakes are becoming embrittled, cracking and detaching from the stay pipes. The impact of their loss on the rain/wind susceptibility of the stay cables needs to be evaluated at some point. Eventually, the HDPE piping may be wrapped to deal with the UV degradation and possibly restore the rain/wind strake function. However, it would be beneficial to wait several years after the HDPE cracking repairs have been made to determine if those are effective.

The condition of neoprene boots at both the deck and tower anchorages requires further study. Some had physical damage (cuts, gouges) or were improperly mounted. The cause of moisture in the boots at the tower anchorages may relate to leakage at the boot seams, loss of material water resistance or water entering the boot from the gap between the transition and guide pipes. Internal inspection of the tower anchorages at the anchor heads may provide insight into the latter possibility. The water-tightness of the deck anchorage boots needs to be evaluated by internal inspections in the space between the transition and guide pipes as well. The implications/consequences of water in the boots has not been assessed. One piece zip-up neoprene sleeves are available to replace boots that are damaged or leaking (Figure 106). The existing neoprene boots can also be painted with a protective coating (e.g., hypalon) to seal them from water and reduce weathering.

The work described above will take several years to complete. Most of the problems encountered on the Natcher Bridge appear to be unique to or at least first identified on this bridge as the result of the Phase I work. Other stay cable bridges have experienced significant strand deterioration that hopefully has not occurred on this bridge. Additional work will be needed to ascertain that fact. Follow-on repairs, both temporary and permanent, will be needed to prevent strand damage that could prove problematic to the long-term structural integrity of the stay cables.

It should be noted that the first cable-stayed bridge built in the continental U.S., the I-310 Hale Boggs Memorial Bridge, at Luling, LA opened in 1983 was the subject of various investigations throughout its service life. A KTC researcher participated in one of those in the late 1980s. In 2007, the

decision was made to re-cable the bridge due to wire corrosion and other issues. That work ran from 2009-2012 and cost \$30.5 million.

4. RECOMMENDATIONS

The following detailed tasks should be performed in the sequence described to address the stay cable problems:

1. Perform tasks on the HDPE piping at all of the deck anchorages including evaluations of the joint repairs/crack-sealing work performed by KTC in 2013, affecting necessary repairs to those locations and the new cracks that have appeared. Tape over white-coextruded HDPE sites where KTC took scrape samples and weld HDPE filler pieces where KTC took test samples in late 2014. It is estimated that this field work will take 2-3 weeks.
2. At 11 stay cables, cut into HDPE piping at the deck anchorages connection sleeves (below grout voids) and inspect the condition of several strands embedded in grout. On four stay cables, cut the stay pipe HDPE and inspect the condition of several strands embedded in grout.
3. Concurrent with Task 2, establish temporary arm's length access to the tower anchorages. Inspect any strands exposed by cracking/gaps in the HDPE piping. Thereafter perform temporary repairs to the damaged piping by wrapping crack openings/gaps with Tedlar tape. Sound the connection sleeves to detect grout voids. Cut access holes – as necessary – in the grout voids and videoscope inside the voids to assess strands for exposure to water. Inside the towers, remove the protective caps and access the anchor heads, wedges and strand tails. Evaluate those for corrosion and slippage. Grind the strand tails flat and perform UT on each wire noting strands with anomalous UT indications. Based on findings of the tower work, cut the HDPE piping – as necessary – to access strands inside the connection sleeves and transition pipes to evaluate their condition. Determine the cause and consequence of the tower voids filling with water. Completion of Tasks 2 and 3 will complete Phase II of the KTC plan to address the stay cable problems.
4. Concurrent with Tasks 2 and 3, engage a consultant familiar with cable-stayed bridges to investigate the initial design and construction of the cables, identify the root cause(s) of the stay cable piping cracking, evaluate the current strand conditions, propose repairs and evaluate the options of repairing or replacing the stay cables. Phase III of the KTC plan will encompass this task.
5. After addressing Task 4, the consultant will prepare plans to either repair the existing cables or to replace them at option of KYTC. This task will be Phase IV of the KTC plan.
6. Let a contract to rehabilitate the Natcher Bridge cables based upon the recommendations of the consultant. This will address Phase V of the KTC plan.

5. REFERENCES

1. Parsons Brinckerhoff, Maintenance Manual for William H Natcher Bridge-Daviess County, February 2005, p. 2-16.

2. VSL: William Natcher Bridge-Owensboro, Kentucky <http://www.vsl.net/Case%20Study/tabid/178/contentid/109/Default.aspx>
3. Op. Cit. 1, pp. 76-96.
4. Glass, G.C. and Ribble, S., Letter of Transmittal and Enclosures from Burgess & Niple to Darrell Dudgeon of the Kentucky Transportation Cabinet dated May 14, 2007, pp. 1-8.
5. Kenaway, M.H., Salaimah, A., Akafuah, N.K. Saito, K., Hopwood, T. and Palle, S., Infrared Thermography-Based Inspection Technique for Void Detection in Bridge Stay Cables, Presentation to the TRB AFF40(1) Subcommittee on Nondestructive Evaluation of Structures, Transportation Research Board Annual Meeting, Washington, DC, January 14, 2013.
6. KTC Proposed Phase I Inspection of Stay Cables on the US 231 Natcher Bridge Near Owensboro, Kentucky Transportation Center, June 2010.
7. US 231 Bridge Inspection – Ultrasonic Testing of Strands/Wires at Cable Anchorages, KPFF Consulting Engineers, Evanston, IL, January 2013.
8. William H. Natcher Bridge, US 231 over the Ohio River – Final Report-Field Investigation at Lower Anchorages, Siva Corrosion Services, SCS Project No. 10053-01, July 2013.
9. Op. Cit. 1, pp. 2-5.
10. Akafuah, N. and Salaimah, A., Evaluation of William H. Natcher Bridge Cables Using Thermal Imaging 0 2013, University of Kentucky College of Engineering, October 17, 2014.
11. Ribble, S., “William H. Natcher Bridge Fracture Critical Inspection Report,” Provided to the Kentucky Transportation Cabinet by Burgess & Niple, June 24, 2013, Appendix A. Stay Cable Connection Deficiencies.
12. Tabtabai, H., “Inspection and Maintenance of Bridge Stay Cable Systems,” NCHRP Synthesis 353, Transportation Research Board, 2005, p. 21.
13. Op. Cit. 11 Appendix A.
14. Email from Jendrzewski, J.P. of IMR Louisville to Hopwood, T. of KTC dated September 24, 2009.
15. “Literature Review of Chloride Threshold Values for Grouted Post-Tensioned Tendons, Federal Highway Administration, Publication No. FHWA-HRT-12-067, 2012.
16. Op. Cit. 1 pp. 4-5.
17. Hamilton, H.R. III, Breen, J.E. and Frank, K.H., “Investigation of Corrosion Protection Systems for Bridge Stay Cables,” University of Texas at Austin, Project 0-1264, November 1995.
18. Stantec Consulting Services Inc., “William Natcher (US 231) Cable Stay Bridge -030B00164N Statewide Fracture Critical Bridge Inspections,” June 19, 2015, pp. 10-14.
19. Verbal communication between Venugopalan, S. of Siva Corrosion Services with Hopwood, T. of KTC, August 2014.
20. Tabatabai, H., Email to Hopwood, October 28, 2010.
21. Information Provided by Crigler, J. at Meeting with KYTC Officials, February 25, 2011.
22. P.E. Specialisten, “Conformity Certification for NOCX-PEHD Pipes, General Report for Coloured HDPE Pipes,” Eschborn, Germany, June 5, 1997, p. 3.
23. Parsons Brinckerhoff, “Maintenance Manual for William H. Natcher Bridge – Daviess County”, February 2005, p. 4-9.
24. Theryo, T.S., Hartt, W.H. and Paczkowski, P., “Guidelines for Sampling, Assessing, and Restoring Defective Grout in Prestressed Concrete Bridge Post-Tensioning Ducts,” FHWA, Publication No. FHWA-HRT-113-028, October 2013.

25. Op. Cit. 23.

26. Burgess & Niple, "William H. Natcher Bridge, KY 231 over Ohio River at Owensboro, Daviess County, KY – Scope of Work for the Fracture Critical Inspection," May 25, 2007.

6. TABLES

Table 1. Dimensionless Defect (Grout Void) Sizing on Deck Anchorage Connection Sleeve Pipe Sections Based Upon Thermal Imaging for Tower B (Op. Cit. 10, p 20).

Upstream		Downstream	
Cable Number	Defect Size	Cable Number	Defect Size
B1U	13%	B1D	40%
B2U	21%	B2D	47%
B3U	24%	B3D	33%
B4U	45%	B4D	31%
B5U	33%	B5D	32%
B6U	24%	B6D	30%
B7U	17%	B7D	21%
B8U	8%	B8D	7%
B9U	14%	B9D	17%
B10U	16%	B10D	17%
B11U	22%	B11D	35%
B12U	12%	B12D	21%
B13U	2%	B13D	26%
B14U	40%	B14D	30%
B15U	21%	B15D	22%
B16U	23%	B16D	24%
B17U	19%	B17D	18%
B18U	23%	B18D	37%
B19U	15%	B19D	32%
B20U	14%	B20D	25%
B21U	15%	B21D	27%
B22U	29%	B22D	25%
B23U	35%	B23D	31%
B24U	40%	B24D	15%

Table 2. Dimensionless Defect (Grout Void) Sizing on Deck Anchorage Connection Sleeve Pipe Sections Based Upon Thermal Imaging for Tower C (Op. Cit. 10, p 20).

Upstream		Downstream	
Cable Number	Defect Size	Cable Number	Defect Size
C1U	27%	C1D	38%
C2U	24%	C2D	30%
C3U	29%	C3D	38%
C4U	38%	C4D	9%
C5U	38%	C5D	10%
C6U	29%	C6D	30%
C7U	20%	C7D	23%
C8U	26%	C8D	29%
C9U	28%	C9D	32%
C10U	18%	C10D	17%
C11U	21%	C11D	21%
C12U	7%	C12D	23%
C13U	9%	C13D	1%
C14U	9%	C14D	9%
C15U	31%	C15D	26%
C16U	9%	C16D	9%
C17U	31%	C17D	12%
C18U	37%	C18D	32%
C19U	34%	C19D	30%
C20U	26%	C20D	44%
C21U	44%	C21D	37%
C22U	38%	C22D	32%
C23U	27%	C23D	13%
C24U	34%	C24D	20%

Table 3 Dimensionless Grout Void Sizes for Upstream and Downstream Tower Anchorage Connection Sleeves in Tower B (Op. Cit. 10, p. 26).

Upstream		Downstream	
Cable Number	Defect Size	Cable Number	Defect Size
B1U		B1D	
B2U		B2D	
B3U		B3D	
B4U	43%	B4D	85%
B5U	47%	B5D	73%
B6U	77%	B6D	20%
B7U	75%	B7D	73%
B8U	60%	B8D	93%
B9U	65%	B9D	67%
B10U	56%	B10D	55%
B11U	60%	B11D	23%
B12U		B12D	
B13U		B13D	
B14U	26%	B14D	35%
B15U	40%	B15D	40%
B16U	35%	B16D	64%
B17U	100%	B17D	10%
B18U	50%	B18D	10%
B19U	30%	B19D	20%
B20U	57%	B20D	43%
B21U	57%	B21D	58%
B22U	45%	B22D	71%
B23U		B23D	
B24U		B24D	

Note: No readings obtained in red cells. Results obscured by shading (blue cells) and solar reflections (yellow cells).

Table 4 Dimensionless Grout Void Sizes for Upstream and Downstream Tower Anchorage Connection Sleeves in Tower C (Op. Cit. 10, p. 27).

Upstream		Downstream	
Cable Number	Defect Size	Cable Number	Defect Size
C1U		C1D	
C2U		C2D	
C3U		C3D	
C4U	10%	C4D	75%
C5U	10%	C5D	75%
C6U	60%	C6D	10%
C7U	88%	C7D	73%
C8U	86%	C8D	97%
C9U	64%	C9D	64%
C10U	65%	C10D	55%
C11U		C11D	23%
C12U		C12D	
C13U		C13D	
C14U	41%	C14D	35%
C15U	48%	C15D	25%
C16U	15%	C16D	34%
C17U	42%	C17D	45%
C18U	85%	C18D	68%
C19U	66%	C19D	15%
C20U	45%	C20D	75%
C21U		C21D	80%
C22U		C22D	73%
C23U		C23D	
C24U		C24D	

Note: No readings obtained in red cells. Results obscured by shading (blue cells) and solar reflections (yellow cells).

Downstream Side (Span 9 Cables 13-24 and Span 8 Cables 1-12)											
Tower B											
Cable	IR4TD Tower Anchorage Void Size as Determined by Thermography	KTC Tower Anchorage Crack Condition States and Burgess & Niple Crack Gap Measurements (inches)		KTC Deck Anchorage Void Measured at 0° (inches)	IR4TD Deck Anchorage Void Size as Determined by Thermography	KTC Deck Anchorage Crack Condition States and Crack Gap Measurements (inches)		KTC Water in Void (Deck Anchorage)	SCS Water in Anchorage (Deck Anchorage)	KPFF UT Indications Typical/Atypical (Deck Anchorage)	
B1D	N/A	8	#	49.25	40%	1	0.240		X	36/4	10%
B2D*	N/A	0	0.000	48.75	47%	1	0.368		X	32/7	18%
B3D	N/A	3	0.125	37.00	33%	1	0.030		X	49/10	17%
B4D	85%	2	0.813	41.25	31%	2	0.150			25/5	17%
B5D	73%	2	0.813	39.25	32%	2,5	0.165, 0.010		X	28/6	18%
B6D	20%	3	0.063	33.25	30%	1	0.243	X	X	29/3	9%
B7D*	73%	3	0.063	22.50	21%	1	0.267	X	X	23/7	23%
B8D	93%	6,2	0.250,0.063	3.00	7%	1	0.075			22/6	21%
B9D	67%	6	0.250	16.00	17%	1	0.295		X	25/1	4%
B10D*	55%	2	0.563	14.00	17%	1	0.213		X	18/6	25%
B11D	23%	2	0.375	38.50	35%	6	HL		X	17/1	6%
B12D	N/A	3	0.125	23.50	21%	1	0.070	X	X	21/4	16%
B13D	N/A	6,2	.063,.063	24.50	26%	1	0.125	X		22/3	12%
B14D	35%	6	0.375	32.50	30%	2	0.090		X	16/2	11%
B15D*	40%	3	0.188	21.25	22%	1	0.172		X	17/7	29%
B16D	64%	2	0.250	18.00	24%	1	0.275		X	20/5	20%
B17D	10%	2,3	HL,0.250	16.75	18%	1	0.165		X	24/3	11%
B18D*	10%	3	HL	7.50	37%	1	0.090	X	X	23/6	21%
B19D	20%	3,2	HL,0.063	31.50	32%	1,6	0.175, 0.030		X	27/5	16%
B20D*	43%	2	0.375	26.00	25%	2,5	0.230, 0.050			26/8	14%
B21D	58%	0	0	30.00	27%	1	0.277		X	28/8	22%
B22D	71%	6,2	0.500,0.063	24.00	25%	1	0.226		X	36/3	8%
B23D*	N/A	3	0.125	34.00	31%	1,6	0.060, 0.030		X	32/6	16%
B24D	N/A	3	0.125	1.75	15%	0	0.000		X	44/7	14%

*	= Crack Monitor installed	N/A	= Cables not imaged
	= Tower Anchorage	#	= Measurement not taken
	= Deck Anchorage	HL	= Hairline Crack (< 0.004)

Table 5. Summary of Stay Cable Conditions for Deck and Tower Anchorages of Tower B Downstream from *KTC* and Various *Consultant* Inspections.

Upstream Side (Span 9 Cables 13-24 and Span 8 Cables 1-12)											
Tower B											
Cable	IR4TD Tower Anchorage Void Size as Determined by Thermography	KTC Tower Anchorage Crack Condition States and Burgess & Niple Crack Gap Measurements (inches)		KTC Deck Anchorage Void Measured at 0° (inches)	IR4TD Deck Anchorage Void Size as Determined by Thermography	KTC Deck Anchorage Crack Condition States and Crack Gap Measurements (inches)		KTC Water in Void (Deck Anchorage)	SCS Water in Anchorage (Deck Anchorage)	KPFF UT Indications Typical/Atypical (Deck Anchorage)	
B1U	N/A	6	0.313	5.25	13%	1	0.060	X	X	33/7	18%
B2U	N/A	3,8	#	40.50	21%	1	0.100	X	X	36/4	10%
B3U	N/A	3,8	#	28.00	24%	1	0.100		X	51/8	14%
B4U	43%	3,8	0.125	50.00	45%	2,6	0.375, 0.080		X	30/0	0%
B5U*	47%	2	0.250	39.75	33%	2	0.223			34/0	0%
B6U	77%	2,5	0.250, 0.375	29.75	24%	2	0.245		X	31/1	3%
B7U	75%	3	0.125	18.25	17%	2,8	0.080		X	26/4	13%
B8U	60%	3	0.250	4.25	8%	1	0.080		X	21/7	25%
B9U*	65%	3	0.125	14.00	14%	2	0.245		X	23/3	12%
B10U	56%	3	0.250	18.00	16%	1	0.275		X	20/4	17%
B11U*	60%	3,5	0.125, 0.375	26.50	22%	2	0.339		X	14/4	22%
B12U	N/A	2,3	0.063, 0.375	7.50	12%	8	0.000		X	22/2	8%
B13U	N/A	5,2,1	0.250, 0.063	0.00	2%	0	0.000		X	20/5	20%
B14U	26%	2,3	0.063, 0.750	38.00	40%	0	0.000		X	16/2	11%
B15U	40%	2,3	0.25, #	21.50	21%	1	0.390		X	24/0	0%
B16U	35%	5,3	0.125, 0.125	26.25	23%	1	0.390		X	23/2	8%
B17U*	100%	3	HL	18.75	19%	1,6	0.246, 0.004		X	25/2	7%
B18U	50%	5,2	0.188, 0.063	46.50	23%	1,6	0.246, 0.004		X	22/7	24%
B19U*	30%	6,2	0.313, 0.125	15.50	15%	2,6	0.332, .0125	X	X	30/2	6%
B20U	57%	0	#	11.75	14%	1,6	0.481, 0.217		X	31/3	9%
B21U	57%	0	0.000	11.75	15%	1,6,7	.220, .218,		X	31/5	14%
B22U	45%	2,5	0.375, 0.063	38.25	29%	1,5	0.224, 0.291		X	35/4	10%
B23U*	N/A	0	0.000	39.25	35%	1,6	0.300, 0.128		X	32/6	16%
B24U	N/A	2	0.125	52.00	40%	1	0.255		X	43/8	16%

*	= Crack Monitor installed	N/A	= Cables not imaged
	= Tower Anchorage	#	= Measurement not taken
	= Deck Anchorage	HL	= Hairline Crack (< 0.004)

Table6. Summary of Stay Cable Conditions for Deck and Tower Anchorages of Tower B Downstream from *KTC* and Various *Consultant* Inspections.

Downstream Side (Span 9 Cables 13-24 and Span 10 Cables 1-12)											
Tower C											
Cable	IR4TD Tower Anchorage Void Size as Determined by Thermography	KTC Tower Anchorage Crack Condition States and Burgess & Niple Crack Gap Measurements (inches)		KTC Deck Anchorage Void Measured at 0° (inches)	IR4TD Deck Anchorage Void Size as Determined by Thermography	KTC Deck Anchorage Crack Condition States and KTC Crack Gap Measurements (inches)		KTC Water in Void (Deck Anchorage)	SCS Water in Anchorage (Deck Anchorage)	KPFF UT Indications Typical/Atypical (Deck Anchorage)	
C1D	N/A	8	0.25	38.0	38%	1,8	0.229		X	31/9	23%
C2D	N/A	3	0.125	31.5	30%	1	0.293		X	30/9	23%
C3D*	N/A	3	0.063	38.5	38%	1	0.143		X	49/10	17%
C4D	75%	2	0.313	8.5	9%	1,5	0.100, 0.121		X	24/6	20%
C5D	75%	2	0.438	38.5	10%	1,5	0.080, 0.060		X	29/5	15%
C6D	10%	1	0.250	30.5	30%	1	0.202		X	28/4	13%
C7D	73%	2	0.188	22.0	23%	1	0.215		X	29/1	3%
C8D	97%	2	0.125	35.0	29%	1,6	0.211, 0.020		X	24/4	14%
C9D	64%	2,3	0.063, 0.250	34.0	32%	1	0.151	X	X	23/3	12%
C10D*	55%	2	0.375	16.0	17%	1,6	0.144, 0.020	X	X	23/2	8%
C11D	23%	2	0.125	21.8	21%	2	0.095		X	18/0	0%
C12D	N/A	2,3	0.063, 0.125	14.8	23%	1	0.120	X	X	23/2	8%
C13D	N/A	6,2,3	0.063, 0.125, #	2.0	1%	1	0.040		X	23/2	8%
C14D	35%	2	0.125	4.0	9%	0	0.000		X	16/2	11%
C15D*	25%	2	0.250	28.5	26%	1	0.050		X	22/2	8%
C16D*	34%	3	0.250	6.0	9%	1	0.030		X	22/3	12%
C17D	45%	2	0.250	4.0	12%	1	0.004		X	24/3	11%
C18D	68%	2	0.250	32.0	32%	1	0.080		X	25/4	14%
C19D	15%	2	0.750	30.0	30%	4	#		X	26/6	19%
C20D	75%	6,3	1.75, #	59.0	44%	4	#	X	X	31/3	9%
C21D	80%	3	1.750	43.5	37%	1,6	0.090, 0.061		X	30/6	17%
C22D*	73%	5	0.375	37.8	32%	1	0.060		X	30/9	23%
C23D	N/A	5	0.500	7.0	13%	1	0.050			32/6	16%
C24D	N/A	8	0.250	22.5	20%	1	0.216		X	43/8	16%

*	= Crack Monitor installed	N/A	= Cables not imaged
	= Tower Anchorage	#	= Measurement not taken
	= Deck Anchorage	HL	= Hairline Crack (< 0.004)

Table 7. Summary of Stay Cable Conditions for Deck and Tower Anchorages of Tower C Downstream from *KTC* and Various *Consultant* Inspections.

Upstream Side (Northbound Side)											
Tower C											
Cable	IR4TD Tower Anchorage Void Size as Determined by Thermography	KTC Tower Anchorage Crack Condition States and Burgess & Niple Crack Gap Measurements (inches)		KTC Deck Anchorage Void Measured at 0° (inches)	IR4TD Deck Anchorage Void Size as Determined by Thermography	KTC Deck Anchorage Crack Condition States and Crack Gap Measurements (inches)		KTC Water in Void (Deck Anchorage)	SCS Water in Anchorage (Deck Anchorage)	KPFF UT Indications Typical/Atypical (Deck Anchorage)	
C1U	N/A	5	0.250	55.5	27%	1	0.294		X	33/7	18%
C2U	N/A	5,3	.25,.25	31.5	24%	1,6	0.218, 0.392		X	32/7	18%
C3U	N/A	2	0.188	42.0	29%	1	0.170	X	X	54/5	8%
C4U	10%	2	0.375	51.5	38%	4	#	X	X	25/5	17%
C5U*	10%	2	0.500	46.8	38%	2	0.280		X	28/6	18%
C6U*	60%	6,2	0.375, 0.063	32.8	29%	2,6	0.302, 0.273		X	28/4	13%
C7U*	88%	2	0.500	23.0	20%	1	0.289		X	29/1	3%
C8U	86%	2	0.375	32.5	26%	1	0.234		X	18/10	36%
C9U	64%	2,5	0.125, #	31.8	28%	1,6	0.244, 0.050		X	20/6	23%
C10U	65%	3,2	HL, 0.188	19.0	18%	1	0.208		X	21/3	13%
C11U	N/A	2	0.375	26.8	21%	2,5	0.260, 0.067		X	13/5	28%
C12U	N/A	2,3	0.125, #	22.3	7%	1	0.179	X	X	23/2	8%
C13U	N/A	2,3	0.063, #	26.8	9%	1	0.130	X	X	24/1	4%
C14U	41%	2	0.063	4.0	9%	6	0.070		X	14/4	22%
C15U	48%	6,3	0.063, 0.063	28.3	31%	1	0.166		X	21/3	13%
C16U	15%	2	0.125	4.5	9%	1	0.080		X	20/5	20%
C17U	42%	2	0.125	27.8	31%	1	0.274	X	X	21/6	22%
C18U*	85%	3	0.063	33.5	37%	1	0.362	X	X	24/5	17%
C19U	66%	5,2	0.250, 0.125	36.5	34%	2,6	0.310, 0.375		X	30/2	6%
C20U	45%	5,2	N/A	25.8	26%	2,5	0.310, 0.375	X	X	27/7	21%
C21U*	N/A	2,3	.125, 0.1875	47.3	44%	1,6	0.388, 0.208		X	33/3	8%
C22U	N/A	6	#	40.0	38%	1	0.222		X	35/4	10%
C23U	N/A	6,2	0.250, #	42.0	27%	1,6	0.294, 0.210	X	X	33/5	13%
C24U	N/A	2,3	0.125, #	35.8	34%	1	0.240		X	50/1	2%

*	= Crack Monitor installed	N/A	= Cables not imaged
	= Tower Anchorage	#	= Measurement not taken
	= Deck Anchorage	HL	= Hairline Crack (< 0.004)

Table 8. Summary of Stay Cable Conditions for Deck and Tower Anchorages of Tower C Upstream from *KTC* and Various *Consultant* Inspections.

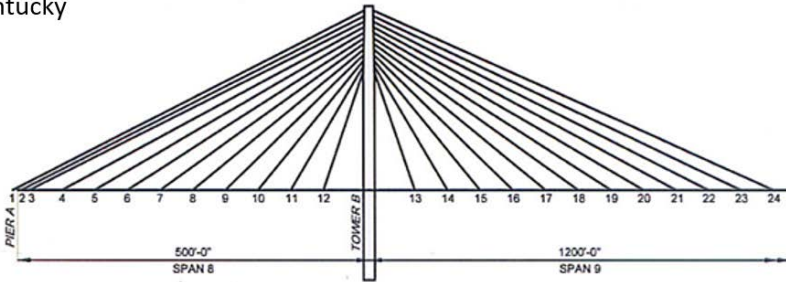
7. FIGURES



Figure 1. US 231 William H. Natcher Bridge over the Ohio River near Owensboro, KY and Rockport, IN.

Cable Layout

← Kentucky



Indiana →

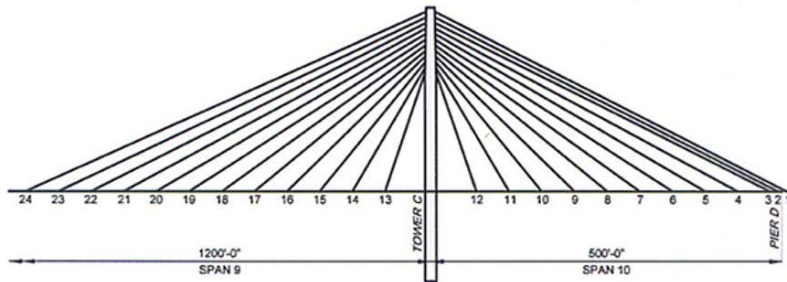


Figure 2. Cable configuration for the Natcher Bridge (Symmetrical for Upstream and Downstream).

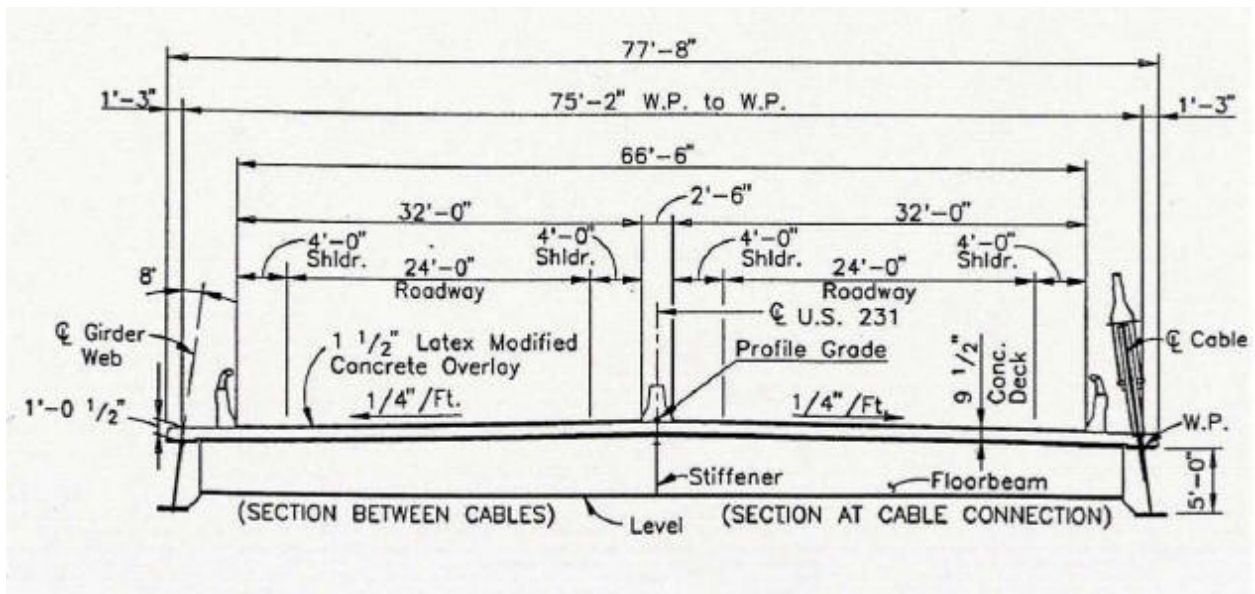


Figure 3. Cross-section of Natcher Bridge Deck on Main and Side Suspended Spans.



Figure 4. Deck Anchorages.



Figure 5. Tower Anchorage.

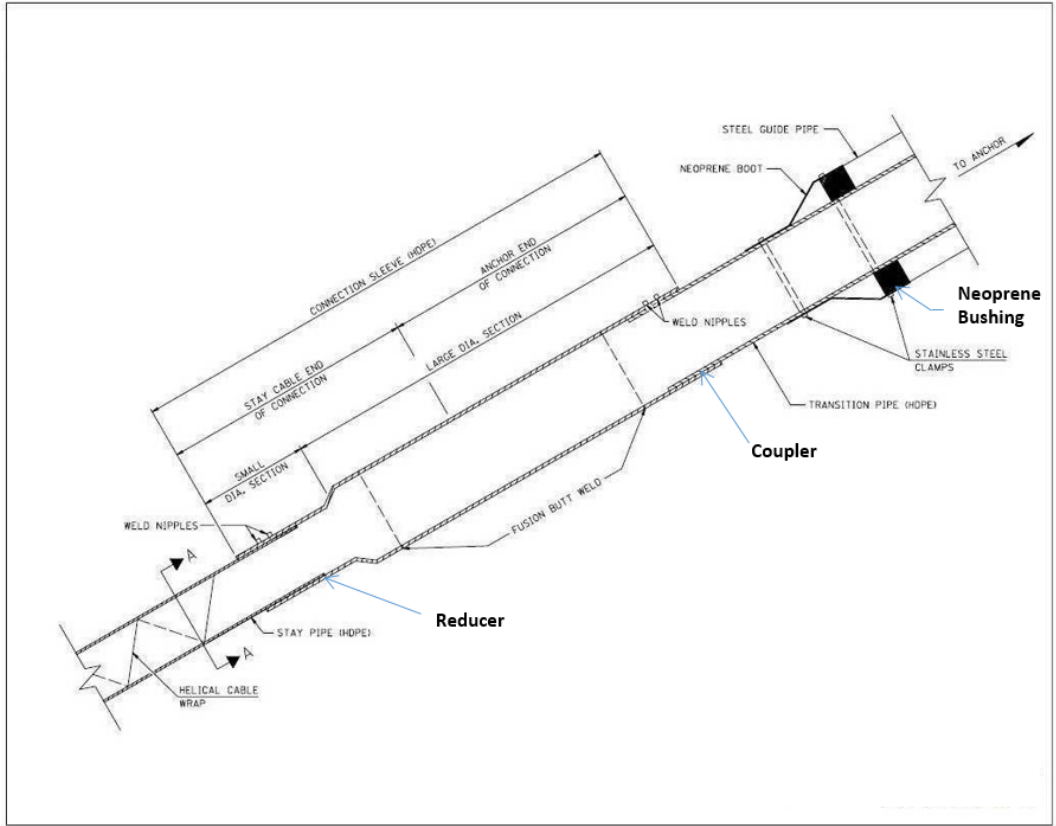


Figure 6. Tower Anchorage and HDPE Piping Terminology.

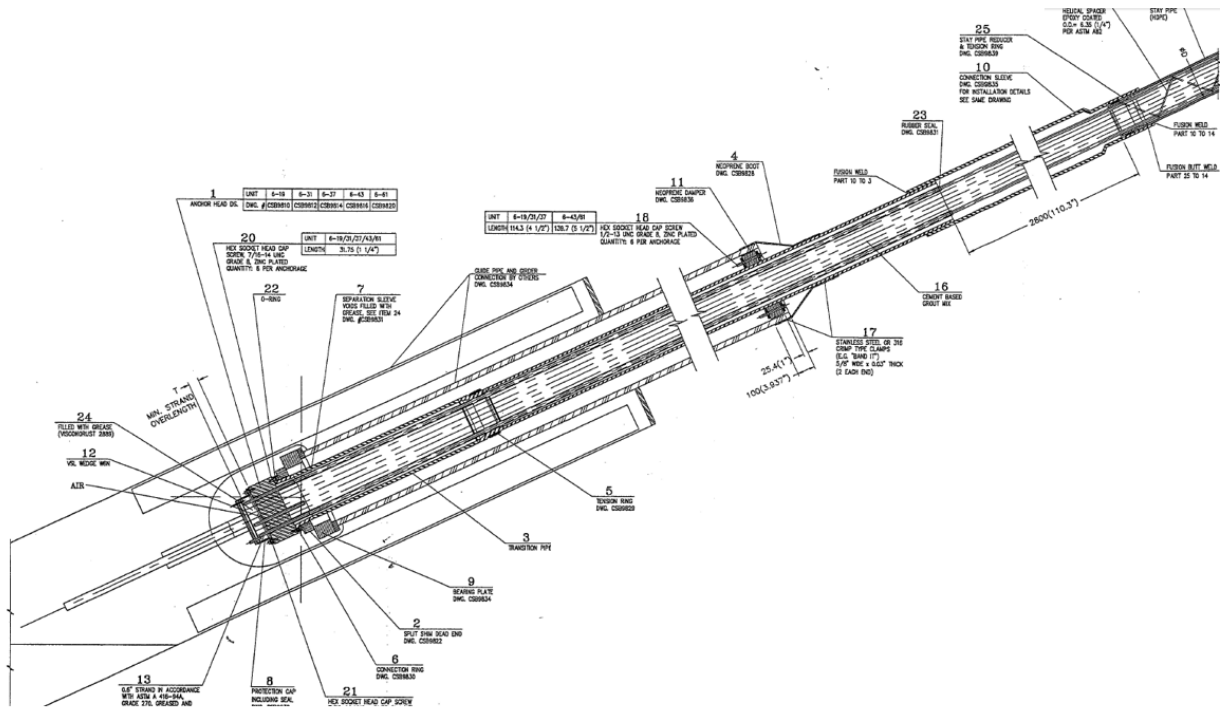


Figure 7. Deck Anchorage Sectional View Showing Key Components (VSL).

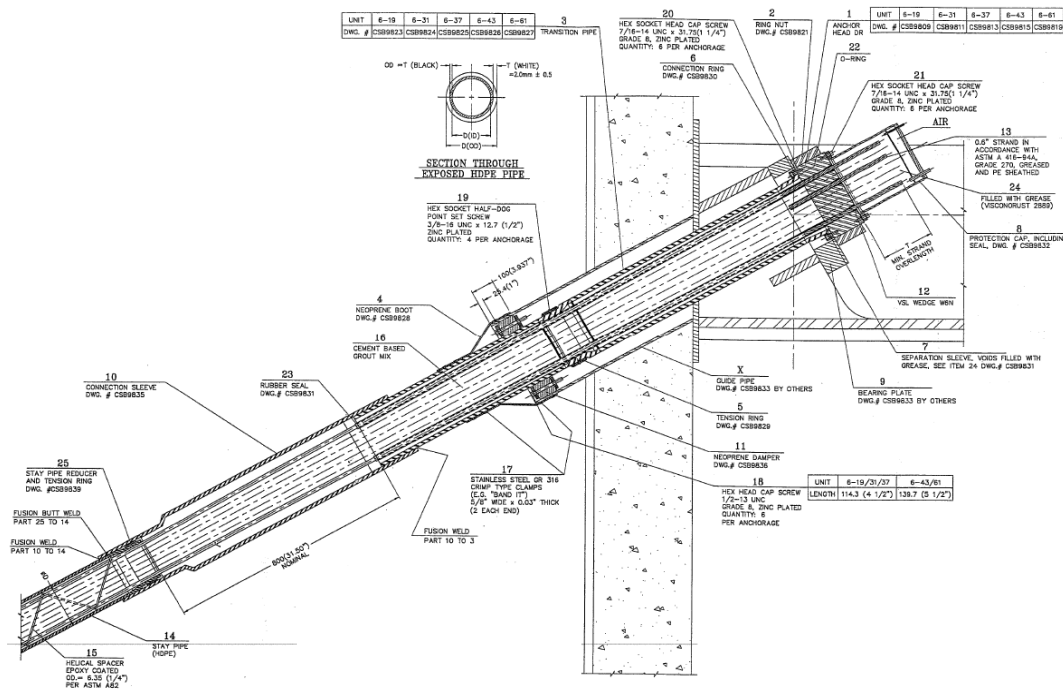


Figure 8. Tower Anchorage Sectional View Showing Key Components (VSL).



Figure 9. Protective Cap on Deck Anchorage during Removal.



Figure 10. Deck Anchorage Showing Heavy Grease Coating on Strands/Wedges/Anchor Head. Note Water inside Anchorage Piping being Collected



Figure 11. Helically Wound Ribbing on Stay Pipes.

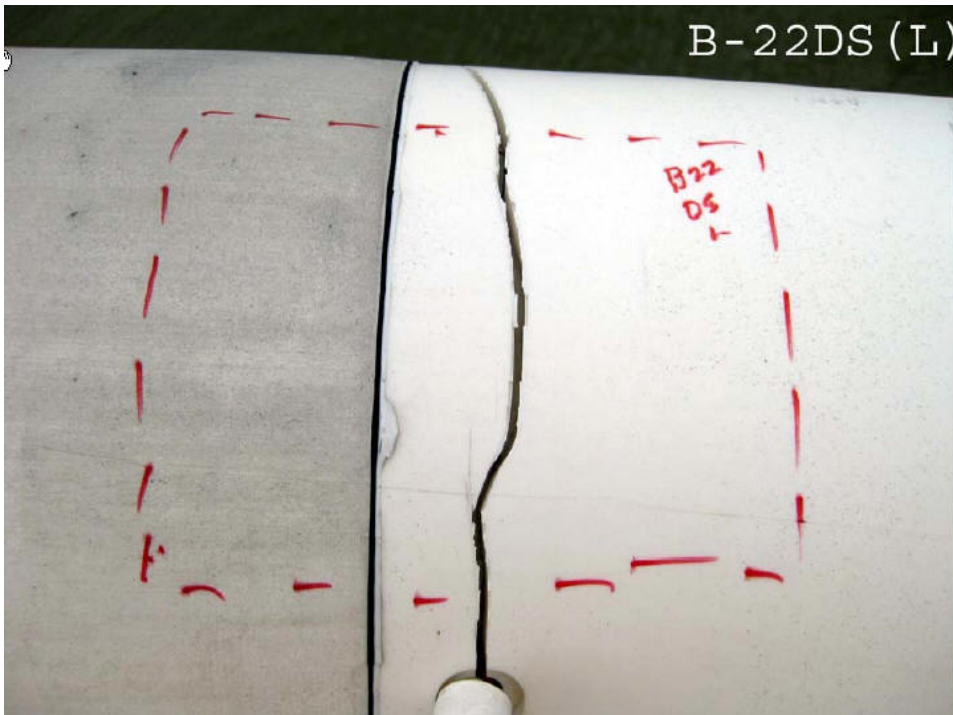


Figure 12. Crack in Connection Sleeve Coupler at Cable B22D. Note Inked Cutting Outline.

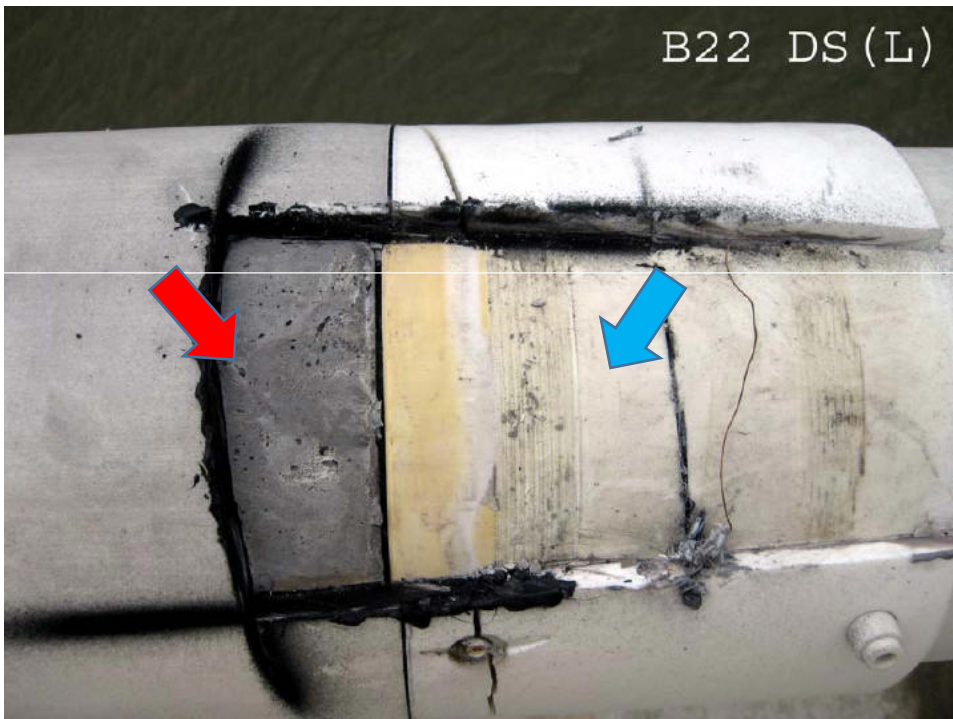


Figure 13. Connection Sleeve and Coupler after Coupon Extraction. Note Grout (Red Arrow) and the Transition Pipe (Blue Arrow).



Figure 14. Extracted Coupon (Inner View). Note Fracture Face (Red Arrow) and Lack of Fusion Area in Electrofusion Weld (Blue Arrow).



Lab 9-23-09 007 [B22 DS(L)]



Lab 9-23-09 012 [B22 DS(L)]

Figure 15. Fatigue Fracture Surfaces. Note Concentric Beach Marks in Top View.



Figure 16. Locating Voids in Deck Anchorage Piping Using Sounding (October 2010).



Figure 17. Locating Voids in Deck Anchorage Piping Using the Time-of-Flight Method (October 2010).



Figure 18. UK IR4TD Personnel Taking IR Pictures of the Deck Anchorage Piping (October 2010).



Figure 19. KTC Personnel Using GPR to Locate Voids in Deck Anchorage Piping (October 2010).



Figure 20. Grout Void Indication on GPR Monitor Screen.

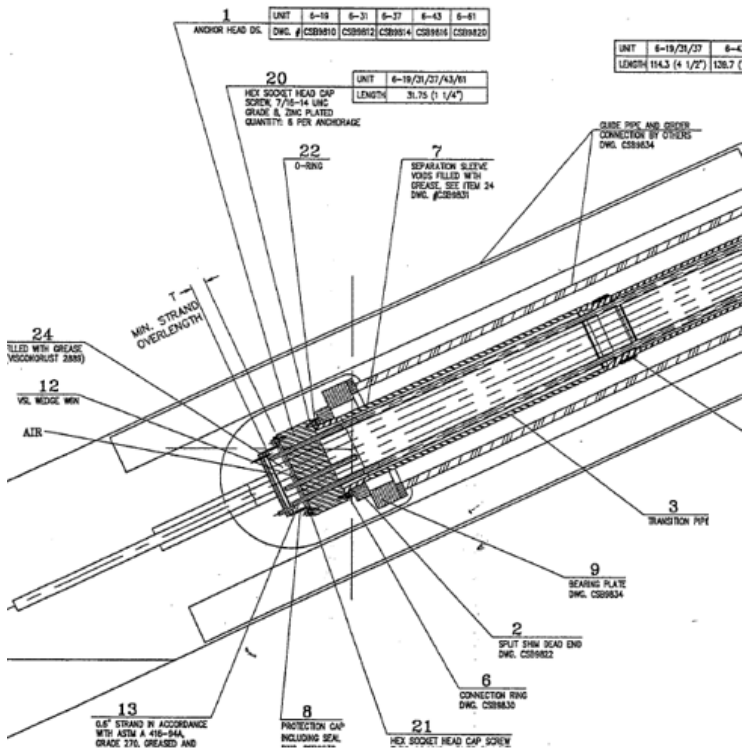


Figure 21. Deck Anchorage Sectional View Showing Strand Wedge Anchor.



Figure 22. Detecting Grout Voids in Connection Sleeves by GPR using a GSSI Palm Antenna.

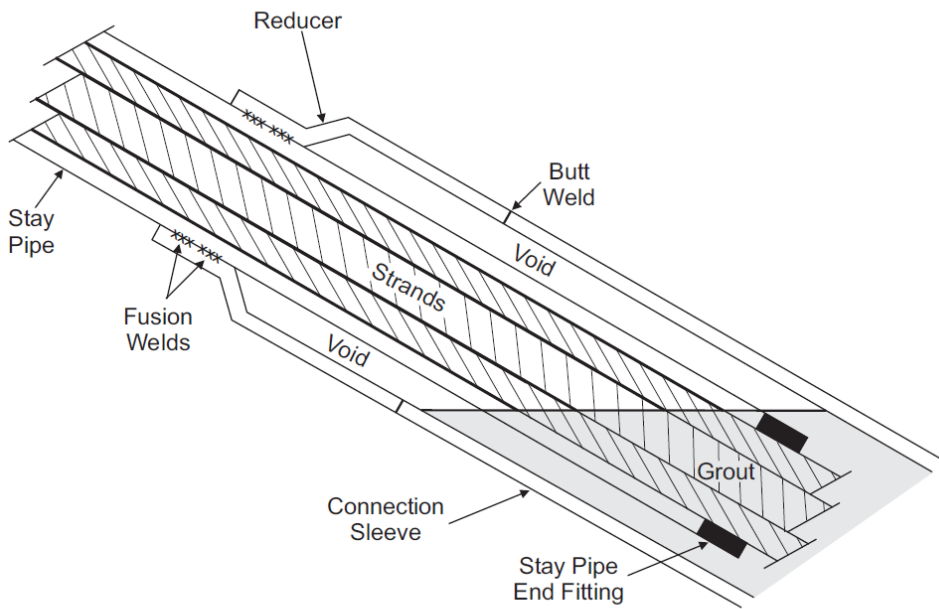


Figure 23. Sectional View of Grout Void Disposition in Deck Anchorage Connection Sleeves.



Figure 24. Measuring Grout Voids Based upon GPR and Sounding Tests.



Figure 25. Use of a Man Lift to Take Thermal Images of the Stay Cable Piping at Various Heights above Deck Level (Op. Cit. 10, p. 11).



Figure 26. Camera Operator Taking Thermal Images of the Stay Cables from a Man Lift.



Figure 27. Camera Operator Taking Thermal Images of Anchorages at the Tower Decks.

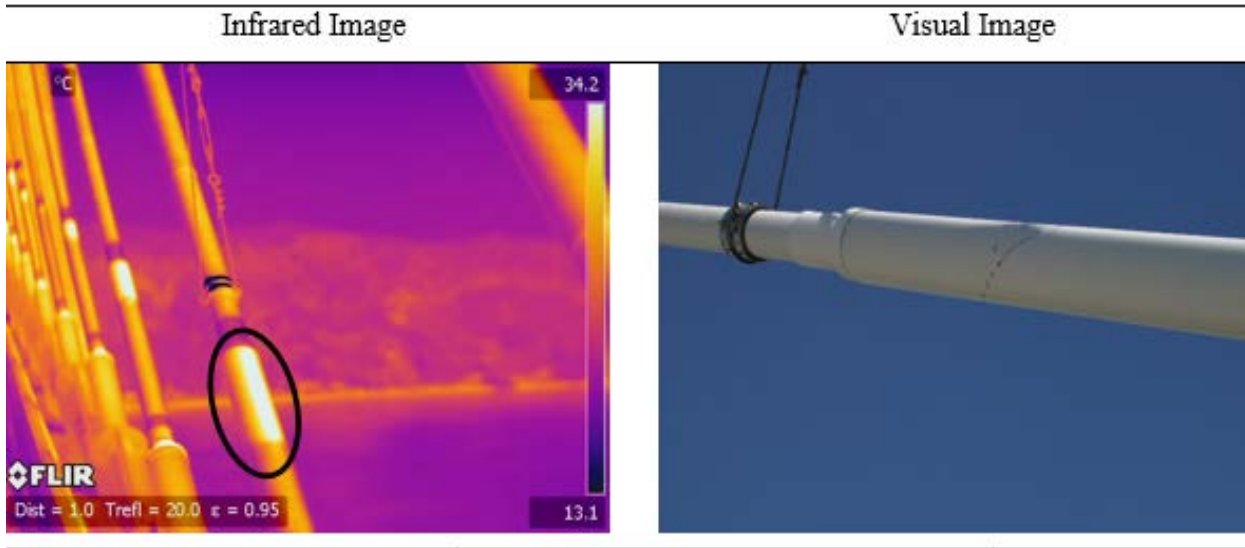


Figure 28. Images of Deck Anchorage Connection Sleeve of Cable B5U Infrared (Thermal) Image (a) Showing Void under Connection Sleeve Piping Compared to (b) GPR Detected Defect Shown in Visual Image (Op. Cit. 10, p. 17).

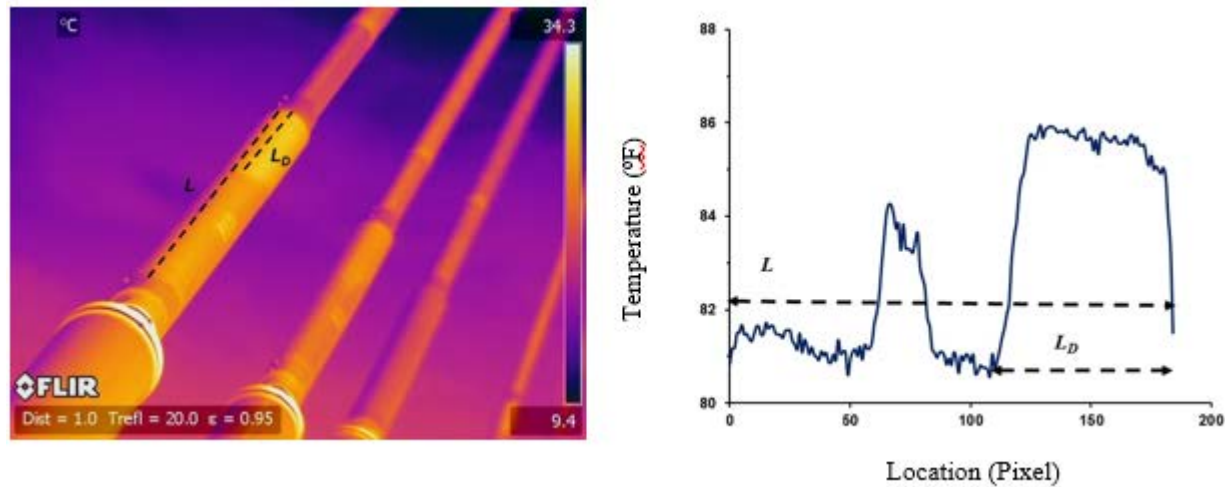


Figure 29. Example of Defect Analysis for the Deck Anchorage Connection Sleeve of Cable B1D. Image Taken a Deck Level Position 0 (Op. Cit. 10, p. 13).

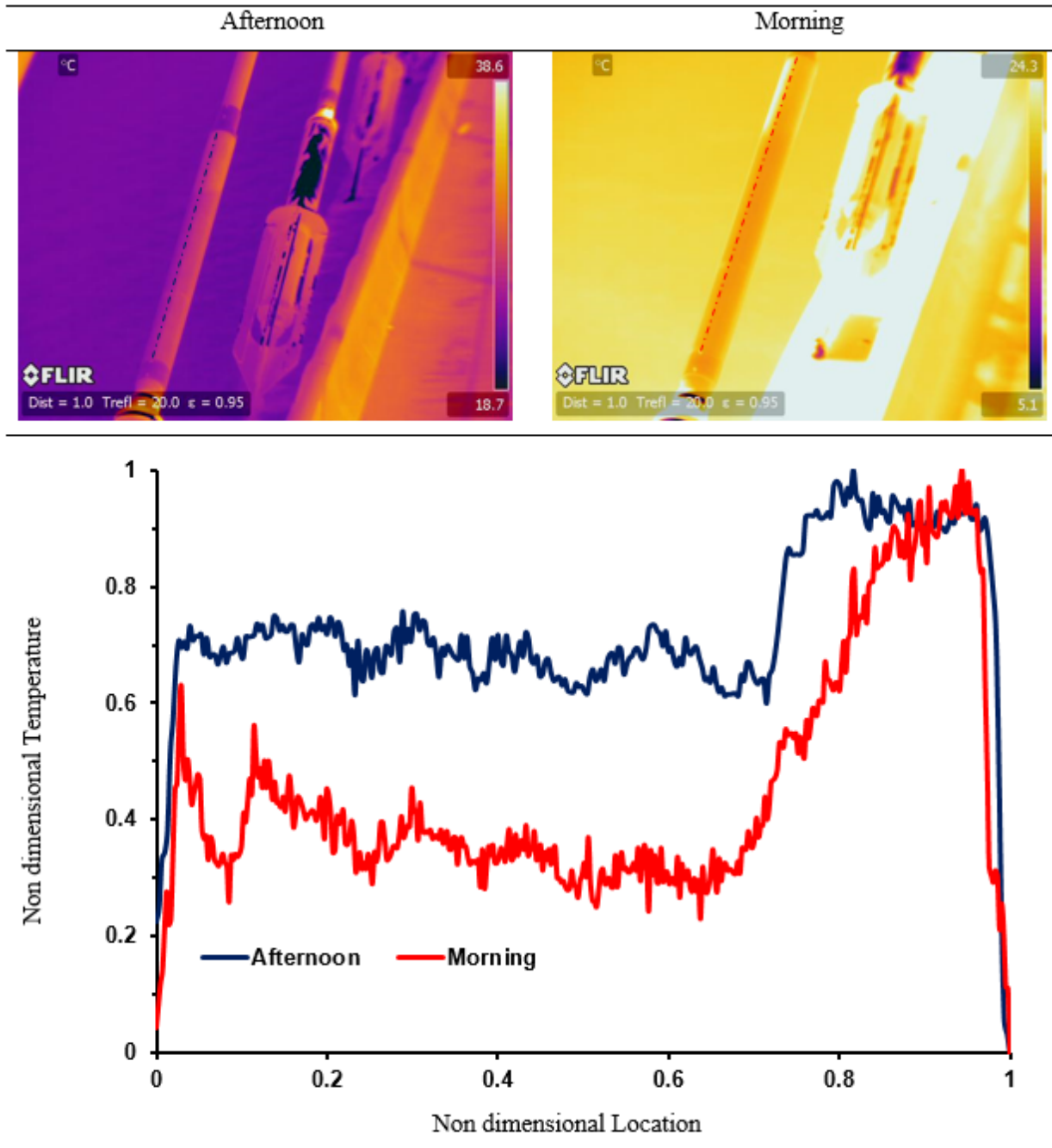


Figure 30. Infrared Images of Deck Anchorage at C6U. Afternoon Imaging was Performed at 4:50 pm CDST (Top Left) While the Morning Imaging was done at 10:50 am (Top Right). Non-dimensional Temperature of the Dashed Lines Show a Distinction between the Void and Grout-Filled Areas inside the Connection Sleeve Pipe in the Both Morning and Afternoon Sessions (Op. Cit. 10, p. 18).



Figure 31. Infrared Image of the Tower Anchorage Connection Sleeve Pipe Section for Cable B3D and Thermal Profile for the Dashed Line Shown in the Infrared Image (Op. Cit. 10, p. 24).

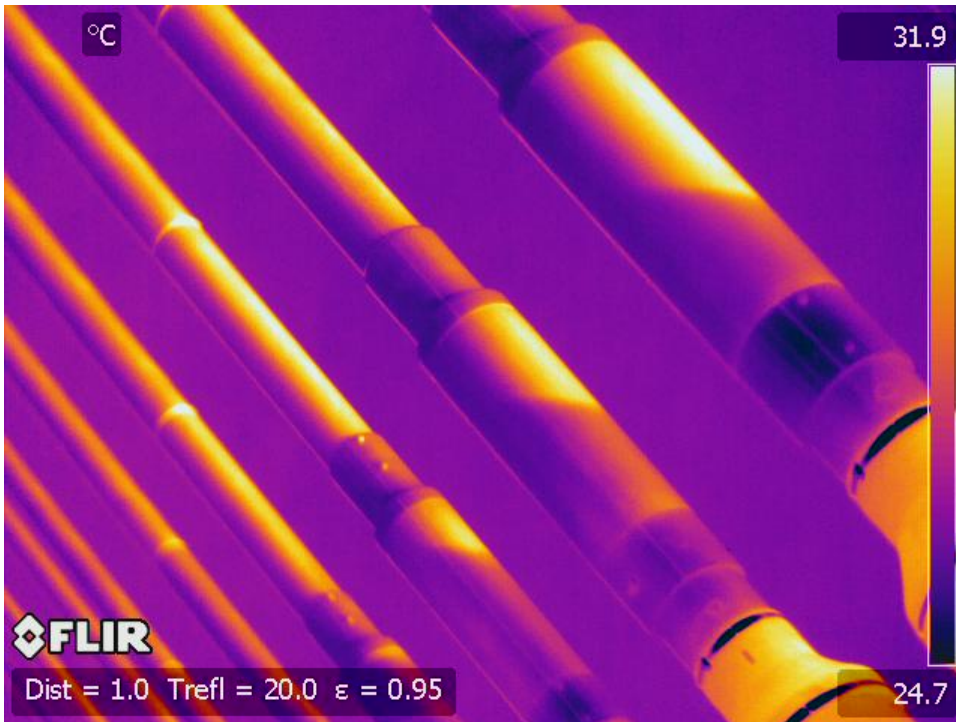


Figure 32. Thermal Image Taken at Tower B of Cables B20D-B22D Showing the Effect of Solar Reflectance in Inhibiting Detection of Grout Voids (Op. Cit. 10, p. 88).

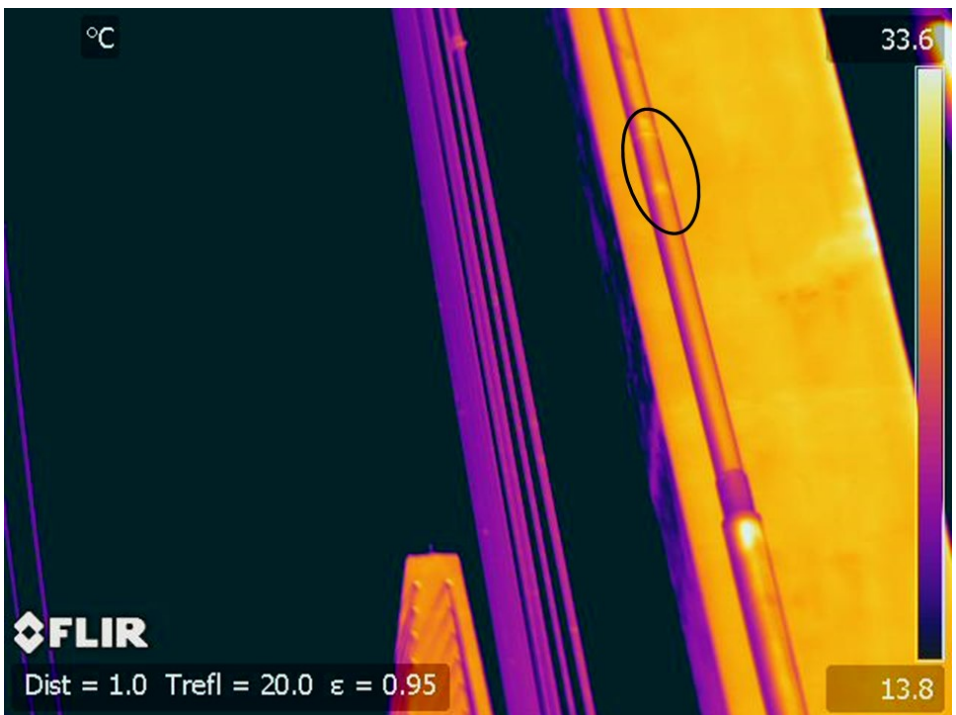


Figure 33. Thermal Image of Stay Pipe at Cable B12U Showing Possible Void (Op. Cit. 10, p. 28).

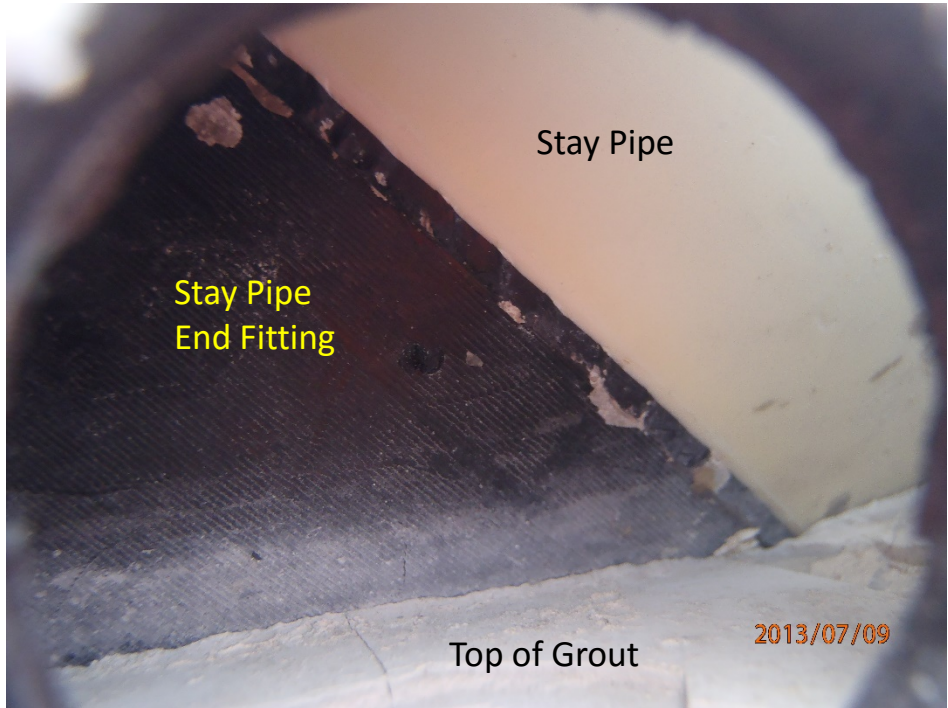


Figure 34. View from Hole Cut in Connection Sleeve Pipe. Grout Void Area Showing Stay Pipe End Fitting Embedded in Top of Grout.



Figure 35. KTC Technician Operating the Articulating Camera of Videoscope inside a Grout Void in a Connection Sleeve.



Figure 36. Grout Interface between the Inner Wall of the Connection Sleeve Pipe and the Stay Pipe.



Figure 37. Picture Taken by Videoscope inside a Grout Void Looking Upward Where the Stay Pipe Passes Through the Reducer.

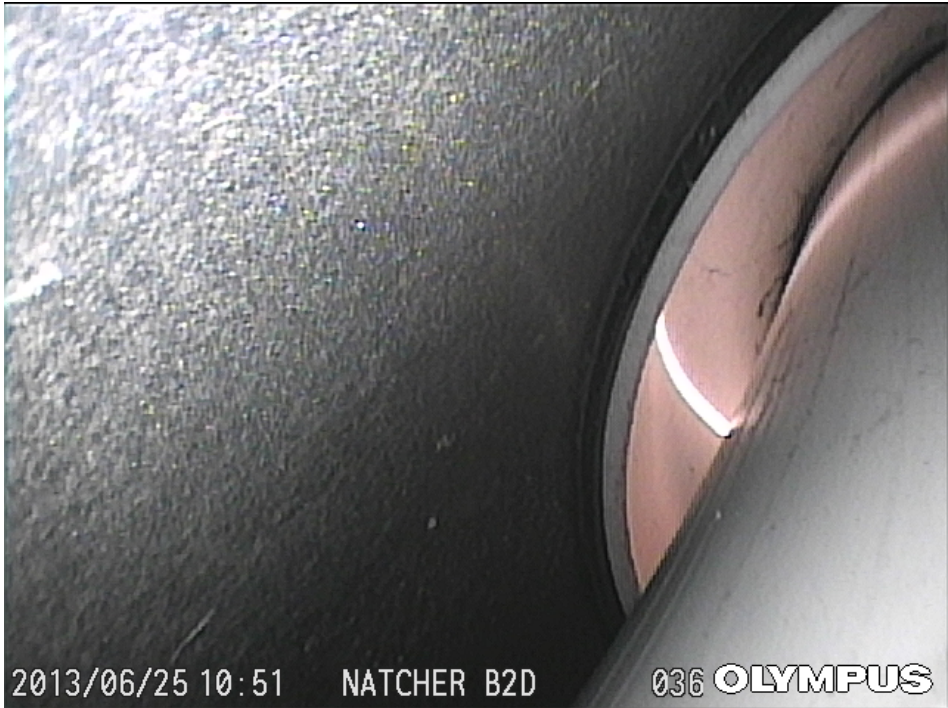


Figure 38. Picture Taken by Videoscope Showing a Reducer Crack inside a Grout Void.

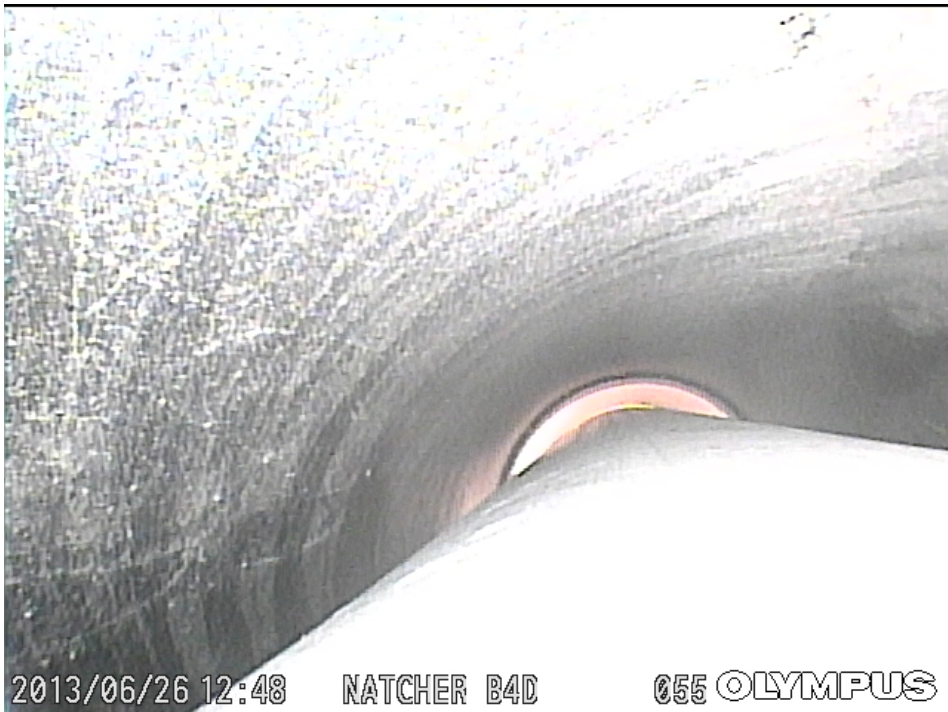


Figure 39. Picture of a Grout Void Taken Upward with Daylight Visible Through a Crack in the Reducer. Note the Tide Mark Rings on the Inner Wall of the Connection Sleeve Indicating Past Presence of Water in the Cable.



Figure 40. Picture inside a Grout Void Showing the Presence of Water in a Grout Void.



Figure 41. Water Leaking from a Grout Void in the Connection Sleeve Pipe at Stay Cable B12D.



Figure 42. Circumferential Crack in Reducer above Grout Void in Stay Cable B12D.



Figure 43. Water Gushing from Void in Cable B2U after Tape Covering Hole was Removed.



Figure 44. Arm's Length Crack Inspection of the HDPE Piping at the Deck Anchorages.



Figure 45. Crack Growth from Coupler Butt Weld into Connection Sleeve Pipe Section (Looking Downward).



Figure 46. Complex Condition State 6 Cracking – A Single Crack at the Top of the Pipe Which Grew Radially in both the Clockwise and Counter-clockwise Direction to the Bottom of a Coupler (Looking Upward).



Figure 47. Simple Condition State 3 Cracking Perpendicular to Axis of Piping.



Figure 48. Bottom Side of HDPE Reducer Where Cracks Growing Clockwise and Counter-Clockwise from the Top Side Merge.

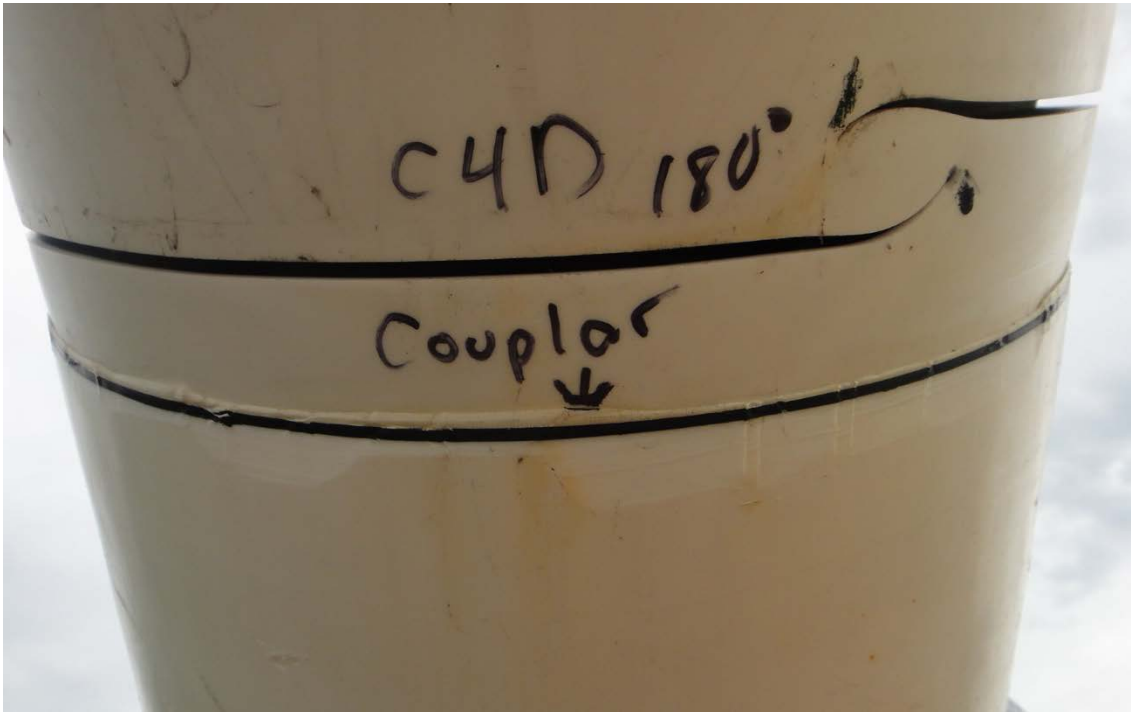


Figure 49. Bottom Side of HDPE Reducer Where Cracks Growing Clockwise and Counter-Clockwise from the Top Side Terminate.



Figure 50. (a) Measuring Large Crack Opening with a Vernier Caliper; (b) Measuring Small Crack Opening with a Comparator Gage.

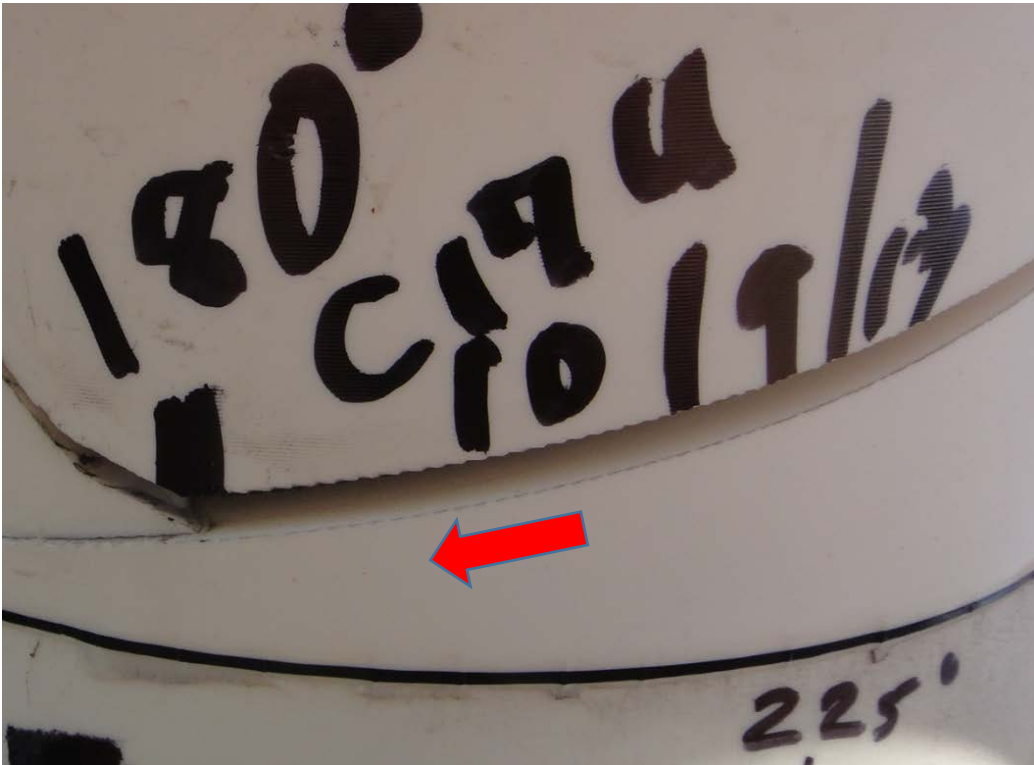


Figure 51. Sawtooth Edge of Fatigue Crack with Arrow Pointing in the Direction of Propagation.

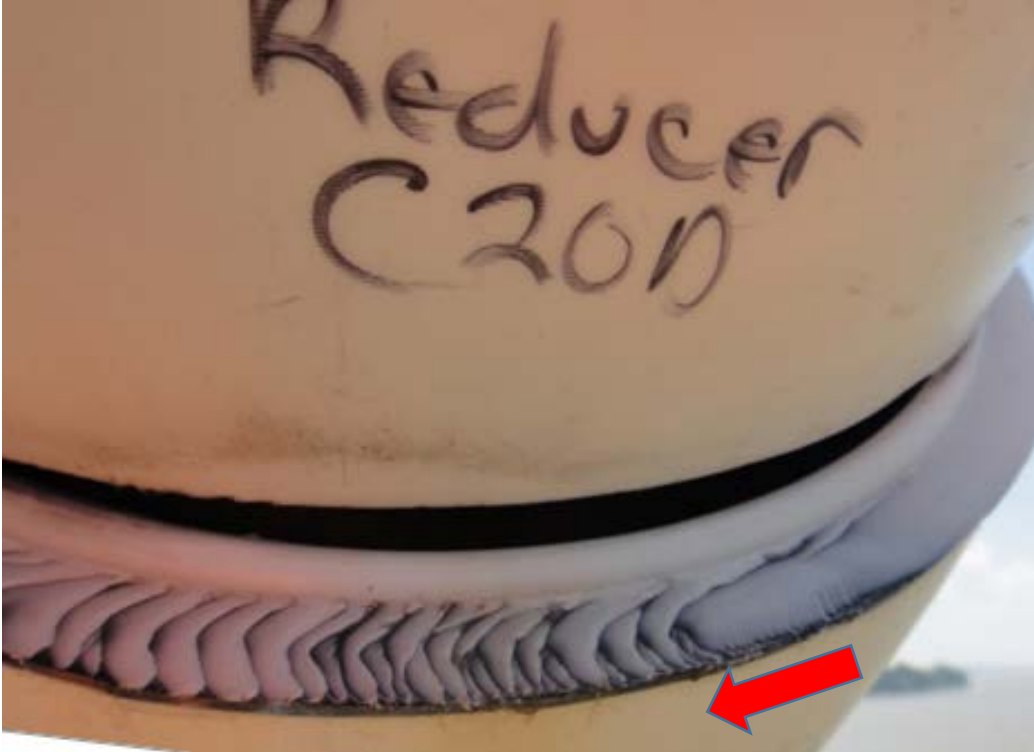


Figure 52. Fracture Surface Marks (Steps) Indicating Clockwise (Right- to- Left) Crack Growth Typical of Low-Cycle Fatigue Crack Propagation at Reducer-to-Connection Sleeve Pipe Butt Weld.

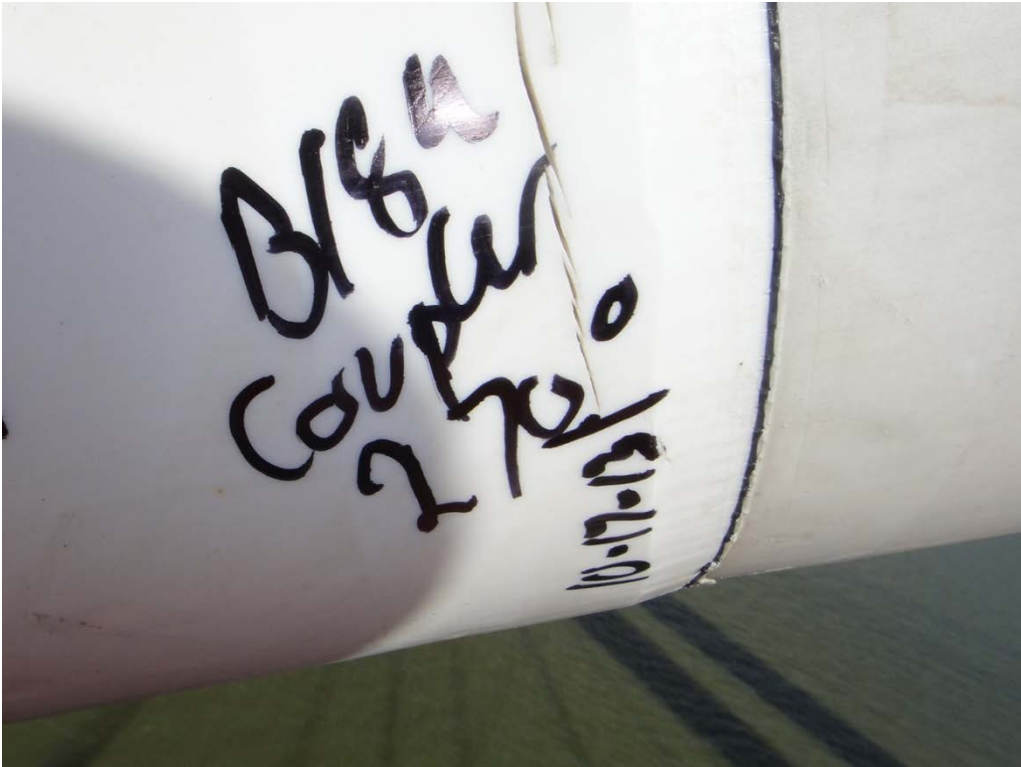


Figure 53. Individual Crack Sites That Merge to Create Stepped Crack Faces.



Figure 54. Large Crack Opening without Signs of Significant HDPE Deformation.



Figure 55. Crack Growth in Reducer Indicated by Marks (5/13 – Consultant and 7/13 – KTC).



Figure 56. Crack Growth in Connection Sleeve Pipe Indicated by Marks (5/13 – Consultant and 10/13 – KTC).



Figure 57. Coupler Crack at Tower Anchorage on Cable B1U.



Figure 58. Cables B4D and B5D at Tower Anchorage Showing Gaps Created by Butt Weld Fracture between Reducers and Pipe Sections of Connection Sleeves.



Figure 59. Slippage of Coupler off Transition Pipe at Tower Anchorage B4D due to Shear Failure of Electrofusion Welds.



Figure 60. Longitudinal Cracking of Reducer at Lag Bolt Retrofit Added During Construction.



Figure 61. Typical 40 ft. Stay Pipe Segment with Helical Ribbing Intact.



Figure 62. Severe Disbonding of Ribbing from Stay Pipe Segment (2009).



Figure 63. Cracking of Ribbing Still Bonded to Stay Pipe (2013).



Figure 64. Ribbing Detaching from Stay Pipe near Deck Anchorage

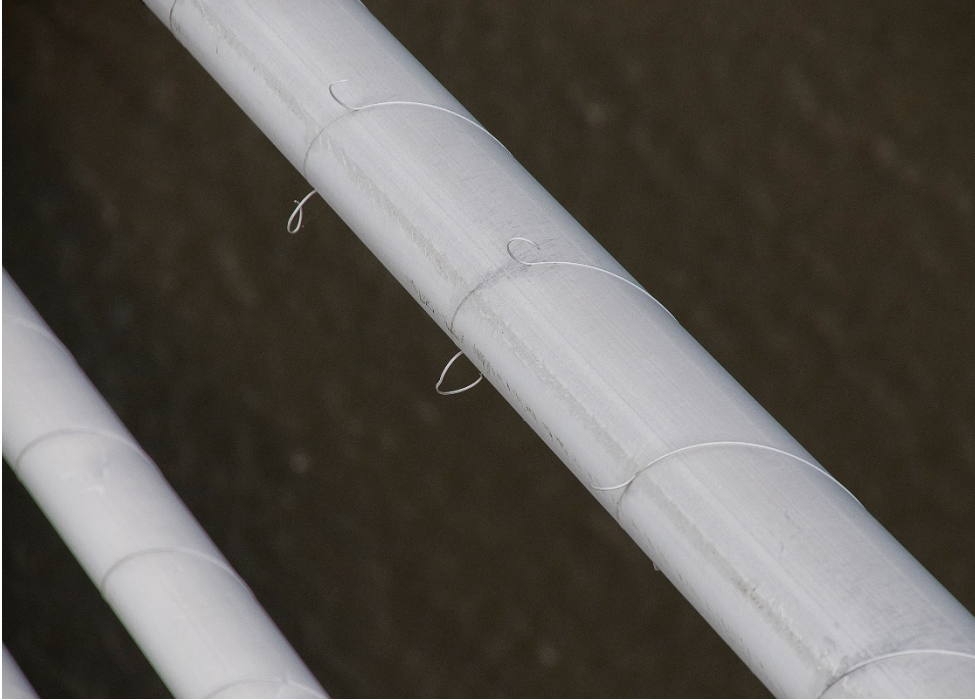


Figure 65. Ribbing Detaching from Stay Pipe near Tower Anchorage (2013).



Figure 66. Grout Plug with Minor Cracking.



Figure 67. Grout Plug in Transition Pipe Having Extensive Cracking.



Figure 68. Missing Grout Plug.



Figure 69. Neoprene Boot at Deck Anchorage with Superficial Damage.



Figure 70. Neoprene Boots at the Upstream Side (Span 9) of Tower B Showing Missing Boot Retaining Bands.



Figure 71. Detached Neoprene Boot at Tower Anchorage of Stay Cable B13U.



Figure 72. Barges Off-Loading Coal at the Neighboring Rockport Power Station in Indiana.



Figure 73. Contrasting Appearance of the Stay Cable HDPE Piping between 2009 and 2013.

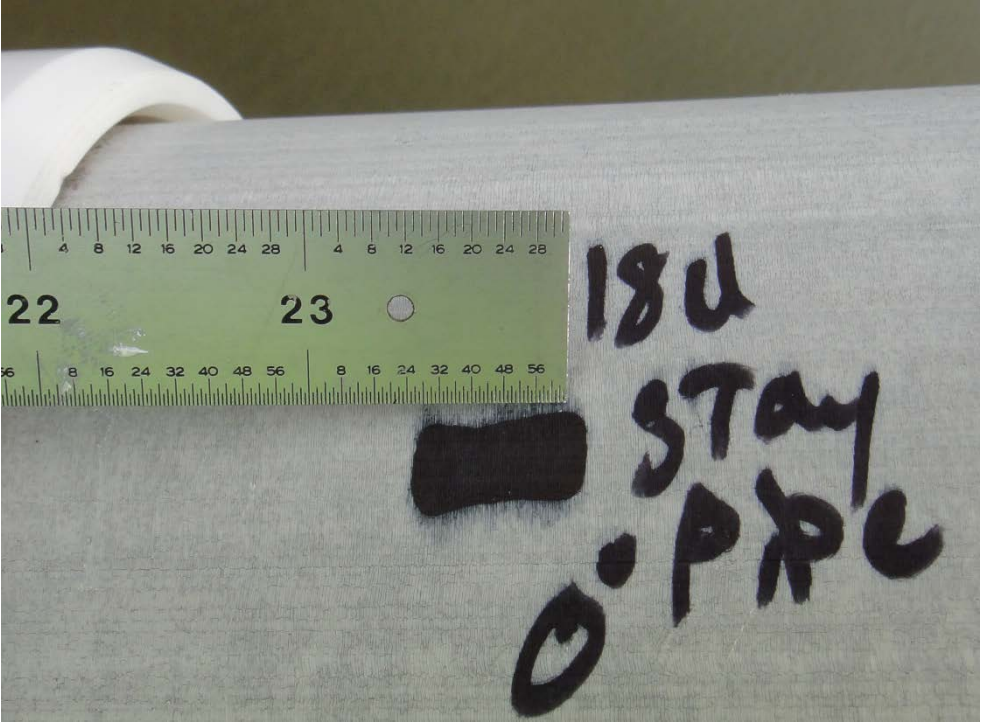


Figure 74. Penetrant Test Showing Indelible Ink Bleeding into Micro-cracks at the Topmost Portion of a Stay Pipe.

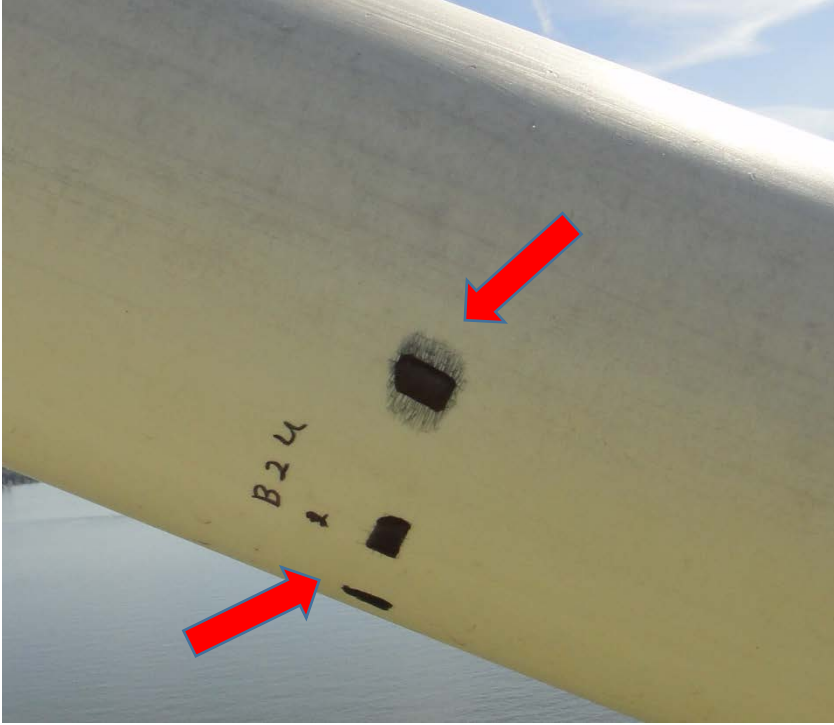


Figure 75. Ink Marks around the Periphery of Stay Pipe B2U Pipe Showing Ink Bleeding into Micro-cracks at the Mid Portion of the Pipe (Upper Arrow) and No Bleeding Is Present on the Lower Portions (Lower Arrow).



Figure 76. Close up Picture of Ink Marks on the Bottom Side of the Connection Sleeve at B20U Showing Signs of Minor Micro-cracking (Ink Bleeding).

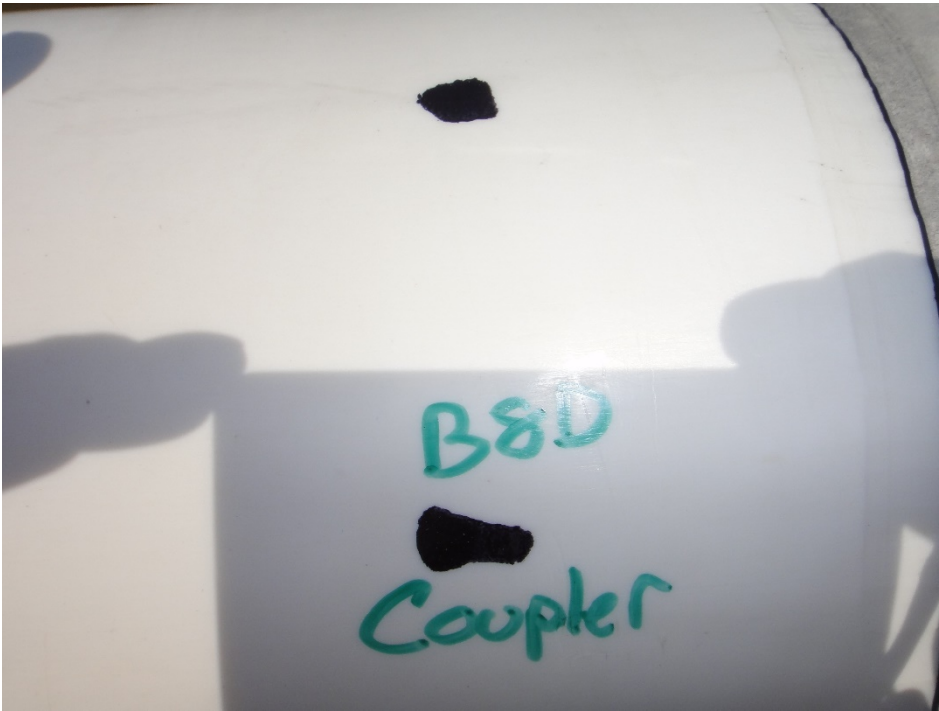


Figure 77. Ink Mark on Coupler Showing the Absence of In Bleeding/Micro-cracking.



Figure 78. Differences in Micro-cracking in a Stay Pipe Adjacent to the Ribbing.



Figure 79. "Candy-Stripe" Appearance of Stay Pipes Due to Micro-cracking Variations at the Helically Wound Ribbing.



Figure 80. KTC Researcher Using a Digital Microscope Camera to Take Close-up Pictures of Micro-cracking on the Surface of the Coextruded HDPE Pipe of a Connection Sleeve.

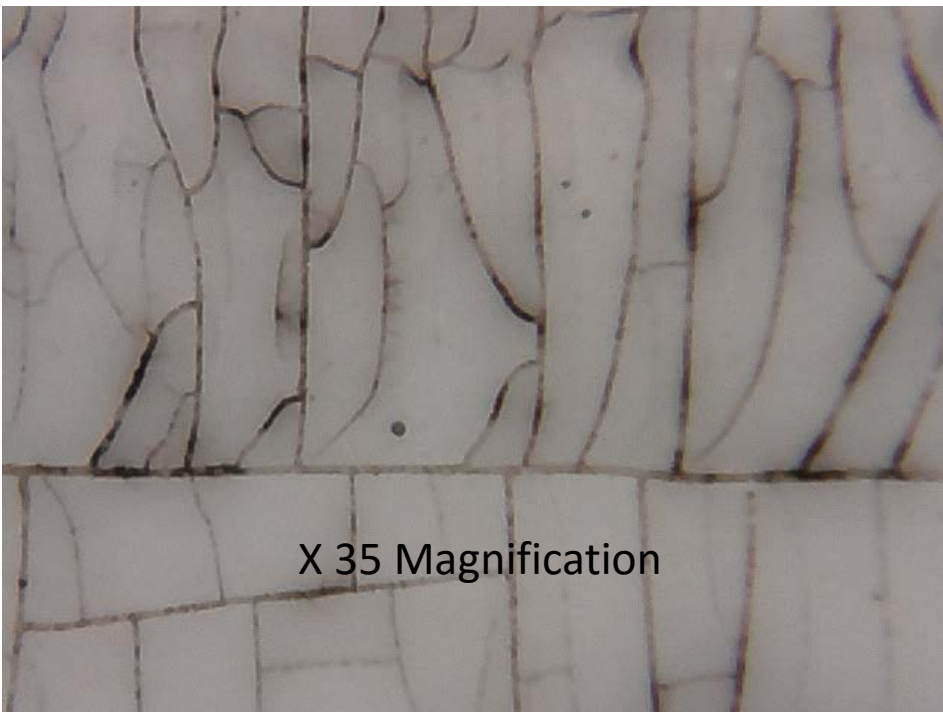


Figure 81. Magnified Image of the Surface of a Coextruded HDPE Pipe Showing Micro-cracking. Note Coat Fines/Soils Embedded in the Micro-cracks.



Figure 82. KTC Technician Using Hand Plane to Take Scrape Samples from the Surface of the White HDPE.



Figure 83. Surface of Coextruded HDPE Piping after Taking a Surface Scrape Sample.

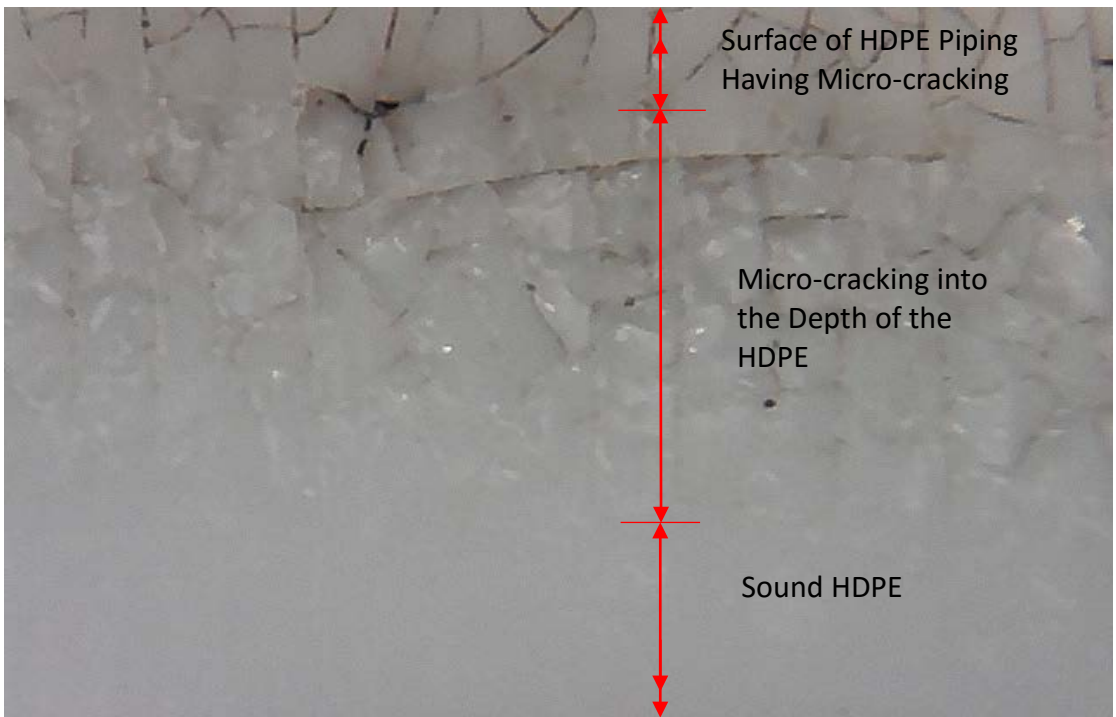


Figure 84. Magnified Picture of the Surface of a Coextruded HDPE Pipe Adjacent to A Scrape Showing the Interwoven Pattern of the Micro-cracking with Depth into Surface down to Sound HDPE.



Figure 85. Scrape Location on Transition Pipe Showing Micro-cracking Penetration of White Coextruded HDPE Down to the Black Base Material.

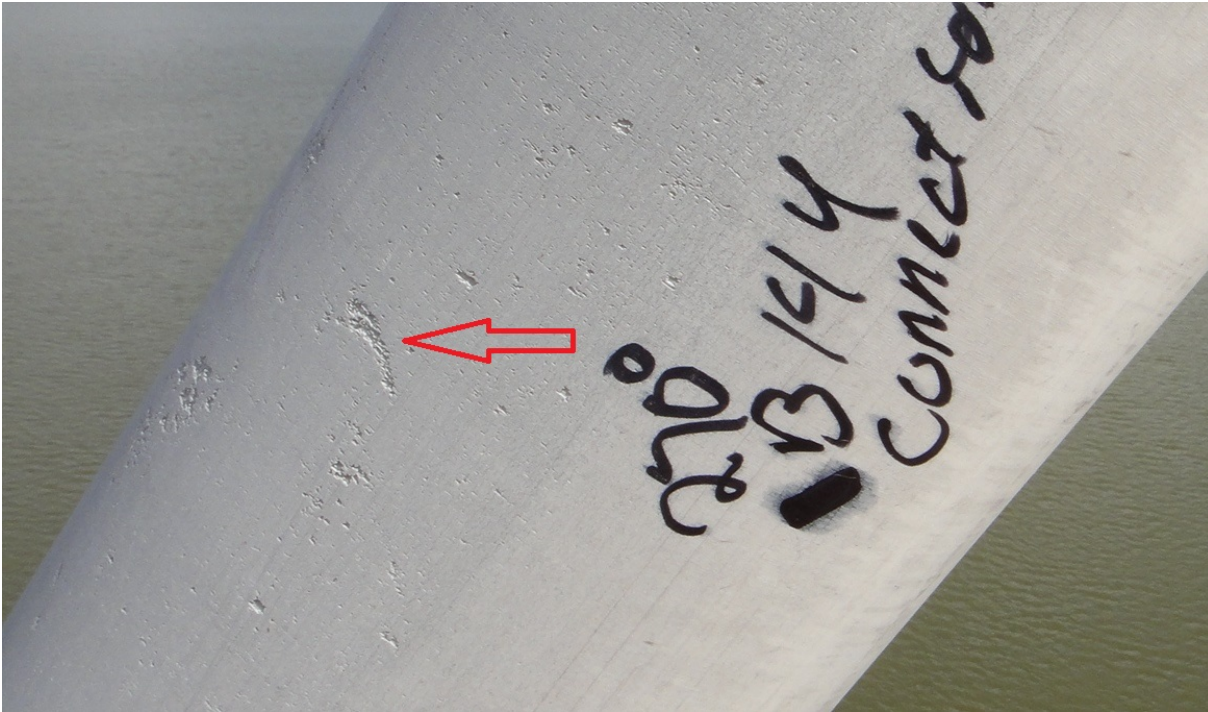


Figure 86. Spalling of Coextruded HDPE on Surface of a Connection Sleeve.

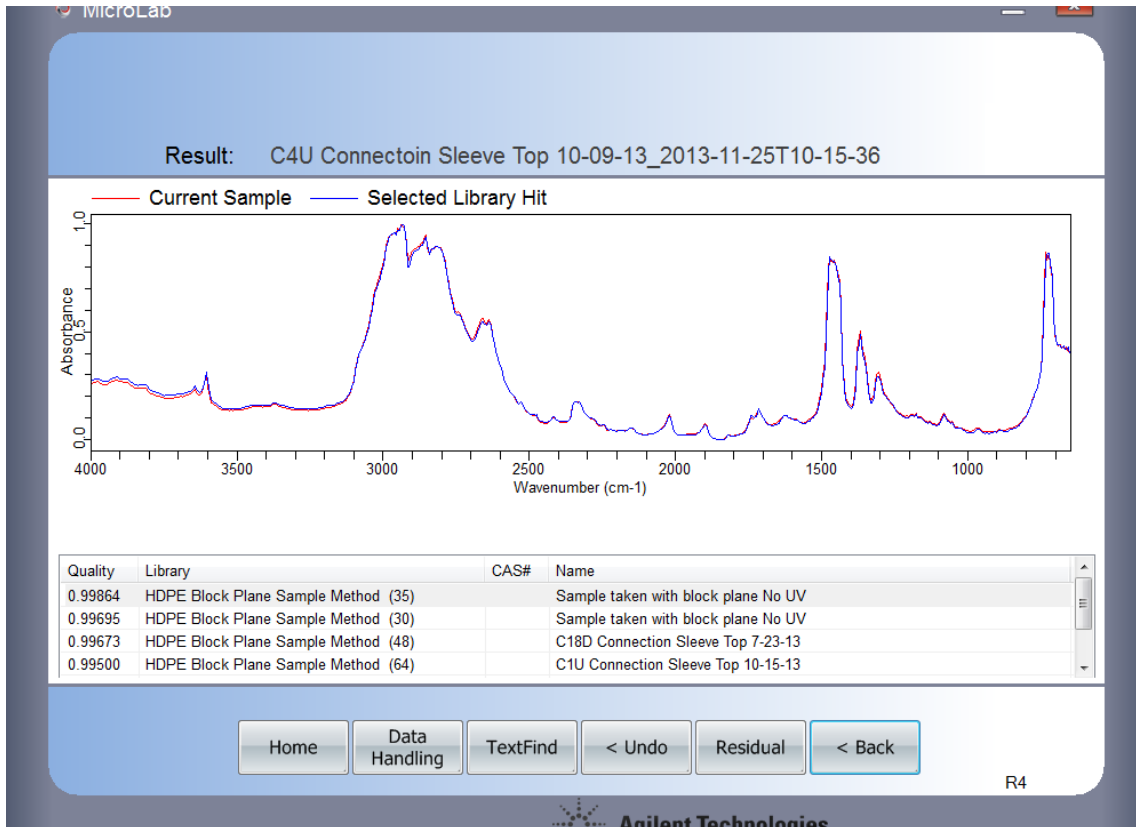


Figure 87. FTIR Scan from Scrape Sample of White Coextruded HDPE from Connection Sleeve Pipe Exhibiting Micro-Cracking.

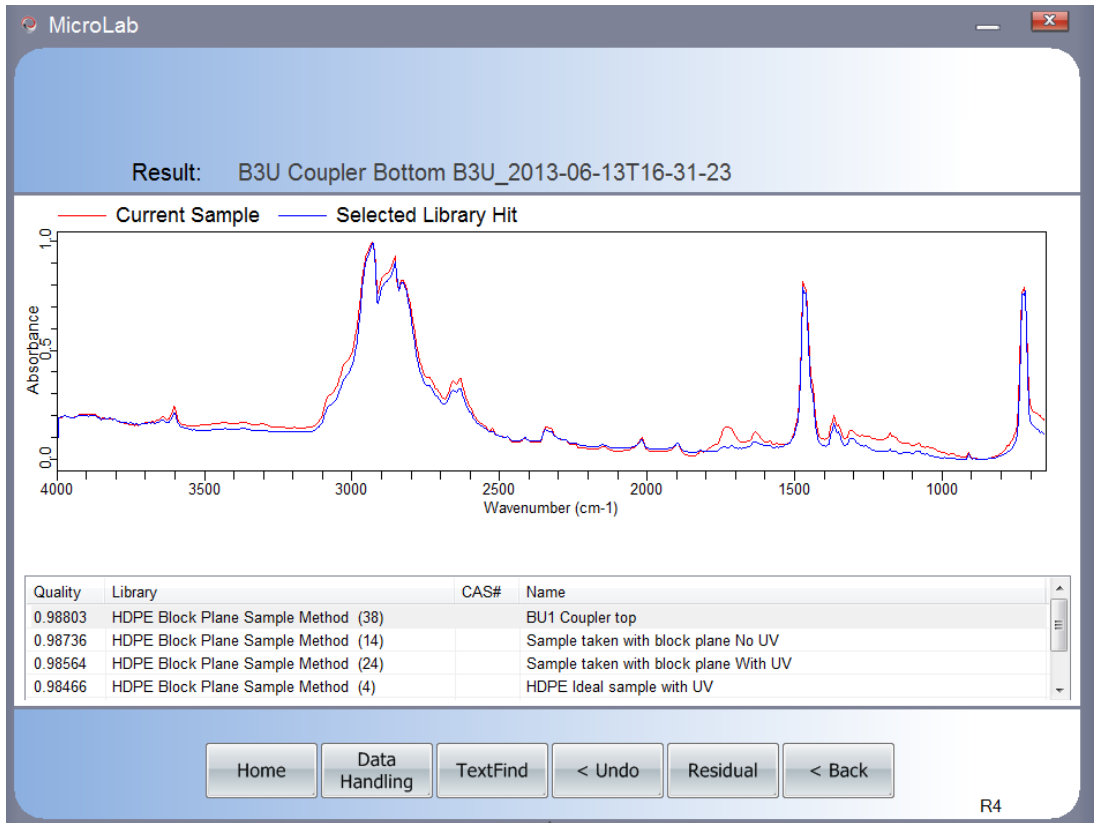


Figure 88. FTIR Scan from Scrape Sample of White HDPE from Coupler with No Signs of Micro-Cracking.



Figure 89. A Porous Grout Sample Extracted from A Void in Connection Sleeve C19D.

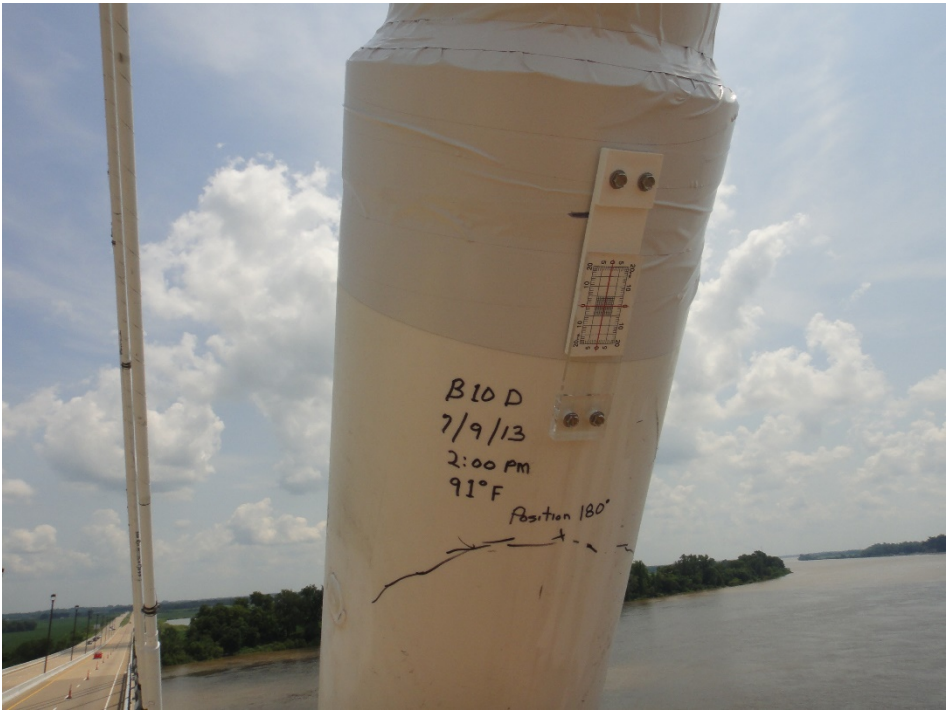


Figure 90. Crack Width Gage Installed at Butt-Weld Crack at a Reducer.



Figure 91. Drill with Rasp Bit Being Used to Create Bevel in a Butt-Weld Crack Prior to Plastic Welding.

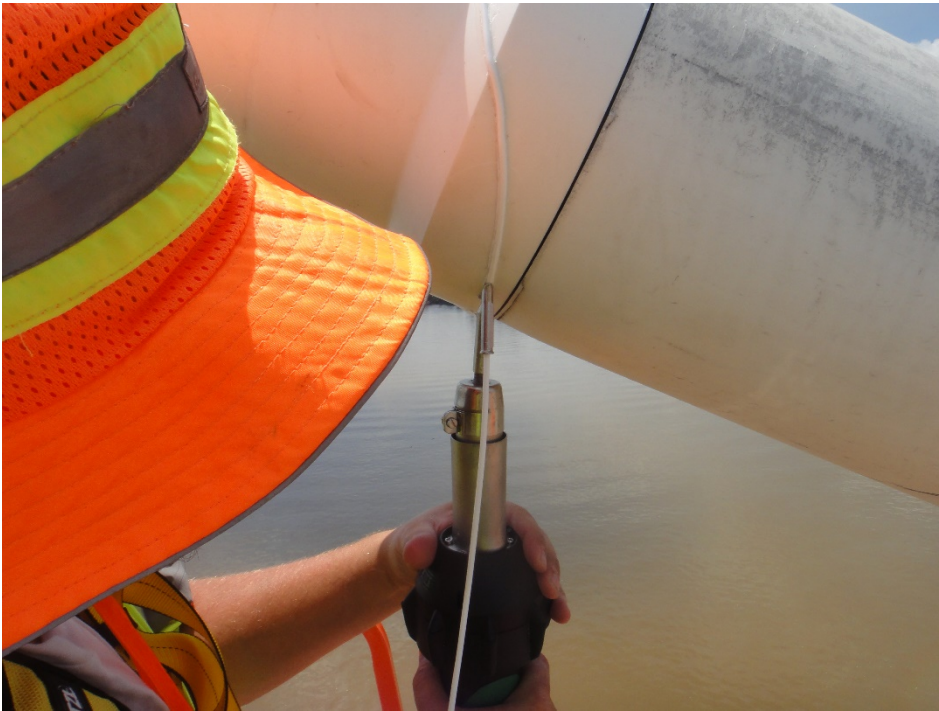


Figure 92. Weld Repair of Crack in Reducer at Stay Cable B23D.



Figure 93. Completed Weld Repair in a Previously Cracked Reducer.



Figure 94. Failed Repair Weld (Ref. Figure 89) Discovered Several Months after Completion of Repair.



Figure 95. Applying Stopaq® Paste to a Seal Crack in a Reducer.



Figure 96. Covering the Stopaq® Paste Seal with Tedlar Tape.



Figure 97. Failure of Stopaq® Paste Seal Found Several Months after the Repair.



Figure 98. Tedlar Tape Applied over Crack in a Reducer and Reducer-Stay Pipe Gap.



Figure 99. The Application of STOPAQ® Tape to Seal the Reducer-Stay Pipe Gap and Prevent Water Intrusion into the Grout Void.



Figure 100. Measuring Resistance of an Electrofusion Weld at the Weld Nipples on a Coupler.



Figure 101. Broken Heating Wire of Electrofusion Weld and Missing Weld Nipples of Cracked Reducer.



Figure 102. Re-welding HDPE Plug Cut from a Connection Sleeve at a Void Access Hole.



Figure 103. Water Leaking from Neoprene Boot at Tower Anchorage of Cable C7D (Ref. 11).

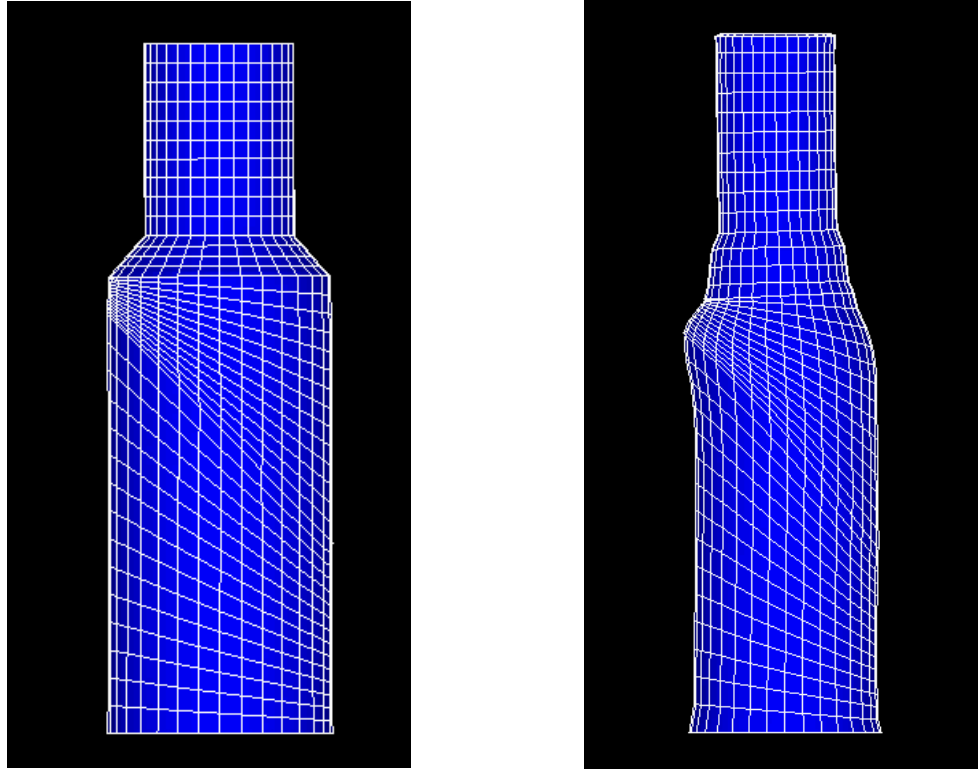


Figure 104. Finite Element Analysis of Effect of a Grout Void to the Reducer-Stay Pipe Area under Loading (Ref. 17).

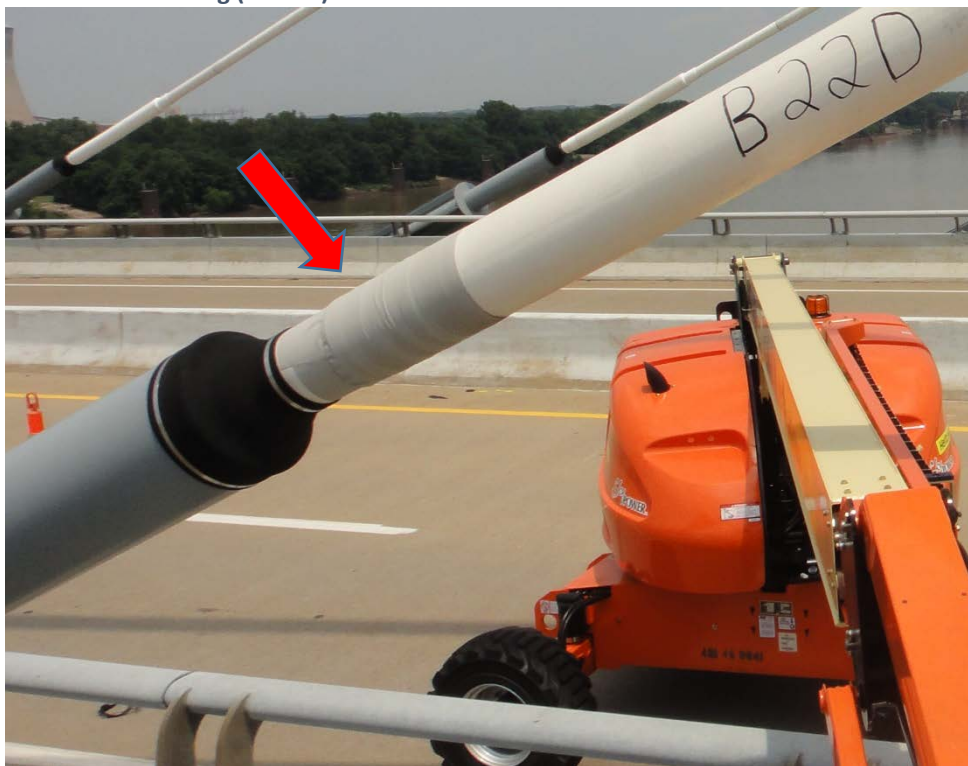


Figure 105. Commercial Cable Wrap Used as a Spot Repair on Stay Cable B22D (Arrow).



Figure 106. Zipper Sleeve on the US 17 Talmadge Memorial Bridge at Savannah, GA.

This page has been intentionally left blank.

8. APPENDIX 1 Description of HDPE Piping Condition States



Condition Category 0:- No Cracking (Applies to Both Connection Sleeve Couplers and Reducers).



Condition Category 1: Crack in Large End of HDPE Reducer.



Condition Category 2: Crack Primarily in Reducer-to-Connection Sleeve Pipe Section Butt Weld.



Condition Category 3: Crack Primarily in Small End of Reducer.



Condition Category 4: Crack in Reducer-to-Connection Sleeve Pipe Section Butt Weld with Lateral Displacement.



Condition Category 5: Crack in Coupler-to-Connection Sleeve Pipe Section Butt Weld.



Condition Category 6: Crack in Coupler.



Condition Category 7: Crack in Connection Sleeve Pipe Section.



Condition Category 8: Failure of Electrofusion Weld between Connection Sleeve Coupler and Transition Pipe with Longitudinal Separation.

**9. APPENDIX 2 Applied Technical Services Review of HDPE
Piping Fractures at the Deck Anchorages**



APPLIED TECHNICAL SERVICES, INCORPORATED

www.atslab.com

1000 Zane St., Louisville, KY 40210 • Ph 502-969-9930 • Fax 502-969-9943

EVALUATION OF CRACKS THROUGH HDPE PLASTIC PIPE REDUCERS AND COUPLINGS FROM THE US-231 WILLIAM H. NATCHER BRIDGE, OWENSBORO, KY

ATS Project #226165

April 28, 2015

Prepared for:

Ted Hopwood University of Kentucky

**Kentucky Transportation
Center 176 Oliver H. Raymond
Building Lexington, KY 40506-
0281**

Digitally signed by John P. Jendrzewski,
Ph.D.

John P. Jendrzewski,
Ph.D., email=johnj@atslab.com,
m,

Date: 2015.04.29 16:04:51 -04'00'

Prepared by: _____ John P. Jendrzewski, Ph.D.

Senior Consultant/Failure Analyst

Digitally signed by Joseph Maciejewski
Joseph Maciejewski,
email=jmac@atslab.com,

Date: 2015.04.29 16:45:16 -04'00' **Joseph Maciejewski, P.E.**

Reviewed by: _____ Joseph Maciejewski, P.E.

Senior Metallurgist

This report may not be reproduced except in full without the written approval of ATS. This report represents interpretation of the results obtained from the test specimen and is not to be construed as a guarantee or warranty of the condition of the entire material lot. If the method used is a customer provided, non-standard test method, ATS does not assume responsibility for validation of the method.

Professional Engineers

Design • Consulting • Testing and Inspection

Members in AAFS, ACS, ASCE, AISC, ASM, ASME, ASNT, ASQC, ASTM, AWS, API, BOMA, FSCT, IAAI, IWCA, NACE, NFPA, NCSL SAI, SAFS, BLRBAC, TAPPI, NSPE, ALSPE, DCSPE, FLSPE, GSPE, MDSPE, VSPE, PSPE



APPLIED TECHNICAL SERVICES, INCORPORATED

SUBJECT

Evaluation of Cracks through HDPE Plastic Pipe Reducers and Couplings from the US-231
William H. Natcher Bridge, Owensboro, KY

EXECUTIVE SUMMARY:

Circumferential cracking was observed primarily in the reducers used to attach the larger diameter pipe at the anchorage base to the smaller diameter piping. The predominant crack location and origin was at the top of the reducer (i.e. 0° location) where the relatively sharp circumferential groove was present where the reducer undergoes the outer diameter size transition. The cracking propagated both clockwise and counterclockwise around the pipe, terminating at the bottom (i.e. 180° location) of the reducer. These crack paths suggest unidirectional bending stresses in the vertical plane putting the top of the reducer in tension and consequently propagating the crack from the top to the bottom of the reducer in both clockwise and counterclockwise directions.

Cracking was also located in the reducer adjacent to the stay pipe butt weld. It was not possible to determine if the crack formed primarily to axial loads, i.e. pure tension, or if tension produced by bending was indicated since the cracks were relatively tight and stayed basically on the sample circumferential plane around the coupling.

Circumferential cracking was identified to a lesser degree in the bottom and top couplings with most appearing to originate at one of the holes identified as the “weld nipple” holes on top (i.e. 0°) of the specimen. Like the reducer cracks at the pipe butt welds, it was not possible to determine if the crack formed primarily to axial loads, i.e. pure tension, or if tension was produced by unidirectional bending.

Since the majority of the cracking was confined to the reducers while remaining failures were present in the couplers, destructive testing of both these components is recommended to ascertain that they meet the expected mechanical and chemical properties for this application. Lack of tensile or impact strengths could have significantly contributed to if not being the primary cause of failure of these components in a relatively short time in service.

BACKGROUND & OBJECTIVE:

Photographs of high density polyethylene (HDPE) reducers, couplers and stay piping from the bottom stay cable anchorage points from the upstream and downstream sides of the two towers of the US-231 William Natcher Bridge in Owensboro, Kentucky (Figure 1) were received for evaluation. Circumferential cracks were observed in reducers and couplers containing holes for weld nipples. A drawing showing the stay cable anchorage piping components is presented in Figure 2. The reducer attached the larger diameter HDPE piping to the smaller diameter HDPE piping in conjunction with the electric fusion welded coupler. The objective of the evaluation was to determine the crack propagation directions of the circumferential cracks present in the components by review of the photographs.

RESULTS:

Photographs for the twenty-four anchorage points on the downstream side on the Kentucky side of Tower “B” are presented as Figures 3 through 26. Photographs showing cracks that varied to some degree from those identified on the downstream Kentucky side of Tower “B” from the upstream Kentucky side and from both the upstream and downstream Indiana side of Tower “C” are presented in Figures 27 through 33. The results of the examination of the cracked HDPE components from the downstream and upstream locations of the two towers “B” and “C” are presented in Tables 1 through 4.

Most failures were observed at the relatively sharp change in diameter of the reducer piece. All these cracks originated at the top, i.e. 0° location, and propagated in a clockwise and counterclockwise direction around and typically into the larger diameter portion of the reducer. Crack propagation directions are indicated by arrows on the attached photographs when possible. The macroscopic features of the cracks are suggestive of a progressive fatigue cracking mechanism induced by unidirectional bending stress in the vertical plane.

A relative small number of reducer cracks were located next to the butt weld on the larger diameter portion of the reducer. These may have been induced primarily by axial tensile stress which was concentrated in the “heat-affected-zone” of the butt weld of the connection

TABLE 1**Tower B (Downstream Kentucky Side Span)**

Anchorage	Crack Location & Origin	Propagation Direction
B1D	Reducer, Top (0°), at size transition	Clockwise & Counterclockwise
B2D	Reducer, Top (0°), at size transition	Clockwise & Counterclockwise
B3D	Reducer, Top (0°), at size transition	Clockwise & Counterclockwise
B4D	Reducer, Next to Stay Pipe Butt Weld	Tension (Clockwise & Counterclockwise?)
B5D	Reducer, Next to Stay Pipe Butt Weld	Tension (Clockwise & Counterclockwise?)
B6D	Reducer, Top (0°), at size transition	Clockwise & Counterclockwise
B7D	Reducer, Top (0°), at size transition	Clockwise & Counterclockwise
B8D	Reducer, Top (0°), at size transition	Clockwise & Counterclockwise
B9D	Reducer, Top (0°), at size transition	Clockwise & Counterclockwise
B10D	Reducer, Top (0°), at size transition	Clockwise & Counterclockwise
B11D	Coupling, Top (0°), at Weld Nipple Hole	Tension/Clockwise & Counterclockwise (?)
B12D	Reducer, Top (0°), at size transition	Clockwise & Counterclockwise
B13D	Reducer, Top (0°), at size transition	Clockwise & Counterclockwise
B14D	Reducer, Next to Stay Pipe Butt Weld	Tension (Clockwise & Counterclockwise?)
B15D	Reducer, Top (0°), at size transition	Clockwise & Counterclockwise
B16D	Reducer, Top (0°), at size transition	Clockwise & Counterclockwise
B17D	Reducer, Top (0°), at size transition	Clockwise & Counterclockwise
B18D	Coupling, Side (90°), at Weld Nipple Hole	Tension/Clockwise & Counterclockwise (?)
B19D	Reducer, Top (0°), at size transition	Clockwise & Counterclockwise
B20D	Reducer, Next to Stay Pipe Butt Weld	Tension (Clockwise & Counterclockwise?)
B21D	Reducer, Top (0°), at size transition	Clockwise & Counterclockwise
B22D	Reducer, Top (0°), at size transition	Clockwise & Counterclockwise
B23D	Reducer, Top (0°), at size transition	Clockwise & Counterclockwise
B24D	No Crack Observed in Photographs	-----

TABLE 2

Tower B (Upstream Kentucky Side Span)

Anchorage	Crack Location & Origin	Propagation Direction
B1U	Reducer, Top (0°), at size transition	Clockwise & Counterclockwise
B2U	Reducer, Top (0°), at size transition	Clockwise & Counterclockwise
B3U	Reducer, Top (0°), at size transition	Clockwise & Counterclockwise
B4U	Coupler-bottom, Next to Pipe Butt Weld	Tension (Clockwise & Counterclockwise)
B5U	Reducer, Next to Lg. Pipe Butt Weld	Tension (Clockwise & Counterclockwise?)
B6U	Reducer, Next to Lg. Pipe Butt Weld	Tension (Clockwise & Counterclockwise?)
B7U	Reducer, Next to Lg. Pipe Butt Weld	Tension (Clockwise & Counterclockwise?)
B8U	Reducer, Top (0°), at size transition	Clockwise & Counterclockwise
B9U	Reducer, Next to Lg. Pipe Butt Weld	Tension (Clockwise & Counterclockwise?)
B10U	Reducer, Top (0°), at size transition	Clockwise & Counterclockwise
B11U	Reducer, Next to Lg. Pipe Butt Weld	Tension (Clockwise & Counterclockwise?)
B12U	No Crack Observed in Photographs	-----
B13U	No Crack Observed in Photographs	-----
B14U	No Crack Observed in Photographs	-----
B15U	Reducer, Top (0°), at size transition	Clockwise & Counterclockwise
B16U	Reducer, Top (0°), at size transition	Clockwise & Counterclockwise
B17U	Reducer, Top (0°), at size transition	Clockwise & Counterclockwise
B18U	Reducer, Top (0°), at size transition	Clockwise & Counterclockwise
B19U	Reducer, Next to Lg. Pipe Butt Weld/ Coupler at weld nipple	Tension (Clockwise & Counterclockwise?)
B20U	Top Coupler into Lg. dia. pipe, Reducer in Small dia. section	Tension (Clockwise & Counterclockwise?)
B21U	Bottom Coupler at weld nipple, Reducer in Small dia. section	Tension/Clockwise & Counterclockwise
B22U	Reducer, Top (0°), at size transition & Bottom Coupler at butt weld	Tension/Clockwise & Counterclockwise
B23U	Reducer, Top (0°), at size transition & at Lg. dia. Butt weld	Tension/Clockwise & Counterclockwise
B24U	Reducer, Top (0°), at size transition	Clockwise & Counterclockwise

TABLE 3

Tower C (Downstream Indiana Side Span)

Anchorage	Crack Location & Origin	Propagation Direction
C1D	Reducer, Top (0°), at size transition	Clockwise & Counterclockwise
C2D	Reducer, Top (0°), at size transition	Clockwise & Counterclockwise
C3D	Reducer, Top (0°), at size transition	Clockwise & Counterclockwise
C4D	Reducer, Next to Stay Pipe Butt Weld	Tension (Clockwise & Counterclockwise?)
C5D	Reducer & Coupler near Butt Welds	Tension (Clockwise & Counterclockwise?)
C6D	Reducer, Top (0°), at size transition	Clockwise & Counterclockwise
C7D	Reducer, Next to Stay Pipe Butt Weld	Tension (Clockwise & Counterclockwise?)
C8D	Reducer, Top (0°), at size transition	Clockwise & Counterclockwise
C9D	Reducer, Top (0°), at size transition	Clockwise & Counterclockwise
C10D	Reducer, Top (0°), at size transition	Clockwise & Counterclockwise
C11D	Reducer, Next to Stay Pipe Butt Weld	Tension (Clockwise & Counterclockwise?)
C12D	Reducer, Top (0°), at size transition	Clockwise & Counterclockwise (most)
C13D	Reducer, Top (0°), at size transition	Clockwise & Counterclockwise
C14D	No Crack Observed in Photographs	-----
C15D	Reducer, Top (0°), at size transition	Clockwise & Counterclockwise
C16D	Reducer, Top (0°), at size transition	Clockwise & Counterclockwise (most)
C17D	Reducer, Top (0°), at size transition	Clockwise & Counterclockwise
C18D	Reducer, Top (0°), at size transition	Clockwise & Counterclockwise
C19D	No Crack Observed in Photographs	-----
C20D	Reducer, Next to Stay Pipe Butt Weld	Tension/Shear (Clockwise & Counterclockwise?)
C21D	Reducer, Top (0°), at size transition	Clockwise & Counterclockwise
C22D	Reducer, Top (0°), at size transition	Clockwise & Counterclockwise
C23D	Reducer, Top (0°), at size transition	Clockwise & Counterclockwise (most)
C24D	Reducer, Top (0°), at size transition	Clockwise & Counterclockwise

TABLE 4**Tower C (Upstream Indiana Side Span)**

Anchorage	Crack Location & Origin	Propagation Direction
C1U	Reducer, Top (0°), at size transition	Clockwise & Counterclockwise
C2U	Bottom Coupler at Weld Nipple-Split	Clockwise & Counterclockwise
C3U	Reducer, Top (0°), & Top Coupler LXS	Clockwise & Counterclockwise
C4U	Reducer, Next to Stay Pipe Butt Weld	Tension (Clockwise & Counterclockwise?)
C5U	Reducer, Next to Stay Pipe Butt Weld	Tension (Clockwise & Counterclockwise?)
C6U	Bottom Coupler at Weld Nipple	Clockwise & Counterclockwise
C7U	Reducer, Top (0°), at size transition	Clockwise & Counterclockwise
C8U	Reducer, Top (0°), at size transition	Clockwise & Counterclockwise
C9U	Reducer, Top (0°), at size transition	Clockwise & Counterclockwise
C10U	Reducer, Top (0°), at size transition	Clockwise & Counterclockwise
C11U	Bottom Coupler, Origins 90°/270°	Clockwise & Counterclockwise
C12U	Reducer, Top near Reducer Butt weld	Clockwise & Counterclockwise
C13U	Reducer, Top (0°), at size transition	Clockwise & Counterclockwise
C14U	Bottom Coupler	Tension/Clockwise & Counterclockwise (?)
C15U	Reducer, Top (0°), at size transition	Clockwise & Counterclockwise
C16U	Reducer, Top (0°), at size transition	Clockwise & Counterclockwise
C17U	Reducer, Top (0°), at size transition	Clockwise & Counterclockwise
C18U	Reducer small end & Top Coupler	Tension/Clockwise & Counterclockwise (?)
C19U	Reducer Large end at butt weld & bottom coupler	Tension/Clockwise & Counterclockwise (?)
C20U	Reducer Large end at butt weld & bottom coupler	Tension/Clockwise & Counterclockwise (?)
C21U	Reducer, Top (0°), at size transition & Bottom Coupler	Clockwise & Counterclockwise
C22U	Reducer, Top (0°), at size transition	Clockwise & Counterclockwise
C23U	Reducer, Top (0°), at size transition & Bottom Coupler	Clockwise & Counterclockwise
C24U	Reducer, Top (0°), at size transition	Clockwise & Counterclockwise

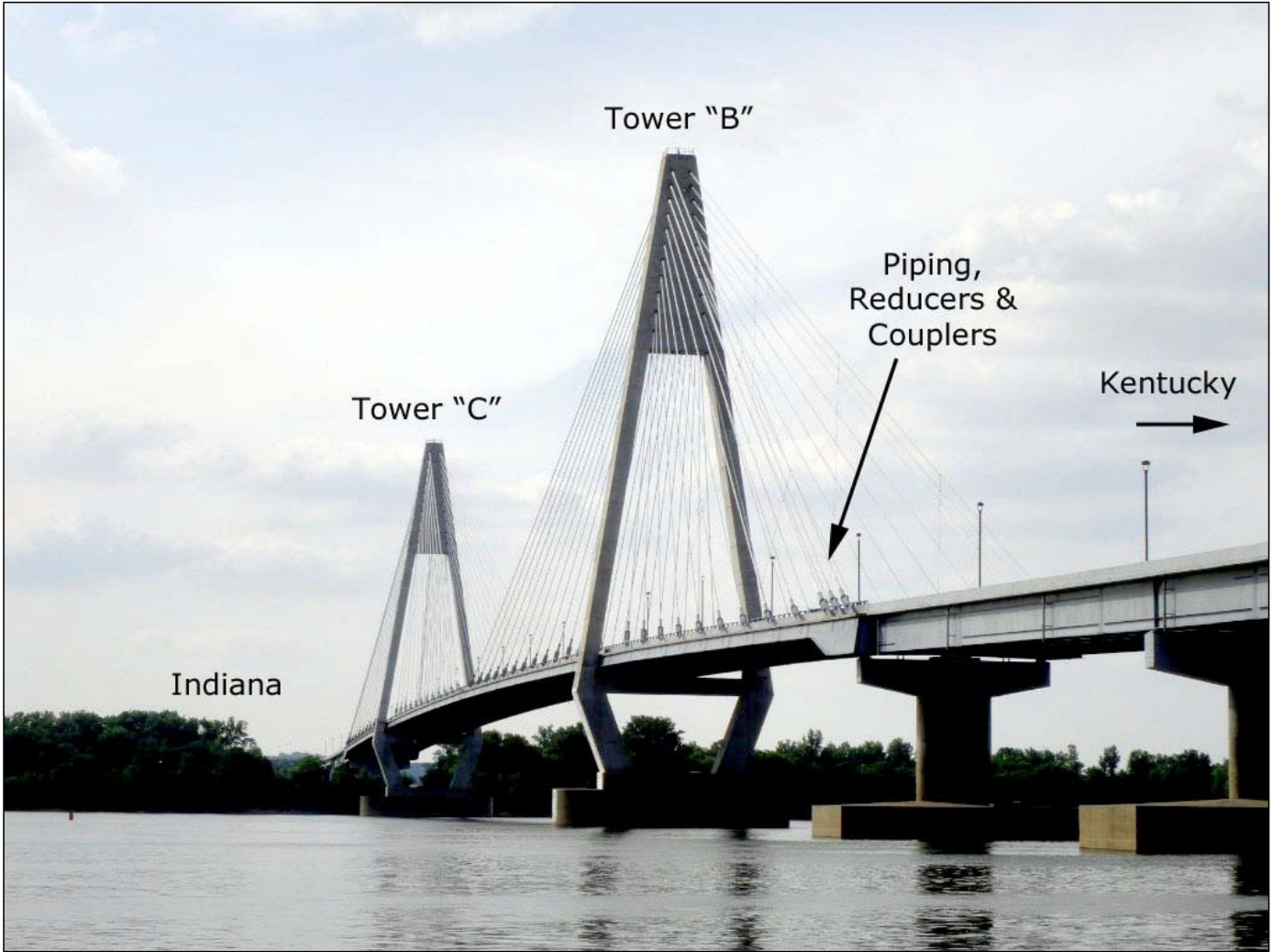


Figure 1: Photograph of the US-231 William Natcher Bridge, Owensboro, KY. The arrow shows the approximate locations of the HDPE couplings and reducers near the bottom of the cable stay bridge.

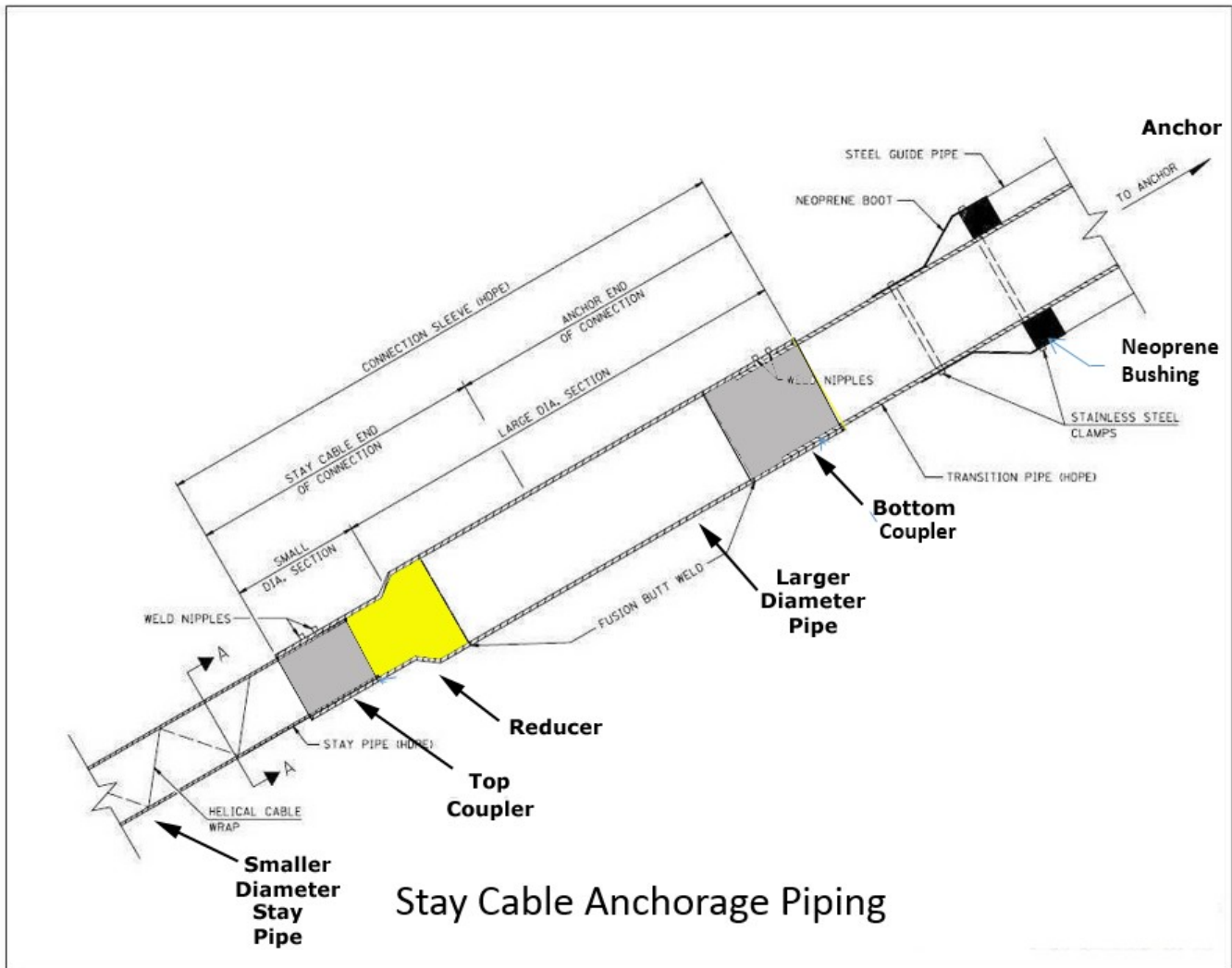


Figure 2: Drawing identifying the Reducer (yellow colored) and Top and Bottom Couplings (gray colored) on the HDPE piping surrounding the cables on the Natcher Bridge.

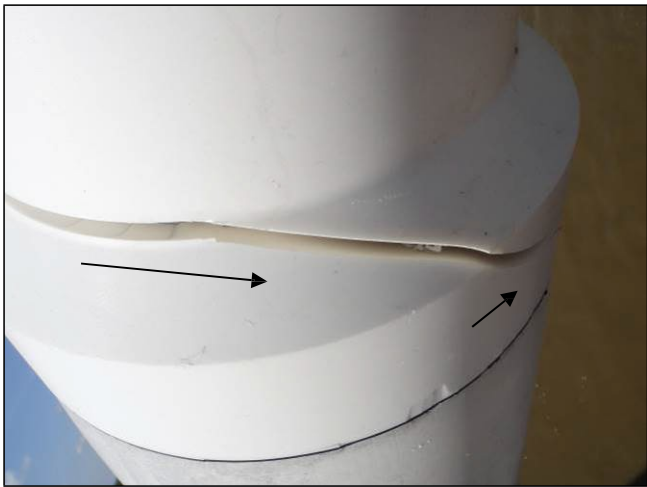
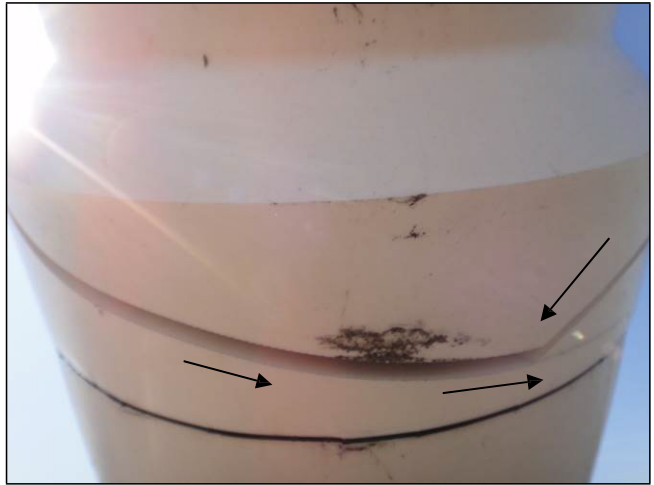
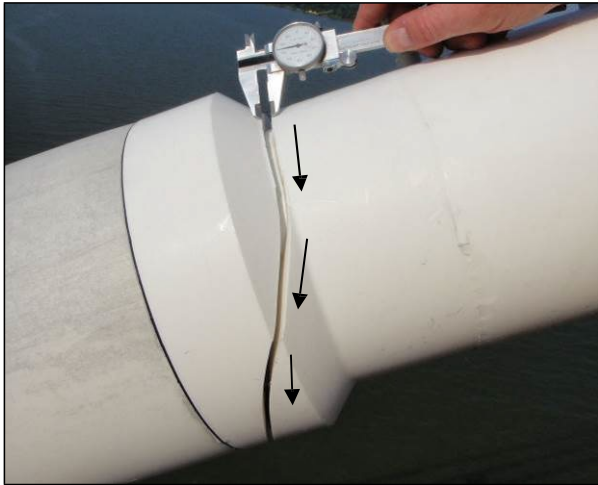
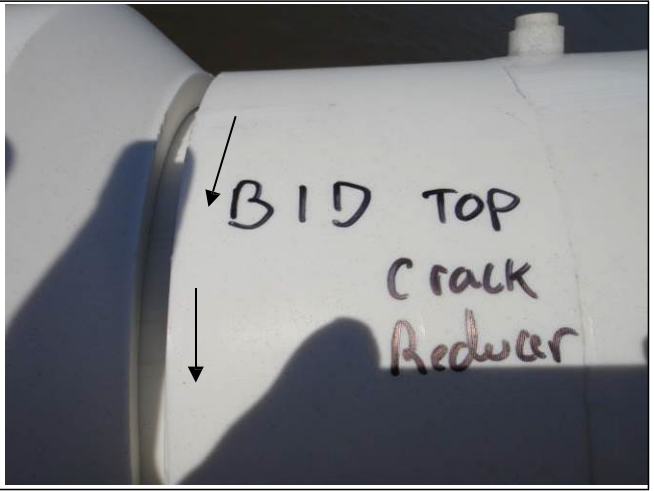


Figure 3: B1D: Reducer Crack at Notch Located at Diameter Transition

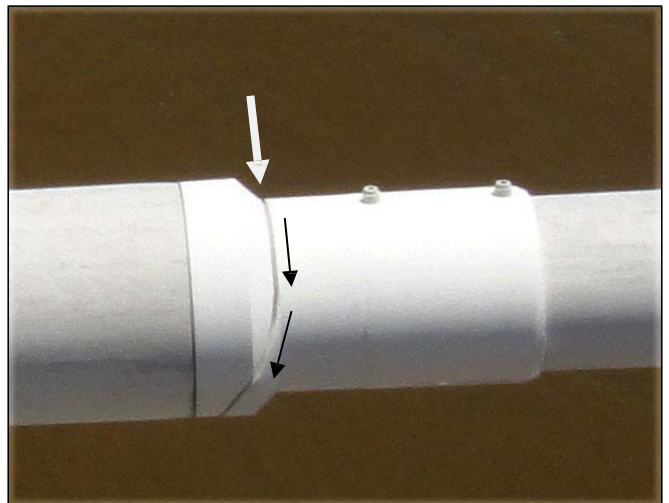
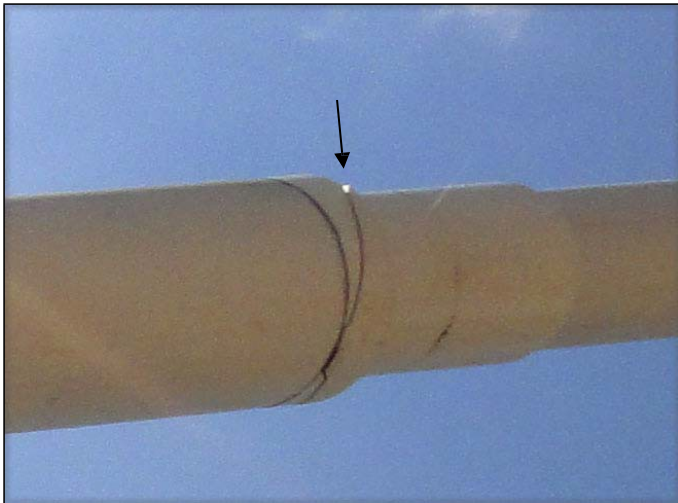


Figure 4: B2D: Reducer Crack at Notch Located at Diameter Transition

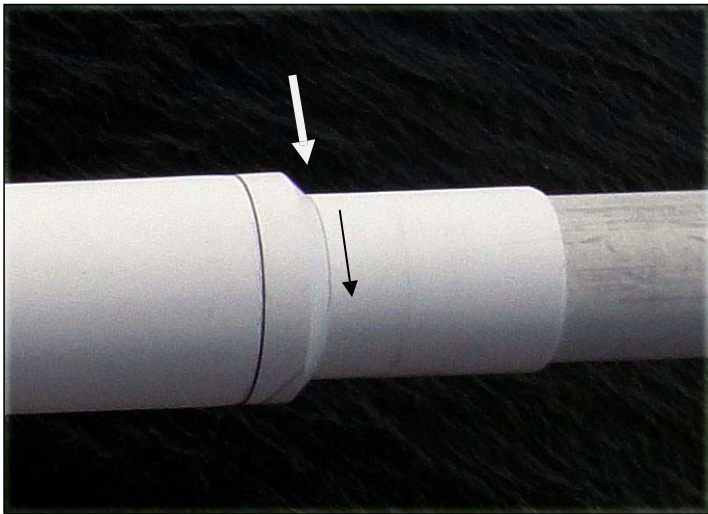


Figure 5: **B3D**: Reducer Crack at Notch Located at Diameter Transition

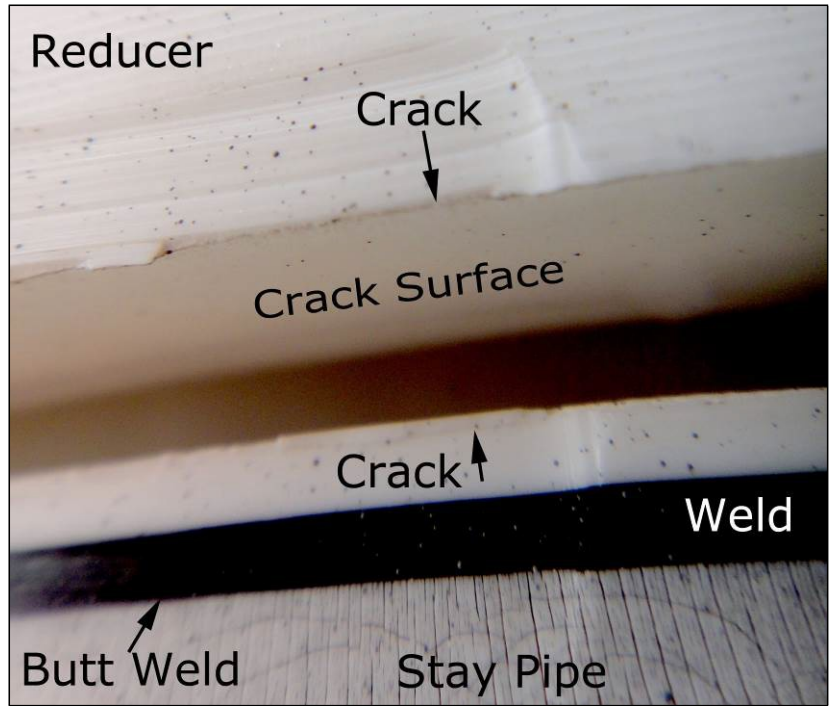
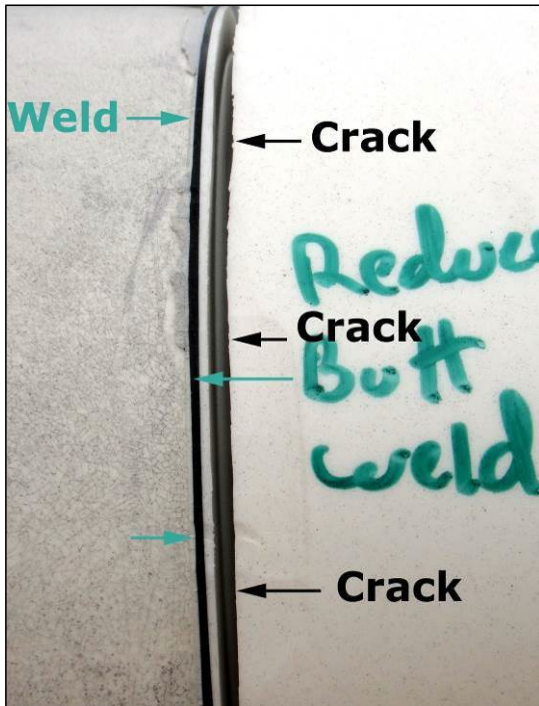
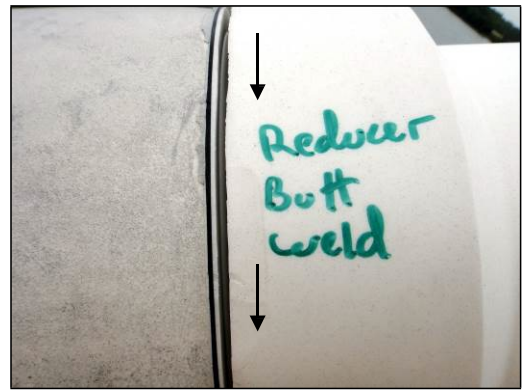
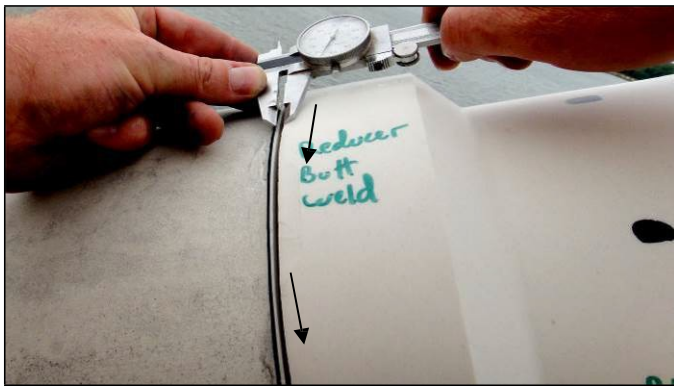


Figure 6: B4D: Reducer Crack Adjacent to Stay Pipe Butt Weld

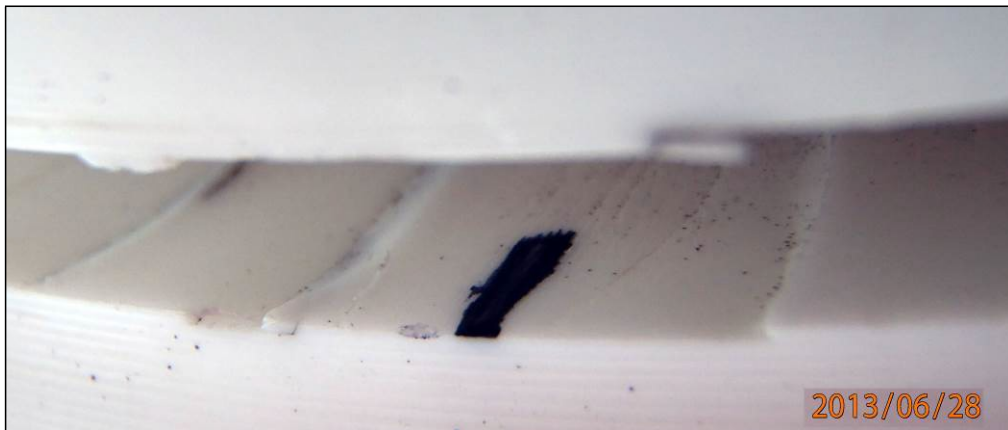
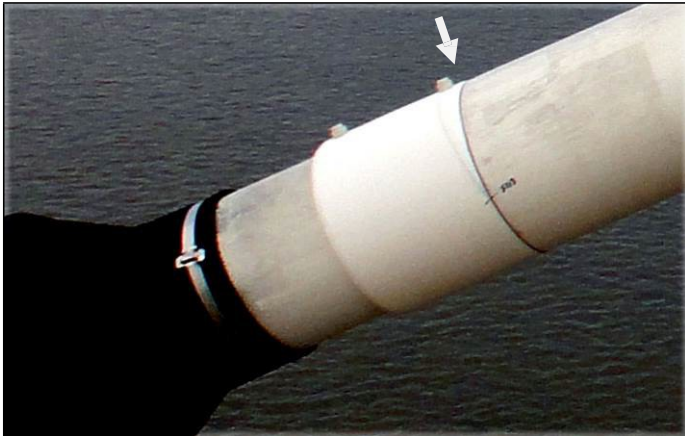


Figure 7: B5D: Reducer Crack Adjacent to Transition Pipe Butt Weld



Figure 8: B6D: Reducer Crack at Notch Located at Diameter Transition

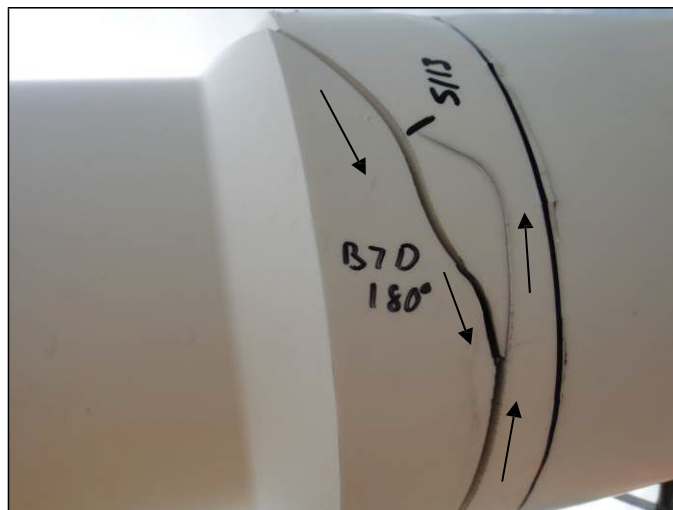
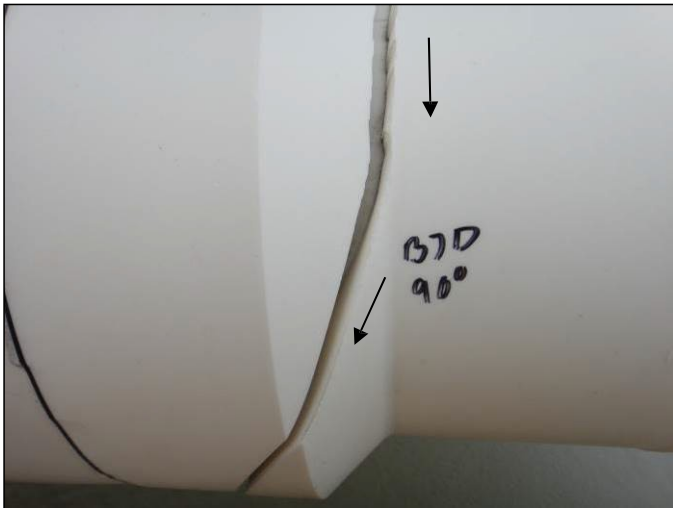
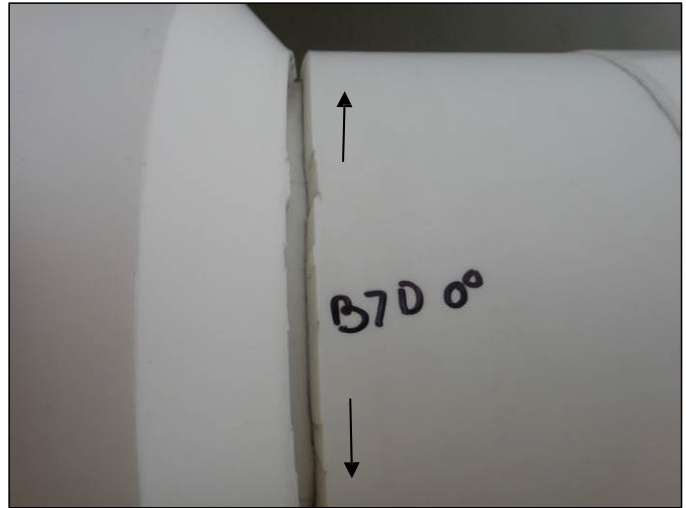


Figure 9: B7D: Reducer Crack at Notch Located at Diameter Transition



Figure 10: B8D: Reducer Crack at Notch Located at Diameter Transition

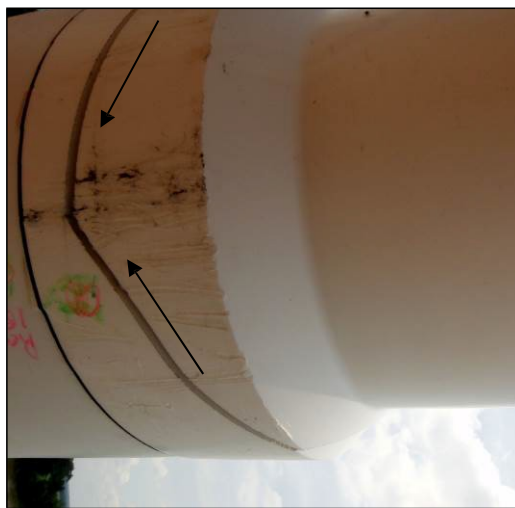


Figure 11: B9D: Reducer Crack at Notch Located at Diameter Transition

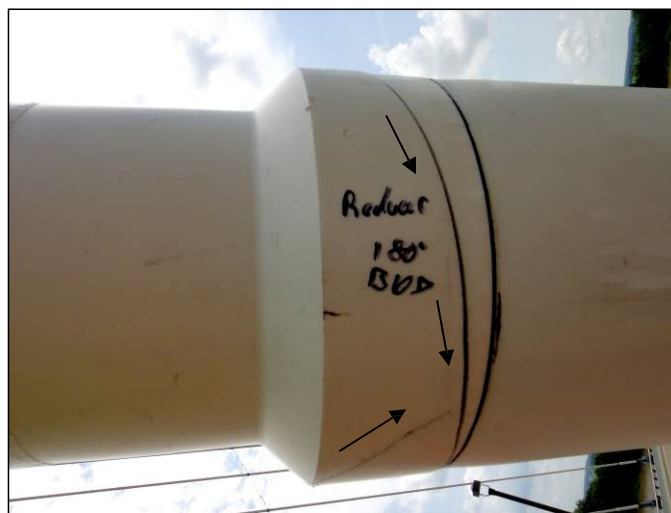
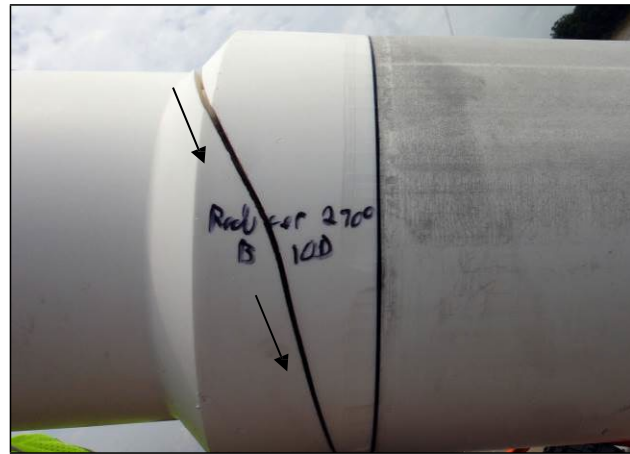
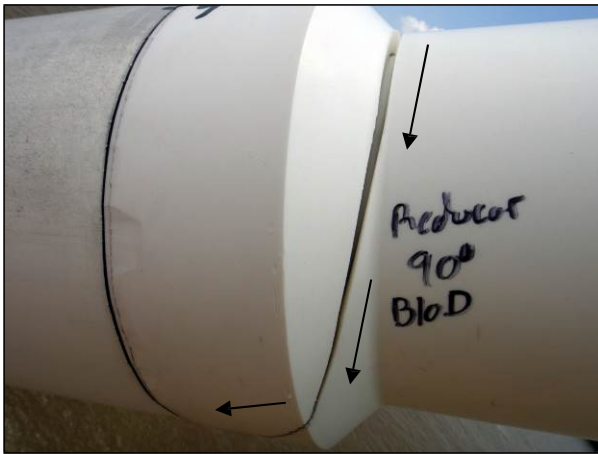


Figure 12: B10D: Reducer Crack at Notch Located at Diameter Transition

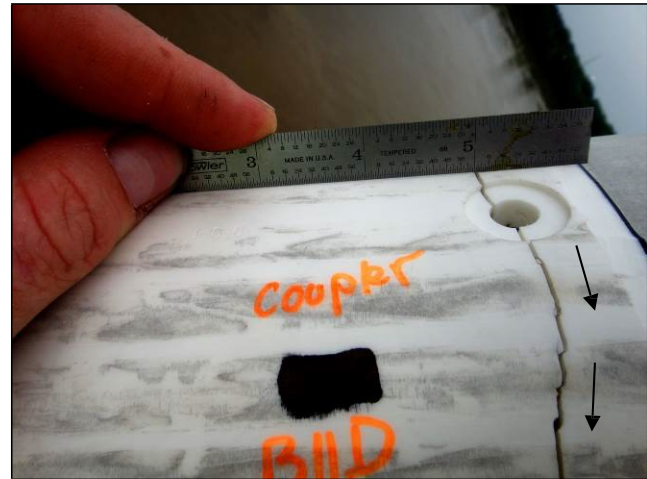
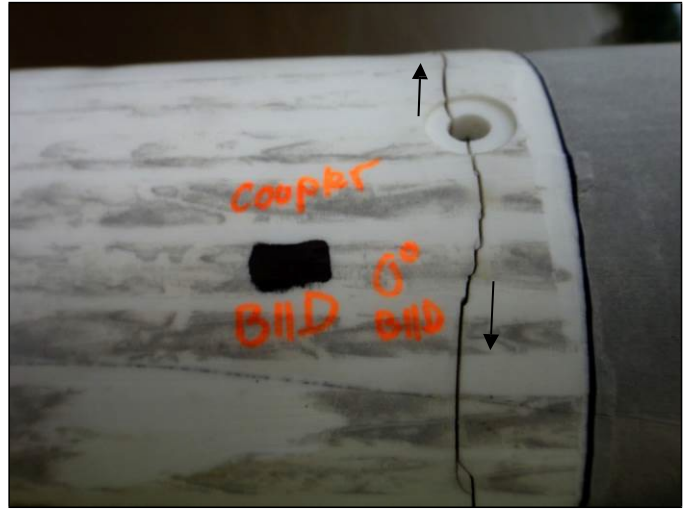


Figure 13: B11D: Reducer Crack at Coupler Hole Used For Electro-Fusion Weld

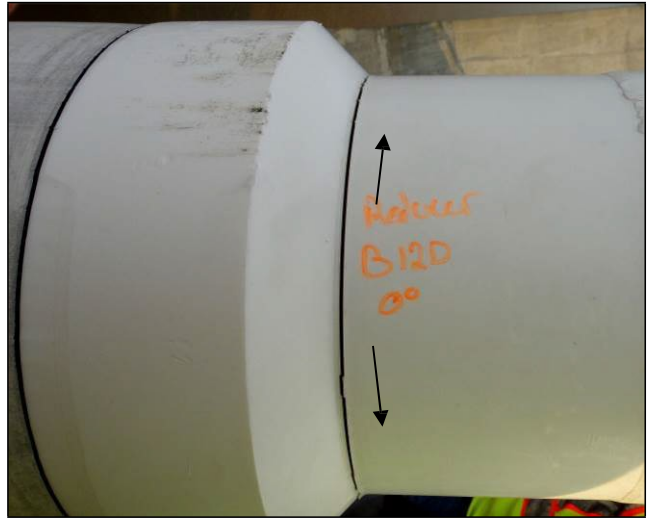


Figure 14: B12D: Reducer Crack at Notch Located at Diameter Transition

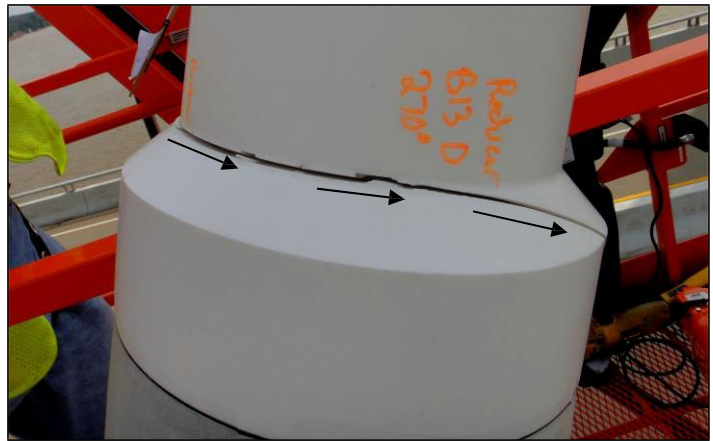
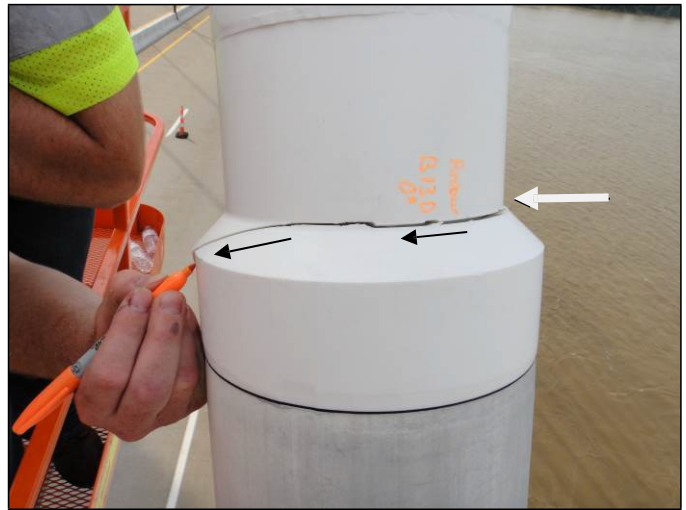


Figure 15: B13D: Reducer Crack at Notch Located at Diameter Transition

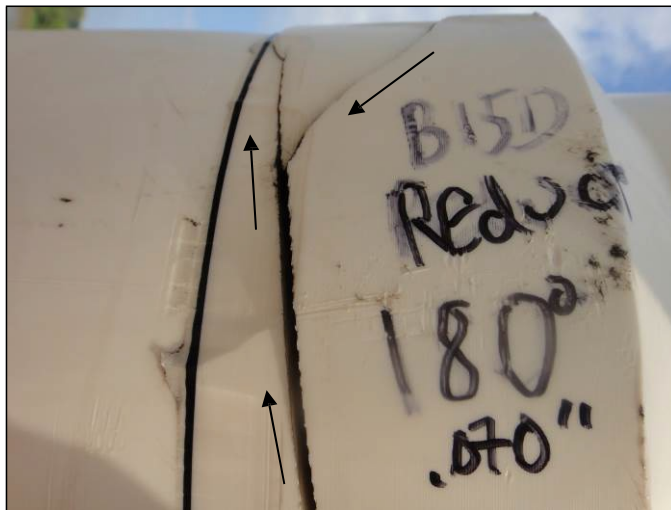
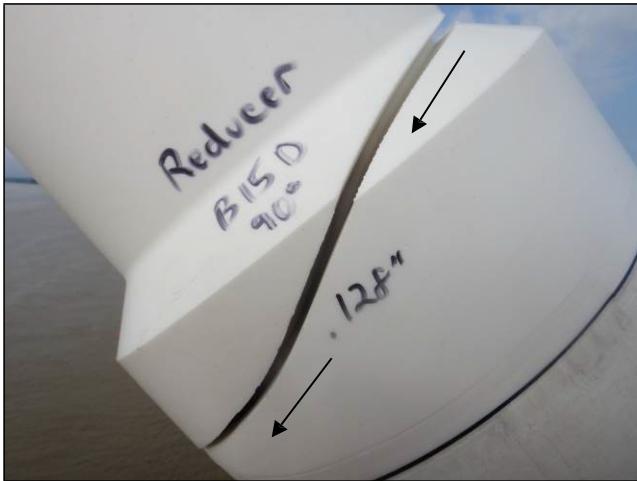


Figure 17: B15D: Reducer Crack at Notch Located at Diameter Transition



Figure 18: B16D: Reducer Crack at Notch Located at Diameter Transition



Figure 19: B17D: Reducer Crack at Notch Located at Diameter Transition

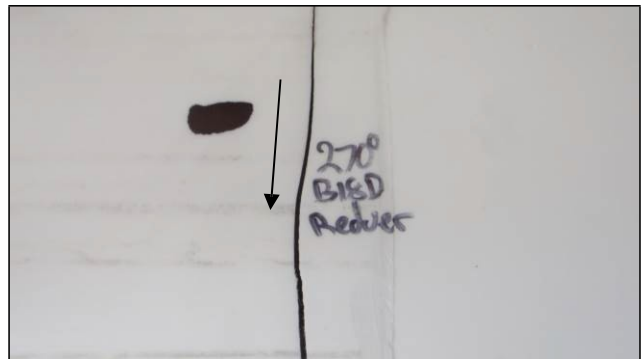
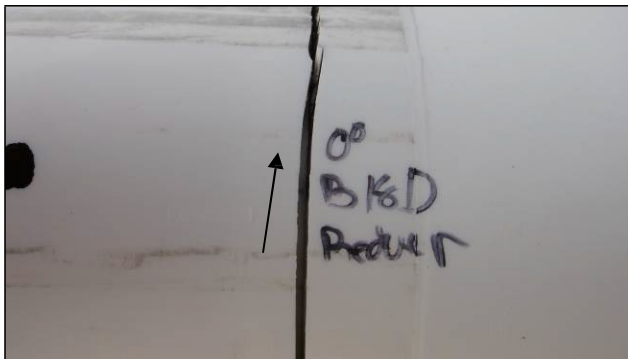
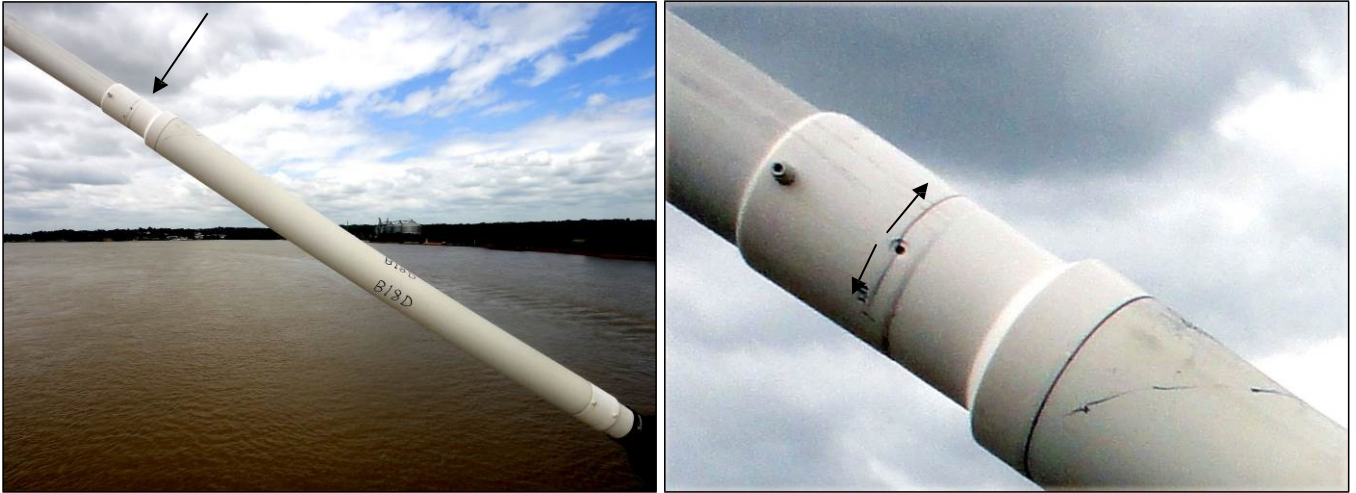


Figure 20: B18D: Reducer Crack at Hole (90°) for Electro Fusion Weld



Figure 21: B19D: Reducer Crack at Notch Located at Diameter Transition

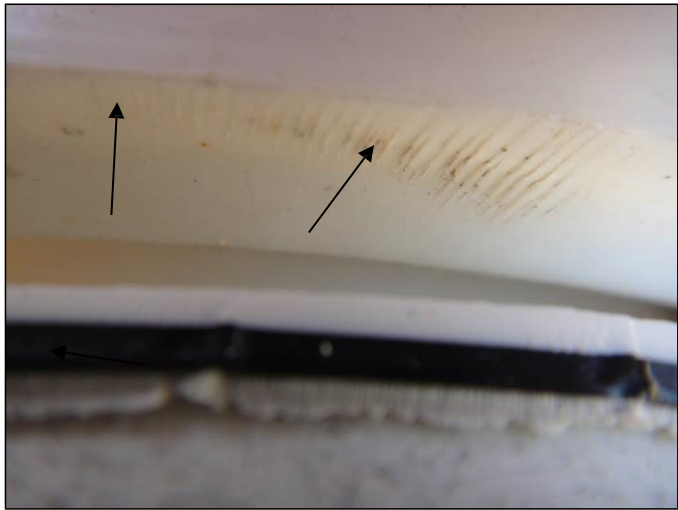
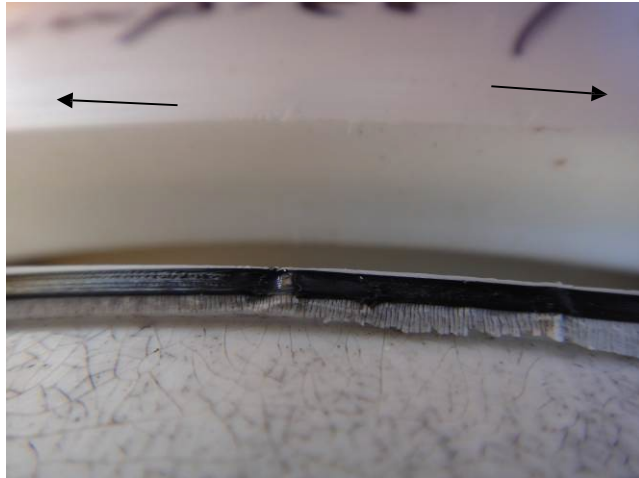


Figure 22: B20D: Reducer Crack at Notch Located at Diameter Transition

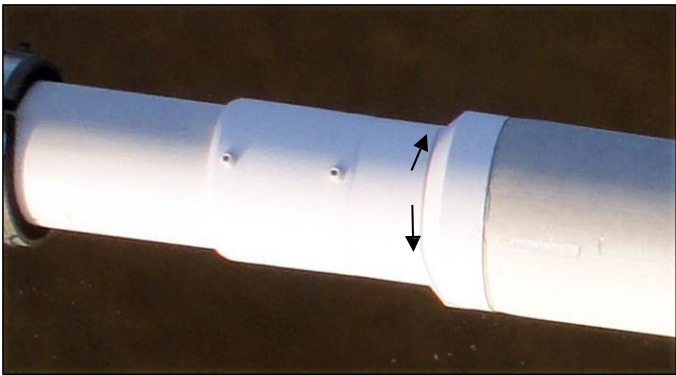
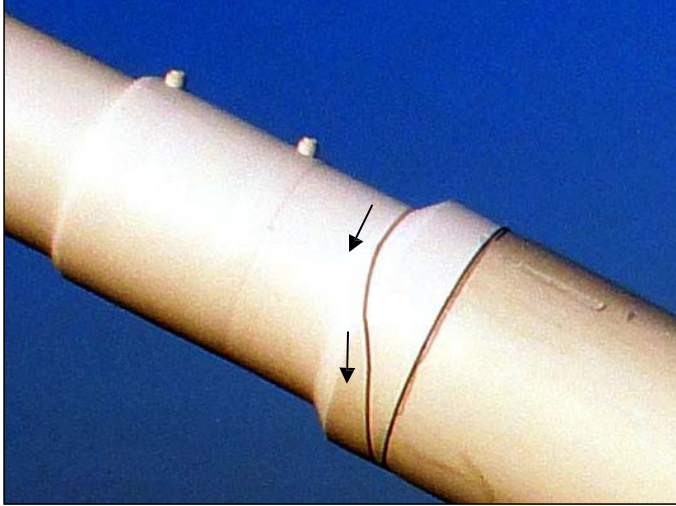


Figure 23: **B21D: Reducer Crack at Notch Located at Diameter Transition**

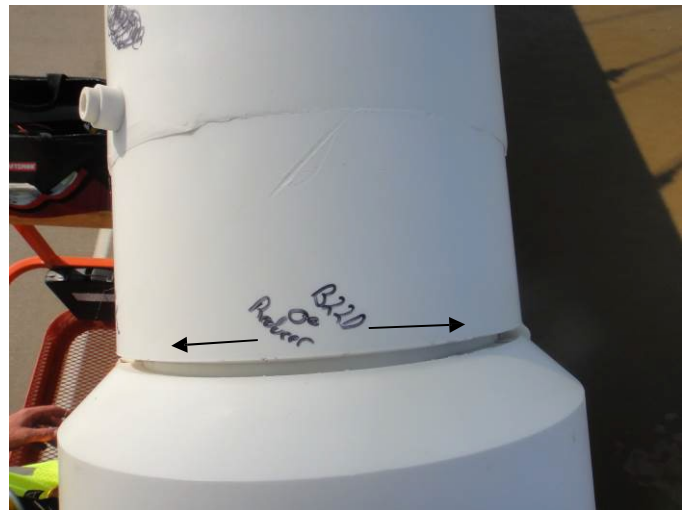


Figure 24: B22D: Reducer Crack at Notch Located at Diameter Transition



Figure 25: B230D: Reducer Crack at Notch Located at Diameter Transition

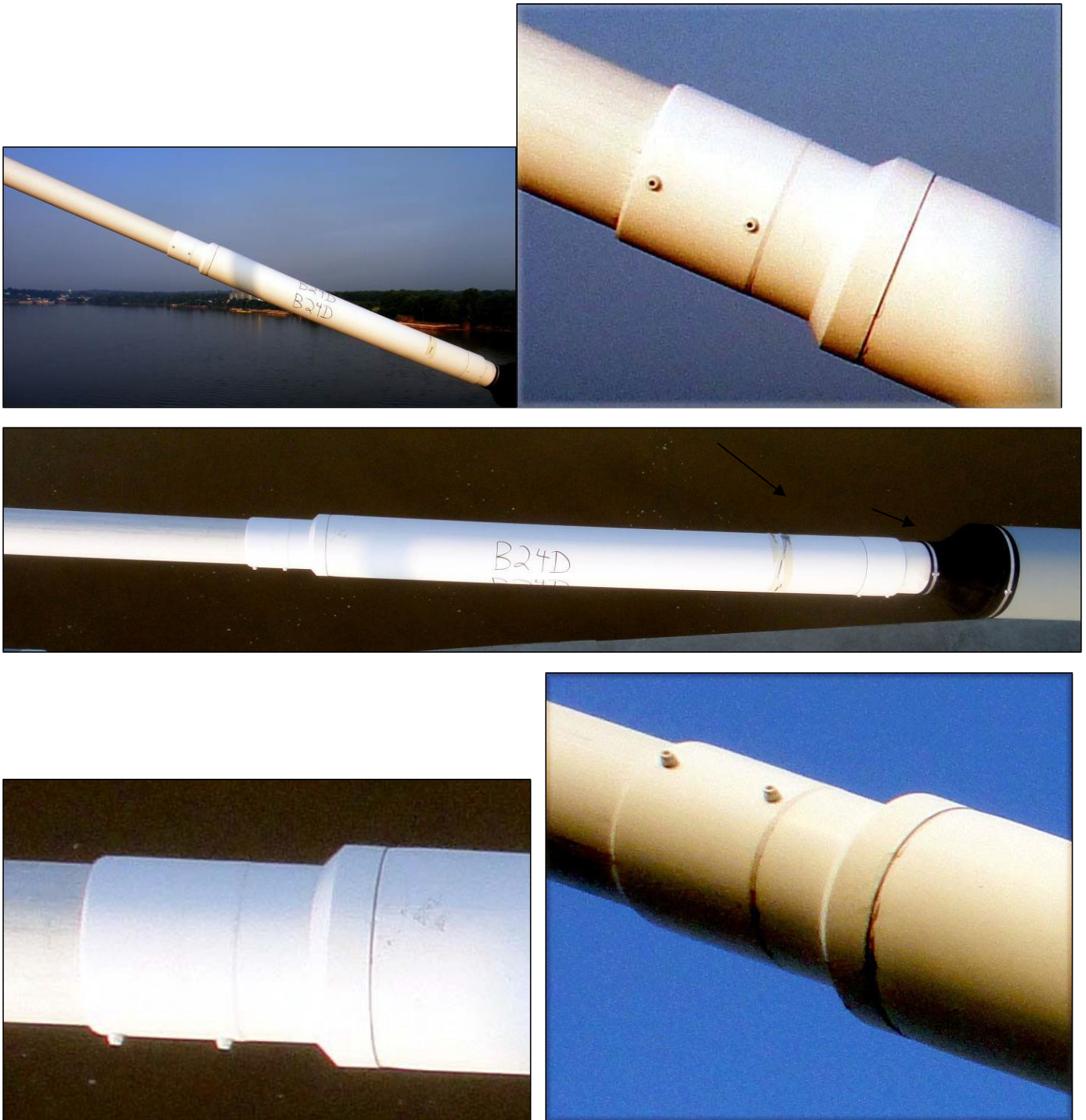


Figure 26: B24D: Reducer to Electro Weld Coupling to Stay Pipe Views (Not Cracked)



Figure 27: B5U: Reducer Crack at Fusion Butt Weld to Larger Diameter Pipe

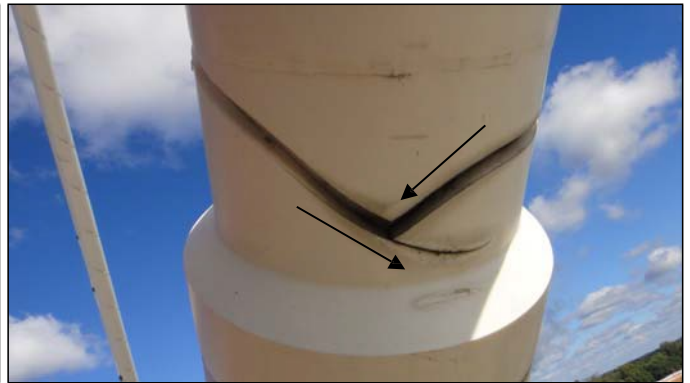
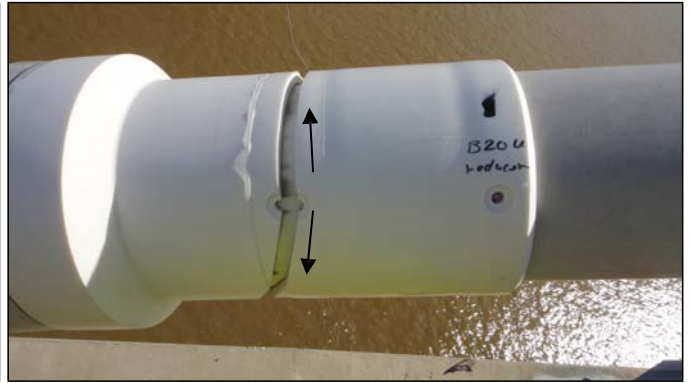


Figure 28: B20U: Top Coupler Crack at Weld Nipple Hole Propagating into and around the Reducer (Top 4 photographs) & Crack at Bottom Coupler (Bottom 2 photographs)

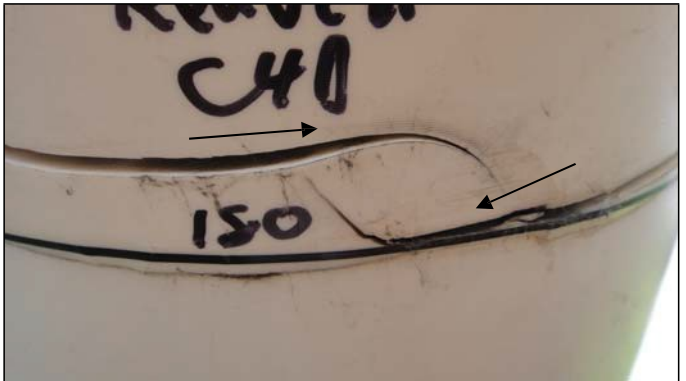
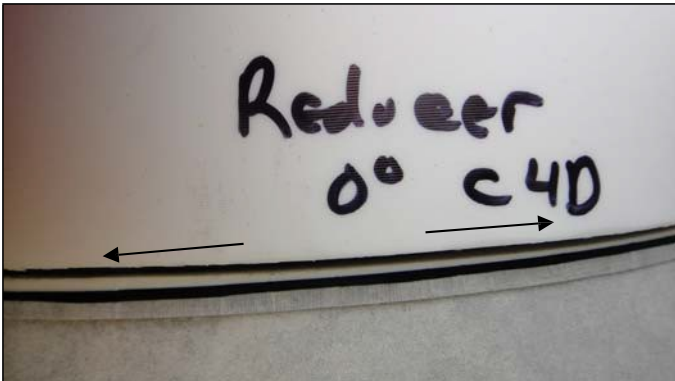
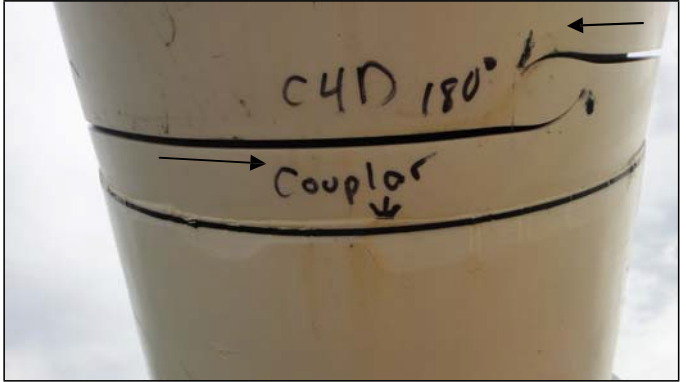
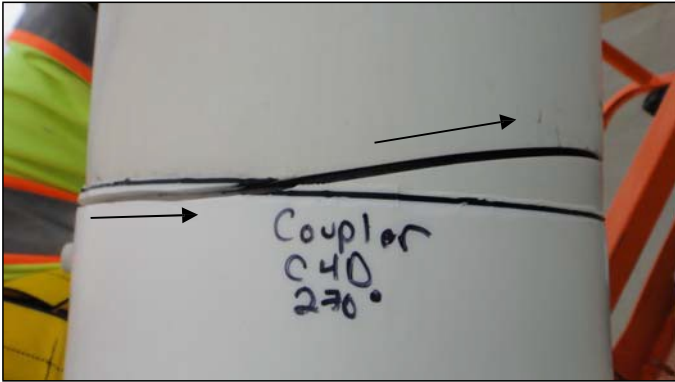


Figure 29: C4D: Bottom Coupler Crack at Butt Weld to Larger Diameter Pipe (4 photographs) & Reducer Crack at Butt Weld to Larger Diameter Pipe (Bottom 2 photographs)



Figure 30: C2U: Bottom Coupler Crack at Nipple Hole (4 photographs) & Reducer Crack at Size Transition Originating at the Top, i.e. 0° (Bottom 2 photographs)



Figure 31: C4U: Reducer Crack at Butt Weld to the Larger Diameter Pipe with Significant Vertical Displacement

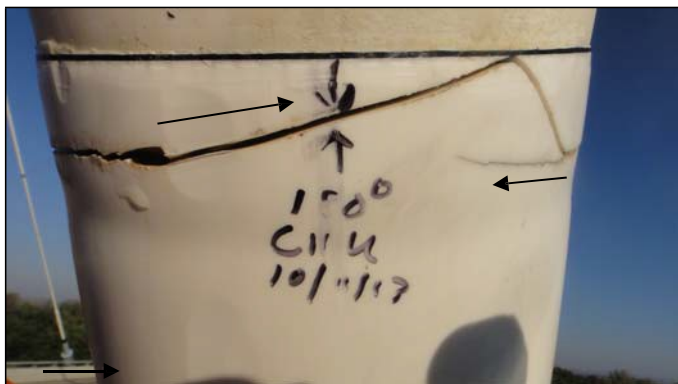
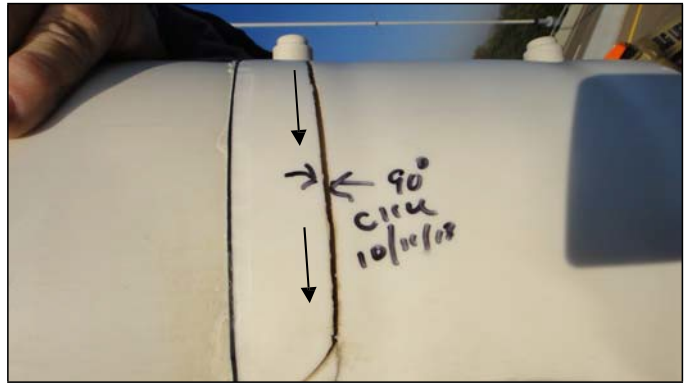
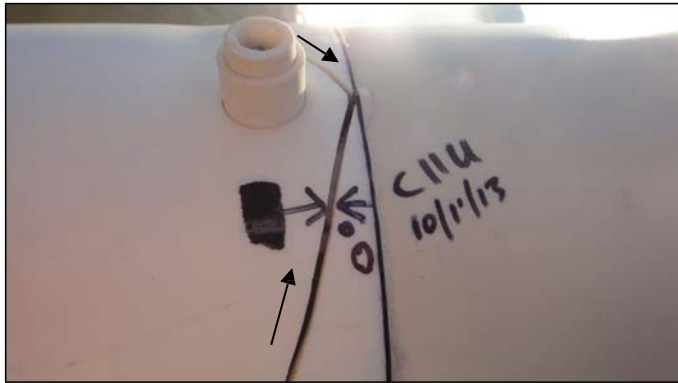
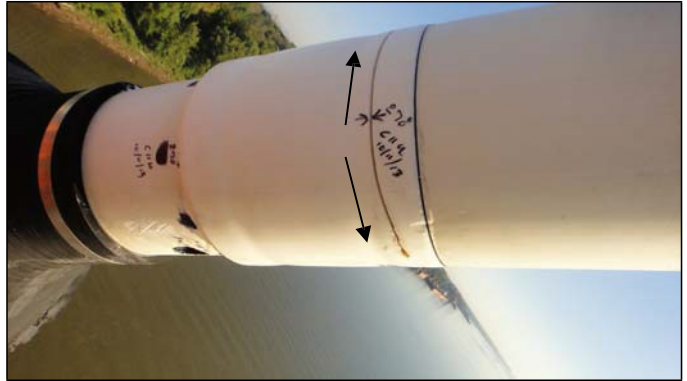
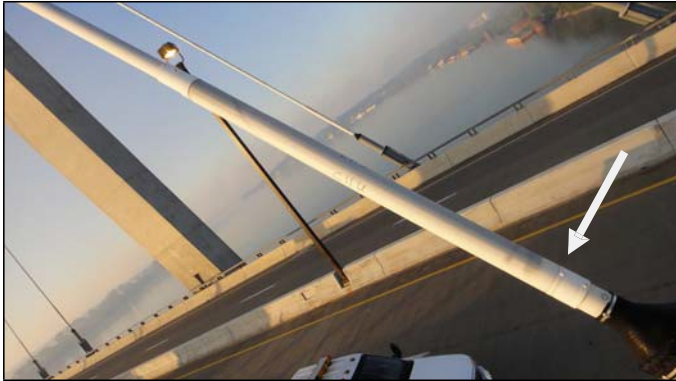


Figure 32: C11U: Bottom Coupler Crack near Butt Weld to the Larger Diameter Pipe Crack Origins at 90° and 270°

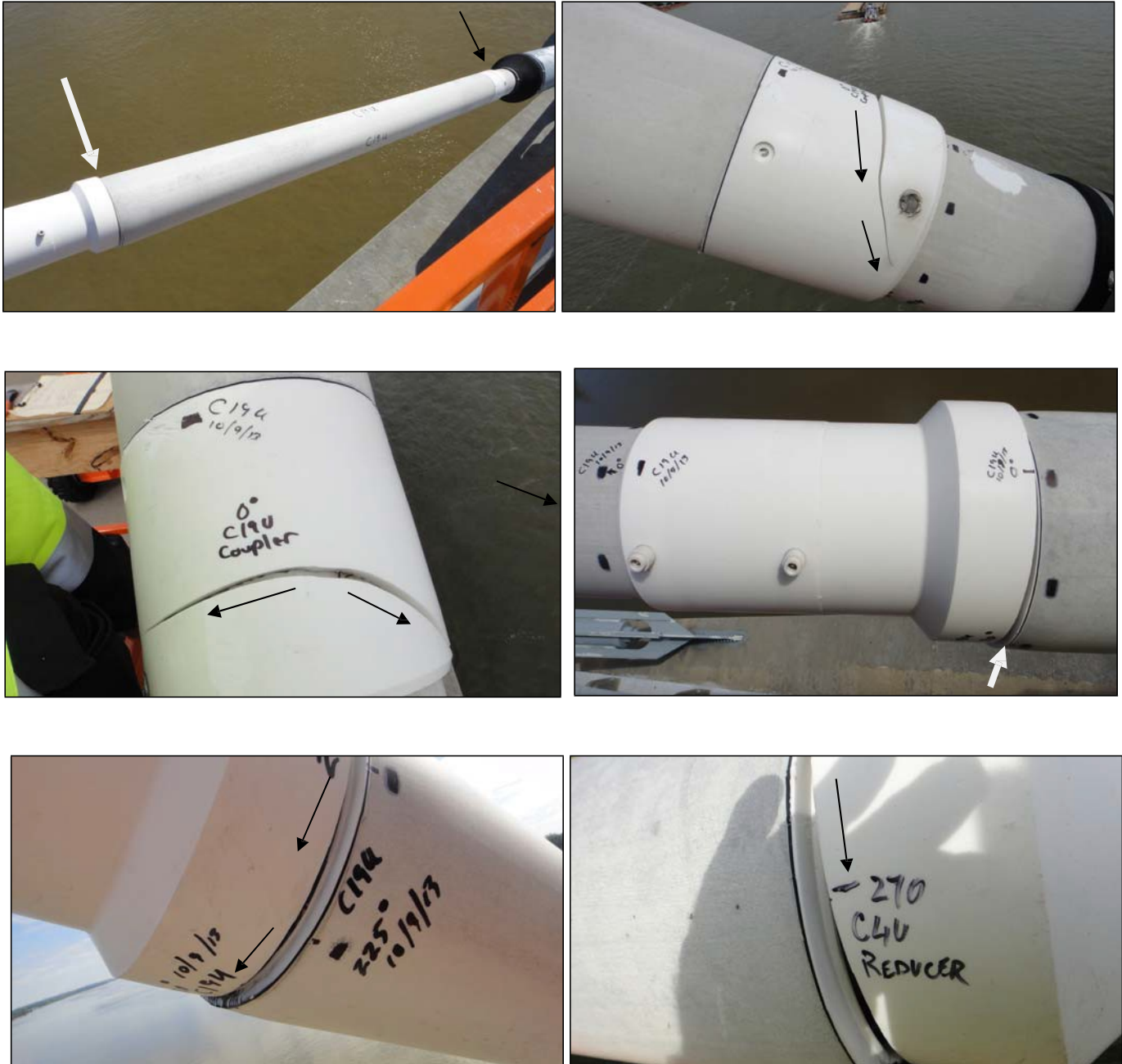


Figure 33: C19U: Bottom Coupler Crack in Middle of Specimen and Reducer Crack at Butt Weld to the Larger Diameter Pipe

**10. APPENDIX 3 Microbac Report on Analysis of HDPE
Piping Specimens from the Natcher Bridge**

TEST REPORT

CLIENT: Kentucky Transportation Center
University of Kentucky
Lexington, KY 40506
Attn: Theodore Hopwood

OBJECTIVE: Evaluate polyethylene materials and products used as bridge stay cable protectors on the Natcher Bridge in Kentucky. In support of this objective a testing protocol was devised to address the main questions proffered by the client of “why do some white HDPE piping components exhibit micro-cracking and some not?” and “does the micro-cracking pose any risk for fracture propagation into (and through) the black base HDPE?”

The following testing methodologies were proposed and (most) performed in order to develop a data set with which the overarching question could be answered:

1. Optical, Digital, and Scanning Electron Microscopy
2. Thermal Analysis by Differential Scanning Calorimetry (DSC)
 - a. ASTM D3350 “Thermal Stability”
 - b. ASTM D3895 Oxidative-Induction Time (OIT)
3. Infrared Spectroscopy (FTIR)
 - a. Carbonyl Index Testing
4. Gas Chromatography/Mass Spectroscopy (GC/MS)
 - a. Pyrolysis P-GC/MS
 - b. Evolved Gas Analysis EGA-GC/MS
 - c. Thermal Desorption TD-GC/MS
5. Liquid Chromatography (HPLC)
6. Various Polymer Materials Characterization tests per ASTM D3350
 - a. Density
 - b. Melt Flow Rate
 - c. Tensile Properties
 - d. Carbon Black (if applicable)
 - e. Stress Crack Resistance
 - i. ASTM D1693 “Bent Strip” method
 - ii. ASTM F1473 “PENT” method

The above tests were chosen as follows: In general the microscopy will allow for an understanding of the failure mode, and the DSC and FTIR testing will characterize differences in the current oxidative state of the PE materials. The GC and HPLC testing will focus on differences in the antioxidant and/or UV protection systems within the materials. Finally, the polymer testing should allow for a comparison to original materials specification requirements as well as shed light on the existing fracture progression and (possibly) future failure probability.

For any feedback concerning our services, please contact the Managing Director of the Hauser Division or Trevor Boyce, President, at trevor.boyce@microbac.com and Cabot Earle, Executive Vice President, at cabot.earle@microbac.com. This report applies only to the sample(s) tested or analyzed. This report may be copied only in its entirety, unless prior written consent has been granted by an authorized agent of the Hauser Division of Microbac Laboratories, Inc.

BACKGROUND:

The client reported that high density polyethylene (HDPE) stay cable pipe sheathing had been installed in the Winter of 2001/Spring of 2002 on the US 231 Natcher Bridge over the Ohio River between Indiana and Kentucky. Subsequent visual inspections of the bridge detected cracking on the piping. In the past five to six years, the white outer surfaces of the stay pipe sheathing have experienced cosmetic color change from a white to a dingy greyish appearance in most but not all piping segments. Upon further inspection extensive micro-cracking was also found to be in evidence, described as “map cracking” by the client. This micro-cracking is most likely the root cause of the cosmetic color change, since environmental contamination (dirt, dust, etc.) gets bound within the extensive surface fracture network, visually darkening the exterior surface.

The stay cable protection system consists of numerous HDPE components, such as coextruded (white over black) stay pipe sheathing and anchorage components consisting of connection sleeves and transition pipes. End fittings were butt fused to the connection sleeves that the client described as (electrofusion) couplers and reducers. The pipe sheathing and connection sleeve piping was manufactured by co-extrusion of white HDPE over a base black HDPE. The end fittings were presumably manufactured via injection molding, of a white only HDPE material. The couplers and reducers were first attached to the connection sleeves via butt fusion. After final installation alignments were obtained the coupler was then electrofused to the transition pipe (at the anchorage side), and in similar fashion the reducer was electrofused to the stay pipe (on the cable side) completing the assembly. Although it is possible to obtain large samples, the effort to remove stay cable protection from existing stay cables and replace with adequate corrosion protection is quite difficult in practice. As such only small “slice” or shaving samples were taken by the client and made available for analysis, excepting some larger pieces as further described in the Samples section below.

Documentation supplied by the client indicated that the plastic used to fabricate the stay pipe sheathing was a Union Carbide (Dow Chemical Co.) DGDA-2483 Black 3408. This is thus the requirement for the stay pipe sheathing black pipe sheathing base material. This Union Carbide DGDA-2483 material has an ASTM D3350 cell classification (per the then-current version of this document as of approximately 1998) of 335434C. This material will have carbon black content almost certainly greater than 2% by weight, and have adequate weathering/UV degradation resistance for prolonged outdoor service. The client also reported that the pipe sheathing was to be manufactured as a coextruded product, with white outer surface coating approximately 2mm in thickness. That document provided by the client indicated the white coextruded layer is to be “UV stabilized colored HDPE” material. The (white) coloring is almost certainly accomplished via the introduction of titanium dioxide, and an absence of carbon black in the exterior coextruded layer. Also, this same document states that “The (pipe sheathing) material provides an equivalent UV resistance as the black HDPE pipe.” As such, since no carbon black is present in the outer white layer, some additional additive should be present to achieve an equivalent UV resistance; this would typically be accomplished via the introduction of hindered amine light stabilizers (HALS).

For any feedback concerning our services, please contact the Managing Director of the Hauser Division or Trevor Boyce, President, at trevor.boyce@microbac.com and Cabot Earle, Executive Vice President, at cabot.earle@microbac.com. This report applies only to the sample(s) tested or analyzed. This report may be copied only in its entirety, unless prior written consent has been granted by an authorized agent of the Hauser Division of Microbac Laboratories, Inc.

SAMPLES: Two (2) sample sets were received from the client. The first sample set consisted of two (2) “chunks” of PE material, and thirty (30) “slices” or shavings of PE material (see Table 1). The second sample set consisted of ten (10) larger sections of PE material (see Table 2). All samples were reported by the client to have been removed from various locations on the Natcher Bridge in Kentucky. In general the bridge stays are labeled with an alphanumeric identifier (“B” for Kentucky-side Tower and “C” for Indiana-side Tower, then a sequential number for stay cable order), followed by “U” or “D” which denotes upstream or downstream installation location. Additional location sampling information is offered as “Top” or “Bottom”, which indicates 12 o’clock (upward facing) or 6 o’clock (downward facing) respectively in service on the cable, regardless of the hanging angle of the cable.

For any feedback concerning our services, please contact the Managing Director of the Hauser Division or Trevor Boyce, President, at trevor.boyce@microbac.com and Cabot Earle, Executive Vice President, at cabot.earle@microbac.com. This report applies only to the sample(s) tested or analyzed. This report may be copied only in its entirety, unless prior written consent has been granted by an authorized agent of the Hauser Division of Microbac Laboratories, Inc.

	Stay	Description	Location	Sample type
1		Sample A		chunk
2		Sample B		chunk
3	B11D	Coupler	Top	slice
4	B11D	Coupler	Bottom	slice
5	B15D	Reducer	Top	slice
6	B15D	Reducer	Bottom	slice
7	C4U	Connection Sleeve	Top	slice
8	C4U	Connection Sleeve	Bottom	slice
9	C10D	Connection Sleeve	Top	slice
10	C10D	Connection Sleeve	Bottom	slice
11	C11U	Transition Pipe	Top	slice
12	C11U	Transition Pipe	Bottom	slice
13	B3U	Transition Pipe	Top	slice
14	B3U	Transition Pipe	Bottom	slice
15	B3U	Connection Sleeve	Top	slice
16	B3U	Connection Sleeve	Bottom	slice
17	B3U	Stay Pipe	Top	slice
18	B3U	Stay Pipe	Bottom	slice
19	B3U	Reducer	Top	slice
20	B3U	Reducer	Bottom	slice
21	B3U	Coupler	Top	slice
22	B3U	Coupler	Bottom	slice
23	B3D	Transition Pipe	Top	slice
24	B3D	Transition Pipe	Bottom	slice
25	B3D	Connection Sleeve	Top	slice
26	B3D	Connection Sleeve	Bottom	slice
27	B3D	Stay Pipe	Top	slice
28	B3D	Stay Pipe	Bottom	slice
29	B3D	Reducer	Top	slice
30	B3D	Reducer	Bottom	slice
31	B3D	Coupler	Top	slice
32	B3D	Coupler	Bottom	slice

Table 1 displaying the first set of samples received from the client. Note that Samples A and B are full wall thickness co-extruded pipe, while all other samples are surface scrapings from the white material only (i.e. no black base material).

For any feedback concerning our services, please contact the Managing Director of the Hauser Division or Trevor Boyce, President, at trevor.boyce@microbac.com and Cabot Earle, Executive Vice President, at cabot.earle@microbac.com. This report applies only to the sample(s) tested or analyzed. This report may be copied only in its entirety, unless prior written consent has been granted by an authorized agent of the Hauser Division of Microbac Laboratories, Inc.

	Stay	Description	Location	Sample type
1	B3U	Connection Sleeve	Top	chunk
2	B3U	Connection Sleeve	Bottom	chunk
3	B7U	Connection Sleeve	Top	chunk
4	B7U	Connection Sleeve	Bottom	chunk
5	B11U	Connection Sleeve	Top	chunk
6	B11U	Connection Sleeve	Bottom	chunk
7	C9U	Connection Sleeve	Top	chunk
8	C9U	Connection Sleeve	Bottom	chunk
9	C24U	Connection Sleeve	Top	chunk
10	C24U	Connection Sleeve	Bottom	chunk

Table 2 displaying the second set of samples received from the client. Note that all of these samples are full wall thickness co-extruded pipe.

TESTS:

Upon receipt of the samples and physical inspection, the testing matrix was truncated either due to limited sample availability and/or a hypothesis that the data obtained would not assist in meeting the overall objective. As such the following tests were performed:

Oxidative-Induction Time (OIT) Testing:

Specimens were tested from various samples per modified ASTM D3895. The testing was conducted in general accordance with ASTM D3895-14, *Standard Test Method for Oxidative-Induction Time of Polyolefins by Differential Scanning Calorimetry*. Modifications consisted of NOT pressing a film, and testing a single replicate test specimen. Locations consisted of outer walls which had been exposed to the environment throughout its service life, and mid-walls and inner walls. The testing was performed using a ramp rate of 20°C/minute, and isothermal dwell temperature of 200°C.

For any feedback concerning our services, please contact the Managing Director of the Hauser Division or Trevor Boyce, President, at trevor.boyce@microbac.com and Cabot Earle, Executive Vice President, at cabot.earle@microbac.com. This report applies only to the sample(s) tested or analyzed. This report may be copied only in its entirety, unless prior written consent has been granted by an authorized agent of the Hauser Division of Microbac Laboratories, Inc.

Thermal Desorption Gas Chromatography/Mass Spectrometry (TD GC/MS)**Testing:**

Specimens were tested from various samples using a Frontier PY-3030D Multi-Mode Pyrolyzer attached to the injection port of a Hewlett-Packard 6890 gas chromatograph coupled to a 5973 mass spectrometer. Detection of polymeric hindered-amine light stabilizers (HALS) was conducted by two separate but complementary methods. Due to the lack of a suitable laboratory control sample (LCS) two methods were used to validate the results:

Coulier Method:

Following the method shown in Coulier, L.; Kaal, E.R.; Tienstra, M.; and Hankemeier, Th. Identification and Quantification of (Polymeric) Hindered-Amine Light Stabilizers in Polymers Using Pyrolysis-Gas-Chromatography-Mass Spectrometry and Liquid Chromatography-Ultraviolet Absorbance Detection-Evaporative Light Scattering Detection. *J. Chromatogr. A*, 2005, 1062, 227-238., approximately 0.001 grams of sample was added to an eco-cup. The eco-cup was placed in the Frontier unit and thermally desorbed at 590°C. All of the volatilized chemicals in the specimen were swept onto the injection port of the GC/MS. Organic compounds detected were identified using a NIST mass spectral database with match quality determined by probability-based match algorithm. The HALS were identified by the major ions and retention times listed in the method.

Kimura Method:

Modifying the method shown in Kimura, K.; Yoshikawa, T.; Taguchi, Y.; Ishida, Y.; Ohtani, H.; Tsuge, S. Direct Determination of a Polymeric Hindered Amine Light Stabilizer in Polypropylene by thermal desorption-Gas Chromatography Assisted by In-line Chemical Reaction., *The Analyst*, 2000, 125, 465-468., approximately 0.001 grams of sample and 5µL of tetramethylammonium hydroxide (TMAH) 25% wt in methanol was added to an eco-cup. The eco-cup was placed in the Frontier unit and thermally desorbed at 300°C. All of the volatilized chemicals in the specimen were swept onto the injection port of the GC/MS. Organic compounds detected were identified using a NIST mass spectral database with match quality determined by probability-based match algorithm. The HALS were identified by the major ion fragments identified in the method.

For any feedback concerning our services, please contact the Managing Director of the Hauser Division or Trevor Boyce, President, at trevor.boyce@microbac.com and Cabot Earle, Executive Vice President, at cabot.earle@microbac.com. This report applies only to the sample(s) tested or analyzed. This report may be copied only in its entirety, unless prior written consent has been granted by an authorized agent of the Hauser Division of Microbac Laboratories, Inc.

High Performance Liquid Chromatography (HPLC) Testing:

Specimens were tested from various samples. A testing methodology was developed based on ASTM D 6953-03, *Determination of Antioxidants and Erucamide Slip Additives in Polyethylene Using Liquid Chromatography*. Samples were milled and extracted with an appropriate solvent, then analyzed using an Agilent 1100 HPLC instrument. A concentration calibration curve was prepared for quantifying reported compounds.

Stress Crack Resistance (SCR)/Slow Crack Growth (SCG) Resistance (via PENT) Testing:

Specimens were tested from various samples in accordance with ASTM F1473-13, *Standard Test Method for Notch Tensile Test to Measure the Resistance to Slow Crack Growth of Polyethylene Pipes and Resins*. Specimens were removed from the connection sleeve pipe sections (black base material only; coextruded white surface layers removed) and tested using a 2.4 MPa (348 psi) test stress at 80°C.

For any feedback concerning our services, please contact the Managing Director of the Hauser Division or Trevor Boyce, President, at trevor.boyce@microbac.com and Cabot Earle, Executive Vice President, at cabot.earle@microbac.com. This report applies only to the sample(s) tested or analyzed. This report may be copied only in its entirety, unless prior written consent has been granted by an authorized agent of the Hauser Division of Microbac Laboratories, Inc.

RESULTS: ASTM D3895 Oxidative Induction Time (OIT) Results:

	Stay	Description	Location	Sample type	OIT (min)
1		Sample A	Outer	chunk	17.0
			Middle		18.7
			Inner		16.9
2		Sample B	Outer	chunk	0.1
			Middle		55.5
			Inner		24.3
13	B3U	Transition Pipe	Top	slice	0.1
14	B3U	Transition Pipe	Bottom	slice	0.1
15	B3U	Connection Sleeve	Top	slice	0.2
16	B3U	Connection Sleeve	Bottom	slice	0.1
17	B3U	Stay Pipe	Top	slice	0.1
18	B3U	Stay Pipe	Bottom	slice	0.1
19	B3U	Reducer	Top	slice	6.4
20	B3U	Reducer	Bottom	slice	5.6
21	B3U	Coupler	Top	slice	0.2
22	B3U	Coupler	Bottom	slice	0.1
23	B3D	Transition Pipe	Top	slice	0.1
24	B3D	Transition Pipe	Bottom	slice	3.8
25	B3D	Connection Sleeve	Top	slice	0.1
26	B3D	Connection Sleeve	Bottom	slice	0.1
27	B3D	Stay Pipe	Top	slice	0.1
28	B3D	Stay Pipe	Bottom	slice	0.1
29	B3D	Reducer	Top	slice	0.1
30	B3D	Reducer	Bottom	slice	0.1
31	B3D	Coupler	Top	slice	0.1
32	B3D	Coupler	Bottom	slice	0.1
33	B3U	Connection Sleeve	Top	chunk	20.7
34	B3U	Connection Sleeve	Bottom	chunk	34.7
35	B7U	Connection Sleeve	Top	chunk	
36	B7U	Connection Sleeve	Bottom	chunk	
37	B11U	Connection Sleeve	Top	chunk	0.2
38	B11U	Connection Sleeve	Bottom	chunk	25.8
39	C9U	Connection Sleeve	Top	chunk	0.2
40	C9U	Connection Sleeve	Bottom	chunk	0.3
41	C24U	Connection Sleeve	Top	chunk	
42	C24U	Connection Sleeve	Bottom	chunk	32.6

Table 3 displaying the OIT test results for the complete group of samples. Within Table 3 blank cells within the OIT results column represent a sample which was not tested. For Samples A and B (1 and 2 respectively) the inner and middle sample locations are black base HDPE material, and the outer location is the white outer layer. For Samples 33 through 42 the test results are from the white outer layer.

For any feedback concerning our services, please contact the Managing Director of the Hauser Division or Trevor Boyce, President, at trevor.boyce@microbac.com and Cabot Earle, Executive Vice President, at cabot.earle@microbac.com. This report applies only to the sample(s) tested or analyzed. This report may be copied only in its entirety, unless prior written consent has been granted by an authorized agent of the Hauser Division of Microbac Laboratories, Inc.

**Thermal Desorption Gas Chromatography/Mass Spectrometry (TD GC/MS)
 Testing Results:**

Coulier Method Results:

The resulting chromatogram for sample B11U-Bottom (Sample 38) is shown in Figure 1. The resulting chromatogram of sample B11U-Top (Sample 37) is shown in Figure 2.

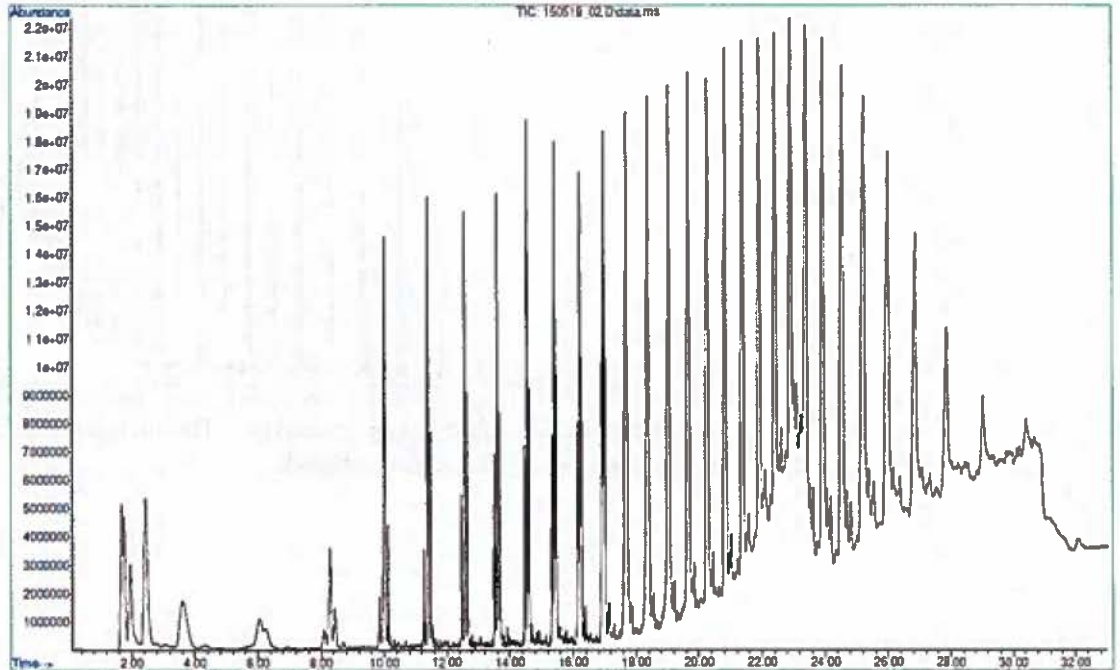


Figure 1 displaying the Gas Chromatogram of B11U-Bottom (Sample 38) after thermal degradation at 590°C using the Coulier method.

For any feedback concerning our services, please contact the Managing Director of the Hauser Division or Trevor Boyce, President, at trevor.boyce@microbac.com and Cabot Earle, Executive Vice President, at cabot.earle@microbac.com. This report applies only to the sample(s) tested or analyzed. This report may be copied only in its entirety, unless prior written consent has been granted by an authorized agent of the Hauser Division of Microbac Laboratories, Inc.

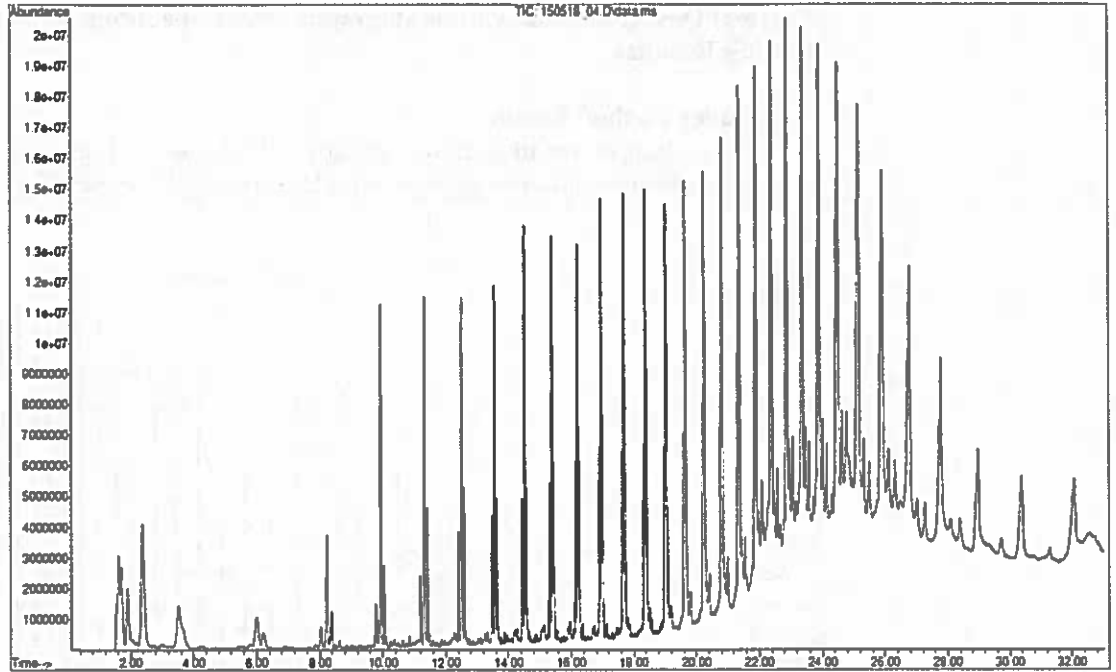


Figure 2 displaying the Gas Chromatogram of B11U-Top (Sample 37) after thermal degradation at 590°C using the Coulter method.

For any feedback concerning our services, please contact the Managing Director of the Hauser Division or Trevor Boyce, President, at trevor.boyce@microbac.com and Cabot Earle, Executive Vice President, at cabot.earle@microbac.com. This report applies only to the sample(s) tested or analyzed. This report may be copied only in its entirety, unless prior written consent has been granted by an authorized agent of the Hauser Division of Microbac Laboratories, Inc.

Kimura Method Results:

The resulting chromatogram for sample B11U-Bottom (Sample 38) is shown in Figure 3. The resulting chromatogram of sample B11U-Top (Sample 37) is shown in Figure 4.

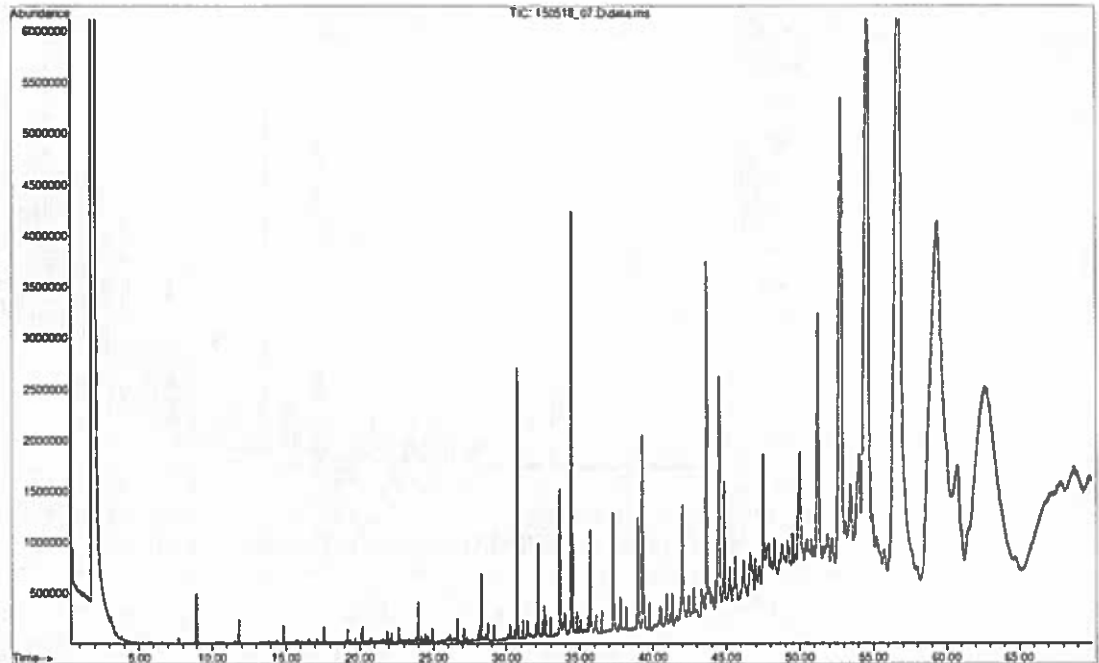


Figure 3 Gas Chromatogram of B11U-Bottom (Sample 38) after thermal degradation at 300°C in the presence of TMAH using the Kimura method.

For any feedback concerning our services, please contact the Managing Director of the Hauser Division or Trevor Boyce, President, at trevor.boyce@microbac.com and Cabot Earle, Executive Vice President, at cabot.earle@microbac.com. This report applies only to the sample(s) tested or analyzed. This report may be copied only in its entirety, unless prior written consent has been granted by an authorized agent of the Hauser Division of Microbac Laboratories, Inc.

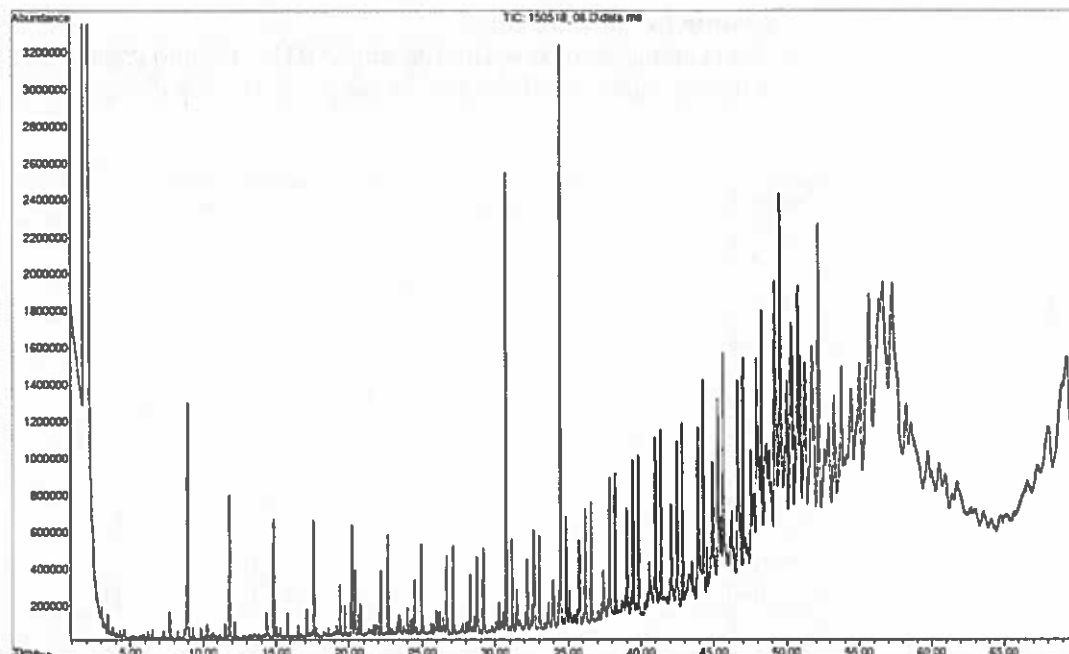


Figure 4 Gas Chromatogram of B11U-Top (Sample 37) after thermal degradation at 300°C in the presence of TMAH using the Kimura method.

HALS were not detected in either method using the major ions and retention times stated in the respective methods. Within the Coulter method hindered amine light stabilizers (HALS) were not present based on (a lack of) identification of characteristic pyrolysis products via selected ion extraction. Within the Kimura method HALS were not present based on (a lack of) identification of methoxylated or hydroxylated substituted piperidine compounds.

Both samples are very similar in chemical composition and were identified as high density polyethylene (HDPE) by software algorithm.

For any feedback concerning our services, please contact the Managing Director of the Hauser Division or Trevor Boyce, President, at trevor.boyce@microbac.com and Cabot Earle, Executive Vice President, at cabot.earle@microbac.com. This report applies only to the sample(s) tested or analyzed. This report may be copied only in its entirety, unless prior written consent has been granted by an authorized agent of the Hauser Division of Microbac Laboratories, Inc.

High Performance Liquid Chromatography (HPLC) Testing Results:

The coextruded white layer was milled off of the larger “chunk” samples and tested for antioxidant (AO) concentration by (modified) ASTM D6953. The test results for the individual AO’s as well as the total AO concentration (all results in ppm) are displayed in Table 4 below.

	Stay	Description	Location	Sample type	Irganox 3114	Irganox 1010	Irganox 1076	Irgafos 168	Total AO
33	B3U	Connection Sleeve	Top	chunk		15		169	183
34	B3U	Connection Sleeve	Bottom	chunk		40		573	613
35	B7U	Connection Sleeve	Top	chunk	105	2163		1054	3322
36	B7U	Connection Sleeve	Bottom	chunk		400		715	1115
37	B11U	Connection Sleeve	Top	chunk		187			187
38	B11U	Connection Sleeve	Bottom	chunk					0
39	C9U	Connection Sleeve	Top	chunk		35		117	152
40	C9U	Connection Sleeve	Bottom	chunk		17			17
41	C24U	Connection Sleeve	Top	chunk				267	267
42	C24U	Connection Sleeve	Bottom	chunk				477	477

Table 4 displaying the antioxidant concentration in the coextruded white layer of the larger “chunk” samples tested.

Stress Crack Resistance (SCR)/Slow Crack Growth (SCG) Resistance (via PENT) Testing Results:

The coextruded white layer was milled off of the larger “chunk” samples, and the black pipe material was then tested for stress crack resistance (SCR) per ASTM F1473. The test results for the single replicate from each sample tested (all results in hours) are displayed in Table 5 below.

	Stay	Description	Location	Sample type	SCR (hr)
33	B3U	Connection Sleeve	Top	chunk	21.9
34	B3U	Connection Sleeve	Bottom	chunk	25.2
35	B7U	Connection Sleeve	Top	chunk	>1000
36	B7U	Connection Sleeve	Bottom	chunk	>1000
37	B11U	Connection Sleeve	Top	chunk	>1000
38	B11U	Connection Sleeve	Bottom	chunk	>1000
39	C9U	Connection Sleeve	Top	chunk	>1000
40	C9U	Connection Sleeve	Bottom	chunk	>1000
41	C24U	Connection Sleeve	Top	chunk	38.2
42	C24U	Connection Sleeve	Bottom	chunk	39.0

Table 5 displaying the stress crack resistance of the black HDPE base layer of the larger “chunk” samples tested.

For any feedback concerning our services, please contact the Managing Director of the Hauser Division or Trevor Boyce, President, at trevor.boyce@microbac.com and Cabot Earle, Executive Vice President, at cabot.earle@microbac.com. This report applies only to the sample(s) tested or analyzed. This report may be copied only in its entirety, unless prior written consent has been granted by an authorized agent of the Hauser Division of Microbac Laboratories, Inc.

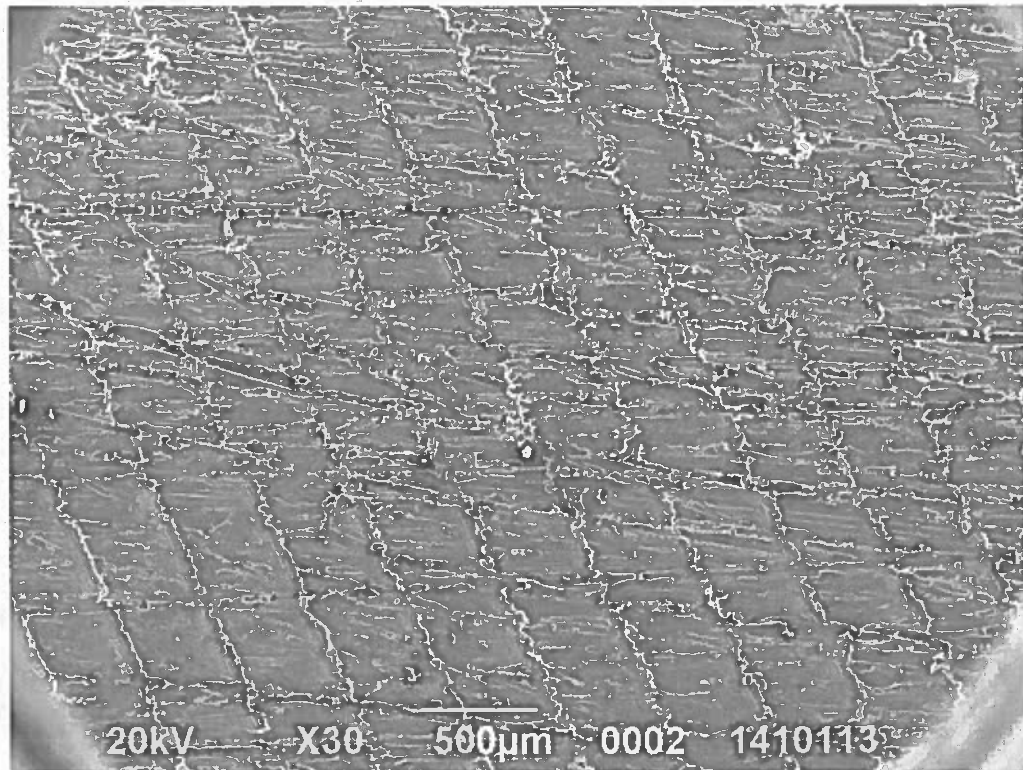


Figure 5 above displays a scanning electron microscope (SEM) image of Sample A. Note high level of surface topography, which is most likely attributed the originally manufactured surface, or to abrasion or some yet to be determined secondary damage.

For any feedback concerning our services, please contact the Managing Director of the Hauser Division or Trevor Boyce, President, at trevor.boyce@microbac.com and Cabot Earle, Executive Vice President, at cabot.earle@microbac.com. This report applies only to the sample(s) tested or analyzed. This report may be copied only in its entirety, unless prior written consent has been granted by an authorized agent of the Hauser Division of Microbac Laboratories, Inc.

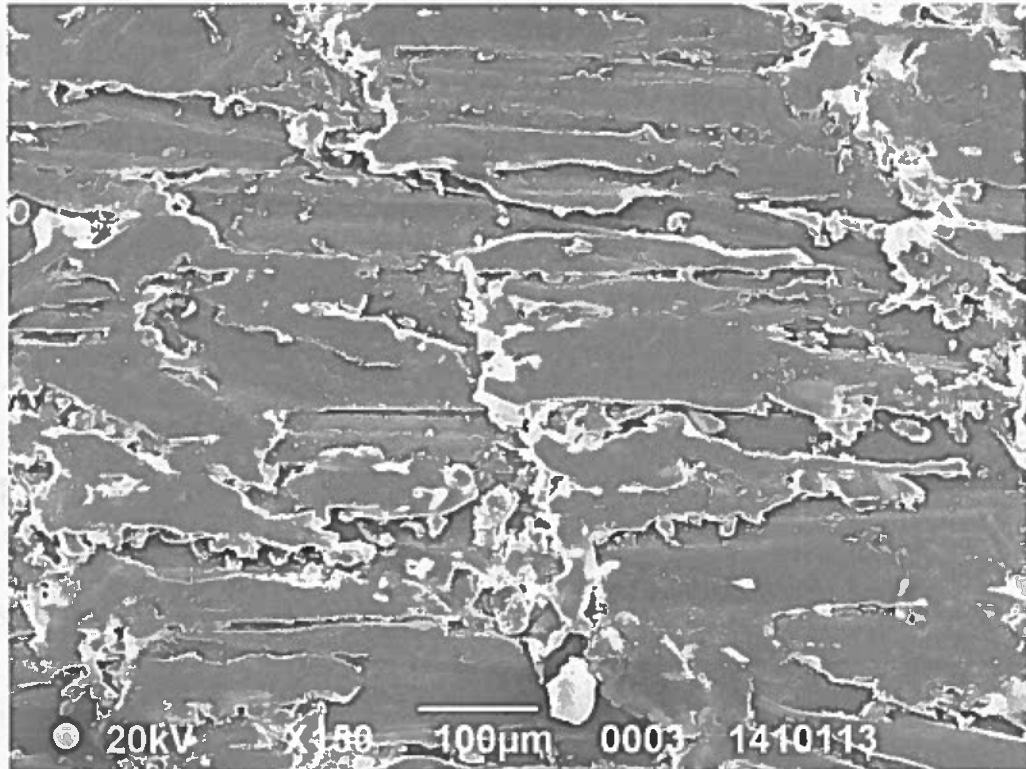


Figure 6 above displays a scanning electron microscope (SEM) image of Sample A, taken at higher magnification from the approximate center of Figure 5. Note surface adhered debris within the abrasion (or some yet to be determined secondary damage).

For any feedback concerning our services, please contact the Managing Director of the Hauser Division or Trevor Boyce, President, at trevor.boyce@microbac.com and Cabot Earle, Executive Vice President, at cabot.earle@microbac.com. This report applies only to the sample(s) tested or analyzed. This report may be copied only in its entirety, unless prior written consent has been granted by an authorized agent of the Hauser Division of Microbac Laboratories, Inc.

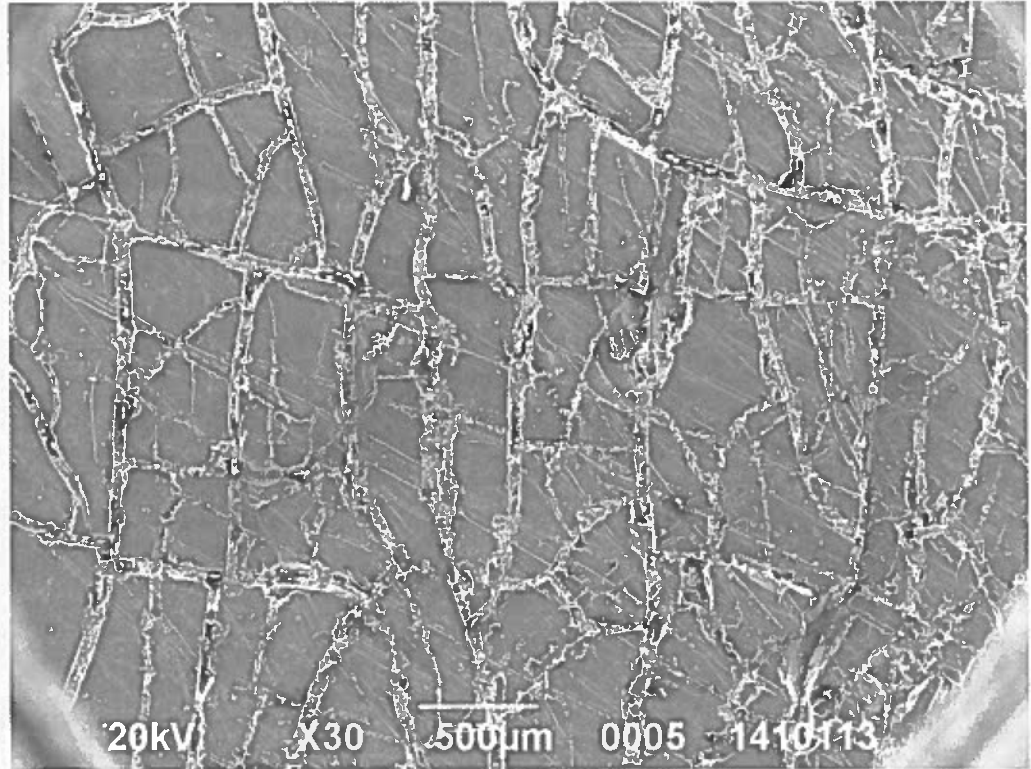


Figure 7 above displays a scanning electron microscope (SEM) image of Sample B. Note extensive micro-cracking networking (“Map Cracking”).

For any feedback concerning our services, please contact the Managing Director of the Hauser Division or Trevor Boyce, President, at trevor.boyce@microbac.com and Cabot Earle, Executive Vice President, at cabot.earle@microbac.com. This report applies only to the sample(s) tested or analyzed. This report may be copied only in its entirety, unless prior written consent has been granted by an authorized agent of the Hauser Division of Microbac Laboratories, Inc.

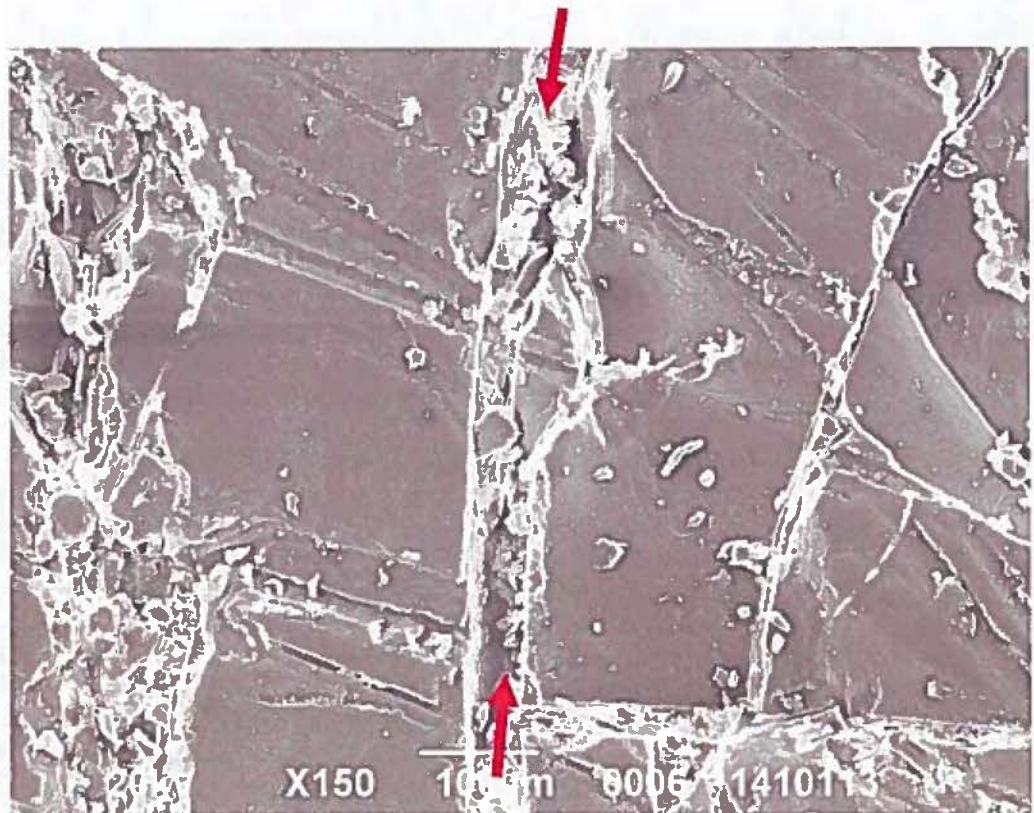


Figure 8 above displays a scanning electron microscope (SEM) image of Sample B, taken at higher magnification from the approximate center of Figure 7. Note debris trapped within the extensive micro-cracking ("Map Cracking") network (e.g. between red arrows).

Detailed test results for all tests performed are available within the project file.

For any feedback concerning our services, please contact the Managing Director of the Hauser Division or Trevor Boyce, President, at trevor.boyce@microbac.com and Cabot Earle, Executive Vice President, at cabot.earle@microbac.com. This report applies only to the sample(s) tested or analyzed. This report may be copied only in its entirety, unless prior written consent has been granted by an authorized agent of the Hauser Division of Microbac Laboratories, Inc.

INTERPRETATION AND CONCLUSIONS:**General:**

In all cases, the use of the test results from the testing methodologies detailed above should be understood to be used for the purpose of understanding the condition of the samples as tested and described herein. In general the assessment of the existing OIT performance, existing AO concentration, and existing SCR performance of the samples is essentially only a limited, although valuable, single point inspection. This assessment is meant as a potential aid to be used in decision-making by the asset owner(s) regarding the potential need for and utility of further investigations and/or other actions. These results are indicative of the condition of the samples received, and more detailed investigations would be required to produce more broad and/or conclusive results.

ASTM D3895 Oxidative Induction Time (OIT) Tests:

Laboratory experience as well as public-domain literature sources typically indicate Oxidative Induction Time (OIT) values at the inner surface of less than 3.0 minutes duration to be consistent with lack of or complete exhaustion of the antioxidant package within PE materials. Additionally, laboratory experience and industry consensus typically indicate OIT values between 3.0 and approximately 10.0 minutes duration to be low in comparison to well stabilized PE materials. It should however be noted that the majority of OIT test results portrayed within this report were obtained from the outer wall of the (white) pipe sheathing which had been exposed to UV radiation throughout the service life of the product. Finally, inner or midwall OIT values of greater than approximately 30+ minutes would typically be considered to be indicative of well stabilized material.

Of significance within the results, the majority of the test results are quite low. This essentially indicates a complete lack of thermal stabilization in the location tested (typically outer wall). In contrast the black base HDPE materials appear to be well stabilized. Some examples of adequate retained thermal stabilization exist (B3U Top and Bottom; Samples 33 and 34) but these are the rare exception. Additionally, bottom locations (with lower UV exposure) typically perform better within the OIT test as expected. Finally, there appears to be no correlation of indicated OIT and field map cracking presence or absence (e.g. B3D Transition Pipe with good still-white field performance and low OIT of 0.1 minute at the Top location).

For any feedback concerning our services, please contact the Managing Director of the Hauser Division or Trevor Boyce, President, at trevor.boyce@microbac.com and Cabot Earle, Executive Vice President, at cabot.earle@microbac.com. This report applies only to the sample(s) tested or analyzed. This report may be copied only in its entirety, unless prior written consent has been granted by an authorized agent of the Hauser Division of Microbac Laboratories, Inc.

Thermal Desorption Gas Chromatography/Mass Spectrometry (TD GC/MS)**Tests:**

It should be noted that the samples tested for HALS via TD GC/MS were the white coextruded outer layer of the larger sections received in the second group of samples only. The material tested would thus have contained significantly affected outer surface materials (i.e. with Map Cracking), as well as the unaffected (or less affected) material below in this approximately 2mm thick white layer. No black PE material was tested in this manner. HALS were not detected via either method using the major ions and retention times stated in the respective methods. Both samples are very similar in chemical composition and were identified as high density polyethylene (HDPE) by software algorithm. Since no HALS were detected whatsoever, the only conclusion that can be drawn is that the white coextruded layer never contained any purposeful addition of HALS for UV resistance.

High Performance Liquid Chromatography (HPLC) Tests:

Similar to the TD GC/MS testing described above, it should be noted that the samples tested for AO via HPLC were the white coextruded outer layer of the larger sections received in the second group of samples only. The material tested would thus have contained significantly affected outer surface materials (i.e. with Map Cracking), as well as the unaffected (or less affected) material below in this approximately 2mm thick white layer. No black PE material was tested in this manner. Antioxidant concentrations were determined, with results essentially segregated into two groups of well stabilized materials (B7U) and poorly (un)stabilized materials (B11U and C9U). Finally, there appears to be no correlation of indicated AO level and field map cracking presence or absence (e.g. C24U Bottom with high OIT of 32.6 minutes and low AO concentration).

Stress Crack Resistance (SCR)/Slow Crack Growth (SCG) Resistance (via PENT)**Tests:**

First, contrary to the TD GC/MS and HPLC testing described above, it should be noted that the samples tested for SCR via PENT were the black inner layer of the larger sections received in the second group of samples only. No white coextruded PE material was tested in this manner (mainly because it would be impossible to prepare a sample from the thin coextruded white layer). Stress Crack Resistance (SCR) performance were determined, with results essentially segregated into two groups of well performing materials (B7U and B11U) and less-well performing materials (B3U and C24U). Overall, if less well performing material stress crack resistance can be correlated with an absence of through wall cracking in empirical field performance, this could be used to establish that the 20-40 hour SCR is enough to stop the map cracking from penetrating into and through the wall of the black base HDPE pipe.

At the time of installation of the PE stay cable protection system, the then-current ASTM D3350 cell classification testing methodology for stress crack resistance was the Bent-Strip method, ASTM D1693. This testing methodology, while currently still valid, has essentially been supplanted by the ASTM F1473 PENT testing methodology for pipe grade resins. As a general rule, the ASTM D1693 test is not typically performed, since the stress crack resistance of current vintage resins cannot be characterized by this testing methodology. As such ASTM F1473 was performed on the samples as reported herein. However, no firm correlation exists between ASTM D1693 test data (and requirements) and ASTM F1473 test data (and requirements). The original cell classification in place circa 1998 for the Union Carbide (Dow) DGDA-2483 Black 3408 material was an ASTM F1693 test result of $F_0 > 1500$ hours (i.e. no failures in less than 1500 hours of test). Again, while no firm correlation exists, this would be expected to be comparable to a 25-100 hour PENT test result.

Figure 9 tabulates the qualitatively interpreted comparison results for all in-depth testing performed on Samples B3U, B7U, B11U, C9U, and C24U and Figures 10 through 14 tabulate the test results for the in-depth testing.

	OIT	AO	SCR
B3U	Low	Low	Low
B7U		High	High
B11U	Mid	Low	High
C9U	Low	Low	High
C24U	High	Low	Low

Figure 9 displaying qualitatively interpreted comparison results for all in-depth testing performed on Samples B3U, B7U, B11U, C9U, and C24U.

White Outer Coextruded Layer						Black Inner Coextruded Layer						
	Stay	Description	Location	Sample type	OIT (min)	Stay	Description	Location	Sample type	Total AO	SCR (hr)	
17	B3U	Stay Pipe	Top	slice	0.1	33	B3U	Connection Sleeve	Top	chunk	187	21.9
18	B3U	Stay Pipe	Bottom	slice	0.1	34	B3U	Connection Sleeve	Bottom	chunk	0	25.2

Figure 10 displaying composite summary results for all testing performed on Sample B3U.

White Outer Coextruded Layer						Black Inner Coextruded Layer	
	Stay	Description	Location	Sample type	OIT (min)	Total AO	SCR (hr)
35	B7U	Connection Sleeve	Top	chunk		3322	>1000
36	B7U	Connection Sleeve	Bottom	chunk		1115	>1000

Figure 11 displaying composite summary results for all testing performed on Sample B7U.

For any feedback concerning our services, please contact the Managing Director of the Hauser Division or Trevor Boyce, President, at trevor.boyce@microbac.com and Cabot Earle, Executive Vice President, at cabot.earle@microbac.com. This report applies only to the sample(s) tested or analyzed. This report may be copied only in its entirety, unless prior written consent has been granted by an authorized agent of the Hauser Division of Microbac Laboratories, Inc.

White Outer Coextruded Layer						Black Inner Coextruded Layer	
	Stay	Description	Location	Sample type	OIT (min)	Total AO	SCR (hr)
37	B11U	Connection Sleeve	Top	chunk	0.2	187	>1000
38	B11U	Connection Sleeve	Bottom	chunk	25.8	0	>1000

Figure 12 displaying composite summary results for all testing performed on Sample B11U.

White Outer Coextruded Layer						Black Inner Coextruded Layer	
	Stay	Description	Location	Sample type	OIT (min)	Total AO	SCR (hr)
39	C9U	Connection Sleeve	Top	chunk	0.2	152	>1000
40	C9U	Connection Sleeve	Bottom	chunk	0.3	17	>1000

Figure 13 displaying composite summary results for all testing performed on Sample C9U.

White Outer Coextruded Layer						Black Inner Coextruded Layer	
	Stay	Description	Location	Sample type	OIT (min)	Total AO	SCR (hr)
41	C24U	Connection Sleeve	Top	chunk		267	38.2
42	C24U	Connection Sleeve	Bottom	chunk	32.6	477	39.0

Figure 14 displaying composite summary results for all testing performed on Sample C24U.

Based on the cumulative body of test results reported herein, one can conclude the following:

1. The white coextruded material (and/or white base material for those samples not manufactured via coextrusion) displays evidence of UV exposure-induced degradation (via outdoor weathering) as evidenced by Map Cracking, which has occurred within approximately ten years of service.
2. The white coextruded material (and/or white base material for those samples not manufactured via coextrusion) displays very poor oxidation resistance as evidenced by very low OIT test results, although some few examples of higher OIT performance are in evidence.
3. The white coextruded material appears to NOT contain any HALS, which would be the typical additive used to stabilize white (non-black) PE materials used in outdoor service applications.
4. The white coextruded material contains varying levels of antioxidants (AO), from poorly-stabilized to well-stabilized.
5. The black pipe sheathing base material displays adequate to good oxidation resistance as evidenced by OIT test results from 19 to 56 minutes.
6. The black pipe sheathing base material displays varying levels of stress crack resistance (SCR) performance, from less well-performing (22-39 hours) to well-performing (>1000 hours).

For any feedback concerning our services, please contact the Managing Director of the Hauser Division or Trevor Boyce, President, at trevor.boyce@microbac.com and Cabot Earle, Executive Vice President, at cabot.earle@microbac.com. This report applies only to the sample(s) tested or analyzed. This report may be copied only in its entirety, unless prior written consent has been granted by an authorized agent of the Hauser Division of Microbac Laboratories, Inc.

The cumulative high-level takeaways from this testing program would be:

7. In general the white coextruded (or otherwise manufactured) material is NOT suitably stabilized for use within an outdoor service environment.
8. It is surmised that multiple different white materials were used in the manufacture of the products used within the stay cable protection system.
9. It is surmised that multiple different black materials were used in the manufacture of the products used within the stay cable protection system.
10. Through wall fractures initiating in the compromised white coextruded layer may arrest in the black material, with higher probability of this occurring for those black base materials with well-performing SCR (i.e. >1000 hours).
11. It should be noted that some system components, specifically the molded couplers and reducers, display acceptable field performance (i.e. they do NOT show map cracking and related weathering), although the materials test data contained herein would indicate the presence of oxidative degradation. No explanation is offered to explain this inconsistency.

Additional testing recommendations include:

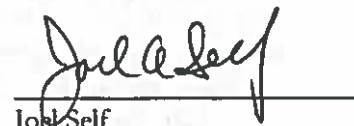
12. Further testing of acceptably field-performing system components to understand why no map cracking is in evidence, and how these components differ from materials that display map cracking.
13. Determination of the type and amount of titanium dioxide content within various components of the system.
14. Determination and possible quantitation of benzotriazole compounds, which are another possible UV stabilizer which could have been used within the white HDPE material.
15. Failure analysis, including fractography, of the typical failure modes in evidence in the field.
16. Selection of a "best case" sample and "worst case" sample (e.g. B3U and B2U respectively) followed by extensive sampling to allow for more in-depth testing with multiple replicates and exhaustive testing via additional techniques to allow a more-complete understanding and interpretation of results.

**DATA REVIEWED AND
REPORT WRITTEN BY:**



Steve Ferris
Independent Contractor to
Microbac Laboratories, Inc.

REPORT REVIEWED BY:



Jobi Self
Engineer III

For any feedback concerning our services, please contact the Managing Director of the Hauser Division or Trevor Boyce, President, at trevor.boyce@microbac.com and Cabot Earle, Executive Vice President, at cabot.earle@microbac.com. This report applies only to the sample(s) tested or analyzed. This report may be copied only in its entirety, unless prior written consent has been granted by an authorized agent of the Hauser Division of Microbac Laboratories, Inc.